A novel approach of power frequency spectrum analysis for residual power loads

Analysis of future grid variabilities among globally distinct regions

Maurin Hörler
EES-2020-423

Master Programme Energy and
Environmental Sciences, University of Groningen

university of groningen / faculty of science and engineering / energy and sustainability research institute groningen

Research report of Maurin Hörler

Report: EES-2020-423

Supervised by:
Dr. R.M.J. (René) Benders, Center for Energy and Environmental Studies (IVEM)
PH.D. Marijn Duvoort, Director Energy Markets (DNV GL)

University of Groningen
Energy and Sustainability Research Institute Groningen, ESRIG

Nijenborgh 6
9747 AG Groningen
T: 050 - 363 4760
W: www.rug.nl/research/esrig

ACKNOWLEDGEMENT

I would like to show my deepest gratitude to my supervisor Dr. R.M.J. (René) Benders for supporting and guiding me during this research. Further, I would also like to thank PH.D. Marijn Duvoort for his valuable inputs and for enabling my graduation project at DNV GL in Arnhem.

TABLE OF CONTENTS

SUMMARY

The current energy transition is not progressing fast enough to meet the targets of the Paris agreement, which asks for limiting global warming well below 2°C and aiming for 1.5°C (Gerwen, Eijgelaar, & Bosma, 2020). As a direct consequence, renewable energy sources are expected to increase enormously in the upcoming years. These renewable sources, such as solar PV and wind, are by nature non- dispatchable and display characteristics of high intermittency. Thus, they are commonly referred to as variable renewable energy sources (VRES). Additionally, the electrification among many power end-consumers of different sectors will increase spreading in the future to phase out fossil-fuel based technologies, such as heat pumps instead of gas boilers. The combination of VRES power generation and enhanced power demand during hours with peak power demand through electrification will put high pressure on the future power grid (Gerwen, Eijgelaar, & Bosma, 2020). As a result, power markets across the globe will experience profound changes in their power supply and demand characteristics, which will eventually lead to higher power variabilities in their grids. Power markets from different regions around the globe are exposed to distinct dynamics regarding the supply and demand side which are, for instance, caused by unique weather regimes or human development indexes (HDI). Thus, it is crucial to analyse current and future power markets of various regions and their corresponding grid variabilities among pre-selected time-cycles such as hourly, daily, weekly, monthly, and seasonal. By doing so, advice for flexibility measures on, for example, energy storage, can be provided for each time-cycle.

This study describes a novel approach to analyse the power variability of geographical and demographical distinct power systems, by examining the residual power load with the aid of a power frequency spectrum analysis. Thereby, the total power load profile was decomposed into relevant power sectors, based on the Netherlands as a benchmark country. In the next step, the decomposed sectorial load profiles were adjusted with country-specific factors to generate new total power loads per examined country. Subsequently, the VRES generation profiles per country were calculated based on solar PV, onshore, and offshore wind. Regional specific development indexes were applied to project the power demand and installed capacity of VRES for low and high scenarios for the years 2030 and 2050. Consequently, the residual power load profiles were created for current and future power markets of four countries: Netherlands, Italy, Egypt, and Singapore, which subsequently were analysed for power and electric energy variability on the pre-selected time-cycles. Additionally, the residual load duration curves (RLDCs) were examined for peaking power demand and VRES surplus or curtailment.

Outcomes revealed significant discrepancies among geographically and demographically distinct regions across the globe. Whereas the Egyptian and Italian power market in 2050 displays strong intra- daily power variation, triggered by the domination of solar PV, the Netherlands also experiences high-power variation on weekly time-cycles, which could be influenced by a high adoption rate of offshore wind in 2015. The Singaporean power market in 2050 has a significant variability peak on seasonal time-cycles caused by high seasonality of wind power in South East Asia (SEA). The RLDC of all examined countries resulted in a significant increase in cumulative VRES surplus by 2050 and thus, requires more investments in more storage facilities or other flexibility measures.

The novel approach of this study can be of importance for future planning and maintenance of power grids for utilities, power producers, transmission system operators (TSO), and the general energy market. The methodology could also be extended and applied to other countries, based on another benchmark country.

1. INTRODUCTION

1.1 Background

Energy markets across the globe are currently undergoing a profound change in their power mix with an increased share of variable renewable energy sources (VRES) to pave the road towards a future society with a net-zero carbon footprint. These VRES technologies will directly enhance the pressure of current grids by intermittent power generation with a characteristic of high weather-dependency, such as wind speed, temperature, and solar irradiance. Additionally, increased electrification within distinct end-consumer of the power sectors, such as high adoption rate of heat pumps, air conditioning (AC), and electric vehicles (EVs), will stress the grid in the upcoming years even further. The manufacturing or industrial sector is also expected to shift to more electrified processes along their supply and production chains. As a result, the global power demand is expected to more than double between 2017 to 2050, increasing from an annual power consumption of 24 PWh to 53 PWh (see Figure 1) (DNV GL, 2019). Thus, the supply side, or power generation, of the current power network will become more variable and unpredictable, by increased shares of VRES, while simultaneously the demand side, or power consumption, will increase in size through enhanced electrification of certain sectors. Consequently, more power generation facilities, utilities, and grid infrastructure are required to operate future power systems. Also, more investments in flexibility measures, for example, energy storage, demand response (DR), vehicle-to-grid (H2G), power-to-gas (P2G) will be needed to mitigate high power variabilities and thus, creating a reliable future power system (Gerwen, Eijgelaar, & Bosma, 2020).

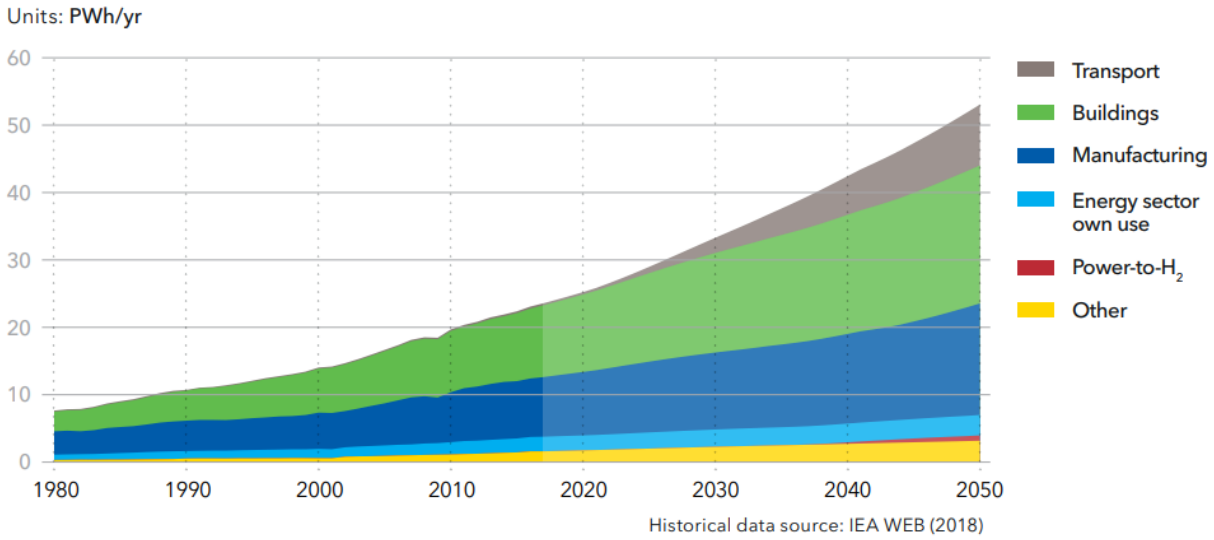

Figure 1: Global power demand by sectors and projections of the future with a time-period of 2018 - 2050 (DNV GL, 2019).

DNV GL's energy transition outlook (ETO) report from 2019 predicts that solar PV will be the global leading power source by 2050, providing 33% of the total power demand (DNV GL, 2019). Onshore wind will be the source that delivers the second most power with a share of 18% (see Figure 2) (DNV GL, 2019). These VRES are, by nature, variable and non-dispatchable at will. The growth of VRES and their correspondent intermittency issues directly enhances the variability of the power supply. Wind power generation exhibits variations among all time-cycles whereas solar PV power output correlates with solar irradiation and thus, displays more defined intra-daily and seasonal cycles (Guozden, Carbajal, Bianchi, & Solarte, 2020).

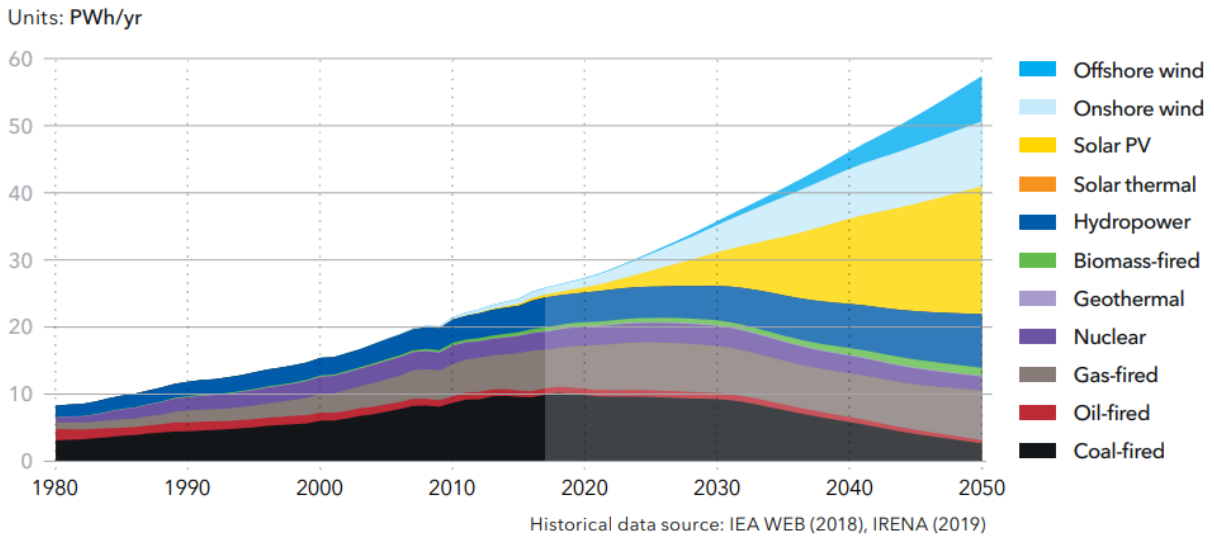

Figure 2: Global power generation by type of technology (DNV GL, 2019).

Aside from the weather-dependency of power generation of VRES, environmental conditions also have an impact on the demand side of the power system. For instance, the power demand for space heating and space cooling within the residential and commercial sectors are strongly correlated with the outside temperature. These environmental conditions display daily and seasonal cycles, resulting in similar patterns in the annual load profile of such end-consumers, such as space heating or space cooling. If current fossil-based heating technologies, such as gas boilers, are exchanged to heat pumps, the mismatch of VRES power supply and power demand will increase and cause more stress during hours with peaking power consumption. Also, the average working schedule is often represented by a workday-weekend cycle, which results in a weekly pattern in the demand profile among all sectors but especially in the industrial, commercial, and transport sectors (Gerwen, Eijgelaar, & Bosma, 2020).

In conclusion, the mentioned cycles of power supply and demand influence the variability of the power system. Thereby, the variability of VRES generation and power demand can reinforce or cancel each other at certain time-cycles. Future power grids with large shares of VRES will be even more exposed to intermittency issues and thus, increased power variabilities, which could have significant impacts for power producers, utilities, and transmission system operators (TSOs). The approach of this research applies a methodology that examines the power variability based on the annual residual power load, which is defined as the total load (demand side) minus the VRES generation (supply side) (see Figure 3). The residual load illustrates the power required by dispatchable sources, for example, natural gas or, if the value is negative, that the power must be stored or curtailed.

Demand side (total load)	Supply side (VRES)	Residual load

• Residential sector
• Commercial sector
• Industrial sector
• Transportation sector
	• Wind
	  • Onshore
	  • Offshore
	• Solar PV
		• Total load minus VRES generation
		• Demand which has to be matched by dispatachble power sources (if positive) or stored/curtailed (if negative)

Figure 3: Demand- and supply side of the power network and their corresponding residual load used in this study.

1.2 Problem Definition

Ideally, the VRES power surpluses during peak generation hours (negative residual load) should be stored and used in off-peak generation times. Nevertheless, in comparison to natural gas or district heating grids, the power grid does not provide intrinsic storage capacity and thus, load variations must be compensated and balanced out almost immediately. Currently, this is primarily achieved through dispatchable generation with the ability to supply electricity almost instantly. Yet, the large shares of VRES in future power systems will gradually diminish the obsolete dispatchable generation source and by doing so enforcing more stress on the power systems stability, flexibility, and adequacy (Gerwen, Sun, Eijgelaar, Bosma, & Dugstad, 2018). Therefore, there is an urgency of applying other measures besides the currently used flexible generation (dispatchable generation) to increase the flexibility of a VRES dominated power grid (see Figure 4). Not all flexibility measures can be implemented on the same time-cycles and thus, it is important to analyse the grid variability during different time-cycles.

On both an hourly and daily basis, flexibility can be introduced by short-term storage options, such as batteries, or so-called demand response and grid interconnectivity (see Figure 4). Demand-side flexibility from smart appliances and EVs can be an effective measure to reduce peak loads and to aid system balancing. Previous research has demonstrated that the demand response increases system flexibility while reducing the requirements for storage (Li & Pye, 2018). Demand response promotes a viable alternative to traditional supply-side remedies and represents the most cost-effective solution to integrate large amounts of VRES in the power grid (Klein, et al., 2016). Weekly and seasonal variations encourage other more long-term measures. These longer variations display different behaviours, like fewer cycles and the necessity of a larger energy storage system. Especially, in a carbon-free future where the carbon price inevitably will increase drastically, seasonal storage systems will be a viable solution in creating long-term flexibility and thus, resulting in a more reliable power grid (Gerwen, Eijgelaar, & Bosma, 2020).

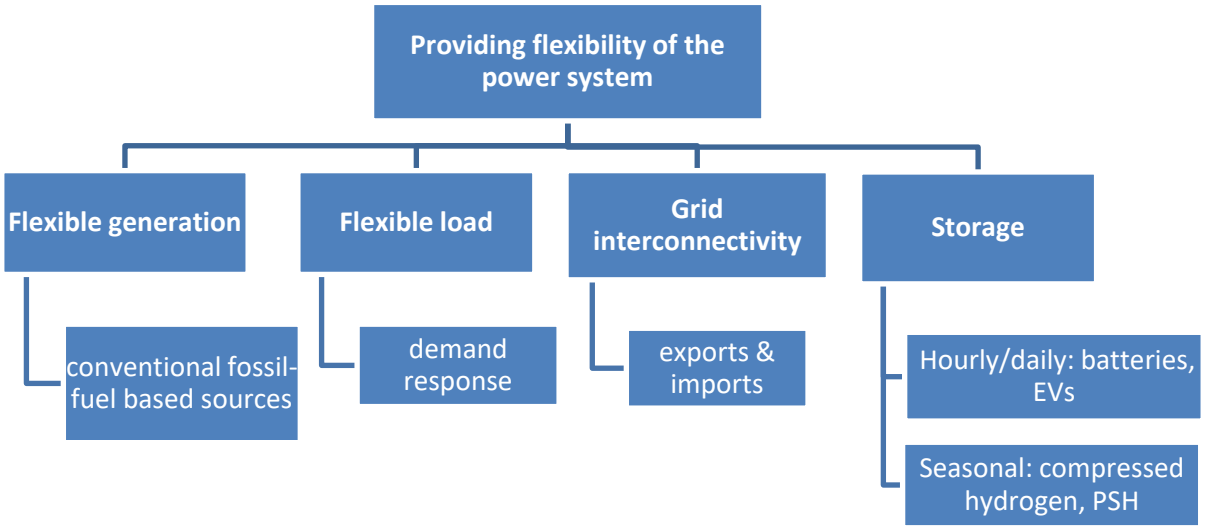

Figure 4: Measures to provide flexibility of variable power grids (ten Klooster, 2017). (PSH = pumped-storage hydroelectricity)

The energy transition is not occurring fast enough to meet the Paris agreement, which asks for limiting global warming well below 2°C and aiming for 1.5°C. Thus, VRES are expected to grow drastically and electrification will occur within many sectors, combining to put high pressure on the future power grids (Gerwen, Eijgelaar, & Bosma, 2020). To advise on flexibility measures (see Figure 4), in terms of what capacity is required during certain time-periods, it is critical to analyse the variability of current and future residual power loads during different time-cycles and among geographically and demographically distinct regions. This is due to differences in weather conditions, power demand, and the human development index.

1.3 Research Aim

This research aims to simulate current and future residual power loads form different countries, located in various regions, and examine their variabilities on pre-selected time-cycles. This is significant for advising on flexibility measures and thereby facilitating more VRES to the power mix which eventually leads to a more sustainable future power system. As previously mentioned, the hourly annual residual power load was used to calculate the grid variability by subtracting the VRES supply from the total load (demand) for every hour within the year. Future power systems will most likely display larger variabilities of residual power loads and therefore the aim was to create VRES forecast scenarios for the years 2030 and 2050. Additionally, it is important to observe these variabilities among different time-cycles because not all flexibility measures share the same characteristics and thus, cannot be applied to all time scales.

This research examined the power [MW] and electrical energy [MWh] variability of the residual power loads among hourly, daily, weekly, monthly, and seasonal time-cycles. Current and future power systems and grid variabilities of the Netherlands (Northern Europe), Italy (Southern Europe), Egypt (the Middle East and Northern Africa (MEA)) and Singapore (South East Asia (SEA)) were analysed by creating scenarios with distinct shares of VRES in the nation's future power mix. This was done to demonstrate spatially distinct regions differences in their VRES supply patterns and to display differences on the demand side, for example, a higher adoption rate of AC systems in warmer climates. Comparing contrasting geographic locations by their residual power loads can help to understand which measures have to be taken to increase the grid-flexibility and facilitate the integration of more VRES to the power mix of different regions. This research generates a novel approach to analysing residual power load variabilities with a power frequency spectrum analysis on pre-selected time-cycles. This analysis gives an overview of the robustness of future power systems among varying geographic locations.

Due to the power sectors displaying differing annual hourly demand patterns, the total power load must be decomposed into relevant sectoral profiles: residential, commercial, and industrial. The novel approach of this research adjusts the decomposed load profiles with country-specific parameters and, by doing so, generates future power loads for each country, which is a requirement for calculating the residual power loads.

1.4 Gap of Knowledge

Previous research has focused on electrical energy variation on multiple time-scales to identify opportunities for flexibility measures (Olsen, et al., 2019; Ueckerdt, et al., 2015; Clerjon & Perdu, 2018). Nevertheless, none of these studies decomposed the total power load into different sectors nor projected them to future scenarios, which neglects the increased variability on the power demand side in future scenarios. Consequently, the impact of electrification in the future, and power demand for electric vehicles (EVs) is not considered. Furthermore, the studies focused only on specific countries (e.g. Denmark for Olsen, et al., 2019) and do not analyse differences of power variabilities among distinct climatic regions. Thus, the methodology of this research, which decomposes the total power load into several sectors and adjusting them with country-specific factors and projecting the total power loads of varying countries to future scenarios, is a novel approach and contributes to this research gap. Olsen, et al., 2019 and Clerjon & Perdu, 2018 calculated both the grid variability with the aid of a Fourier analysis which is a similar statistical method to the power frequency spectrum analysis applied in the current study.

1.5 Research Question

RQ: How can the power grid variability be analysed, based on the residual power load, of geographically and demographically distinct current and future power markets (2030 and 2050) among different time-cycles?

- *How can one decompose the total hourly power load profile into sub-profiles of all significant sectors (demand side)?*
  - *What are the relevant sectors which should be considered?*
  - *What are the hourly, daily, weekly, and seasonal load profiles of these sectors?*
  - *How do these load profiles differ among the pre-selected countries and how are they expected to change in the future?*
- *What are the hourly annual power generation profile and installed capacities of the VRES for the pre-selected countries (supply side)?*
  - *What are the realistic scenarios of future VRES shares of the total supply?*
- *What is the power and electric energy variability of the resulting residual power load per country, when analysed on hourly, daily, weekly, and seasonal cycles?*
  - *How much peaking power demand and VRES surplus will remain when analysed on residual load duration curves (RLDC)?*

1.6 Scope and System Boundary Setting

A methodology was generated for this study, which describes a novel approach to decompose total power loads into relevant sectors and adjusting them with country-specific parameters. Two generic models were created with the ability to create country-specific load profiles and to analyses variabilities of the residual power load through a power frequency spectrum analysis. The system boundary of the current research is illustrated in Figure 5, which simultaneously represents the layout of the generic models. In total, the load profiles of three main sectors (residential, commercial, and industrial) were decomposed resulting in a remainder, which includes the remaining power demand (e.g. fishery sector). Additionally, the power consumption EVs was added to the total load profile.

The Netherlands was used as a benchmark country to create the basis of the load profiles for each sector. To compare different geographical and demographical power systems, one pre-selected country of each examined region was selected and served as a representation for their corresponding region. The following countries/regions were selected: Netherlands/Northern Europe, Italy/Southern Europe, Egypt /Middle East and Northern Africa (MEA), and Singapore/South East Asia (SEA). Hourly data of environmental conditions, such as temperature, of the examined countries were employed to adjust the temperature-sensitive load profiles of certain sectors, for example, of space heating in the residential sector. Thermosensitive end-consumers, such as heat pumps and AC in the residential and commercial sectors, are assumed to correlate with the outside temperature and thus, display contrasting profiles between unique locations. Therefore, this research created load profiles of these end-consumers for each examined country separately. Non-thermosensitive end-consumers, like appliances, EV, and the industrial sector, are assumed to display the same load profile between distinct regions. The effect of daylight length on the power consumption for lighting was neglected.

The power generation of VRES for each country was calculated based on three technologies: solar PV, onshore, and offshore wind. Periods of four consecutive years (2015-2018) were selected for the analysis. The residual power load was generated by subtracting the VRES supply from the total power load on an hourly basis. This remaining part, the residual power load, was analysed on power and electrical energy variability of hourly, daily, weekly, seasonal and inter-yearly time-cycles. As a result, the grid

stability and thus, demand for flexibility was observed. In addition, residual load duration curves (RLDC) were created to examine the required capacity of installed dispatchable electrical power sources, like natural gas, and flexibility capacity required, such as energy storage. Because this research aimed to examine solely grid variabilities, the effect of flexible generation, grid interconnectivity, demand response, and electrical storage flexibility measures on the residual power load was neglected and thus, allocated outside the system boundaries (see Figure 5). Nevertheless, the current research advises on the required capacity of flexibility measures on the examined time-cycles.

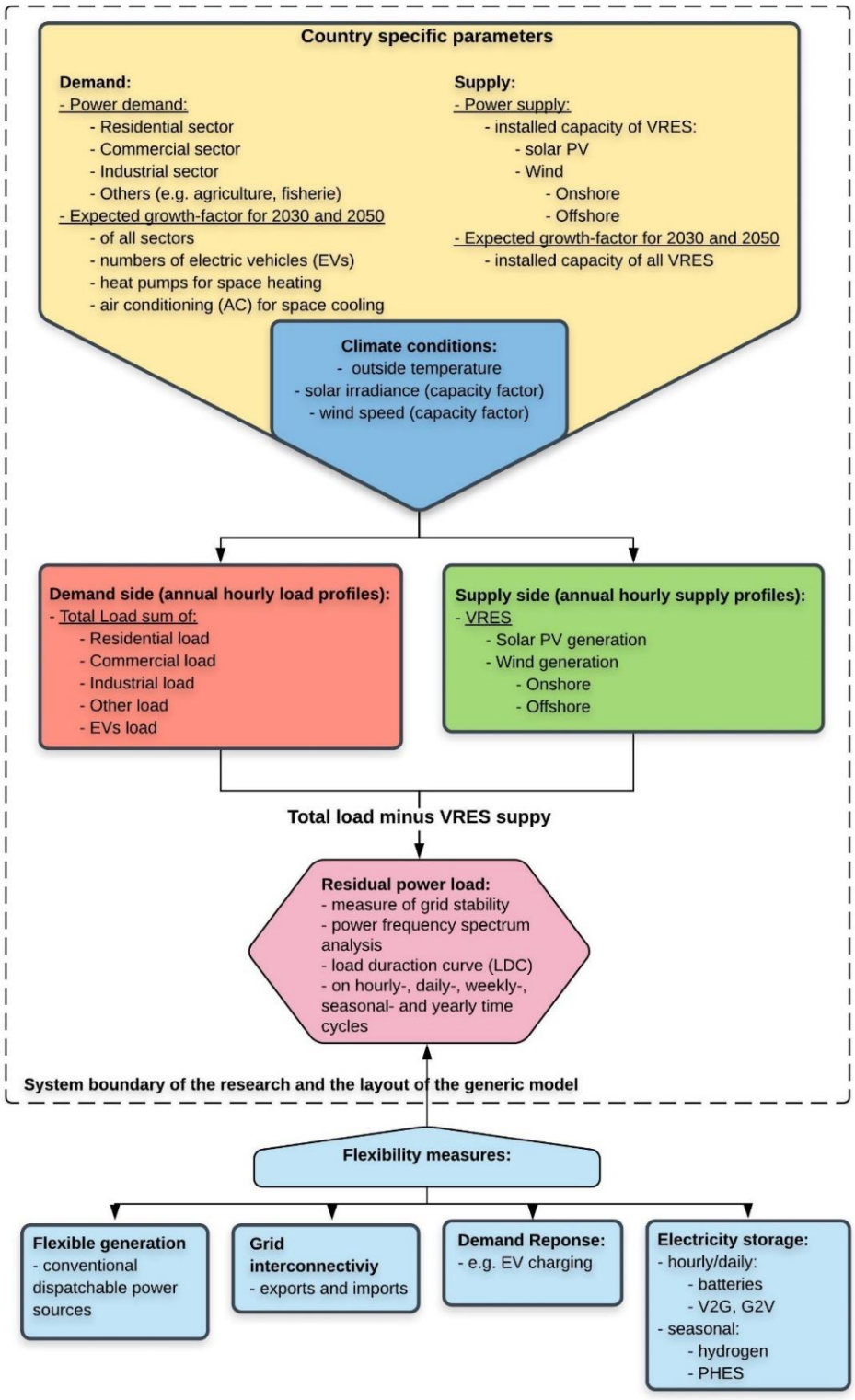

Figure 5: System boundary of the current research and the layout of the generic models.

2. RESEARCH METHODOLOGY

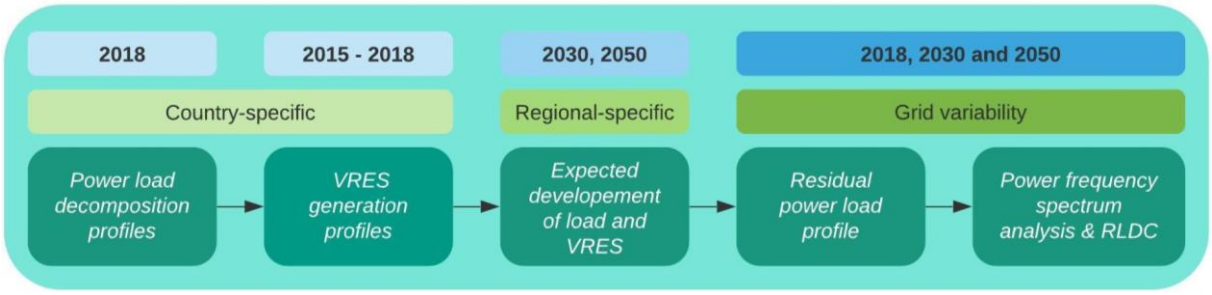

Figure 6: General overview of the applied research methodology. (RLDC = residual load duration curve)

A general overview of the research methodology is illustrated in Figure 6 and serves as the basis of the analysis paragraph (see Chapter 3), which explains each step more thoroughly. The primary objective of the research methodology is to produce hourly profiles of the demand and supply side of the current and future power system, which will then be used to create the residual power load profiles. This has been done for each examined country and the resulting residual power load profiles for 2018, 2030, and 2050 were subsequently analysed with a power frequency spectrum analysis and residual load duration curve (RLDC) to examine the grid variability (see Figure 6).

The methodology of the demand side includes the decomposition of the total annual power load into various sectors. This power load decomposition was based on the load profiles in 2018 from the Netherlands. However, the decomposed sectorial load profiles were adjusted with country-specific parameters from the other examined countries which resulted in sector- and country-specific profiles. After the total load profiles for each sector and country in 2018 were generated, future power load profiles were created based on the expected power consumption of each sector. The anticipated development (e.g. increase in power demand, the adoption rate of heat pumps) of each sector was used to scale the original profiles to the predicted future scenario of 2030 and 2050. These predicted growth-rates are regional-specific because they are based on the regional-development of each examined country (see Figure 6).

The methodology of the supply side considers the VRES generation profiles of each country. The power supply of solar PV, onshore, and offshore wind were calculated based on solar irradiance and wind speeds occurring on sites within the country and thus, are country-specific (see Figure 6). The observation period of the supply profile prolongs over four years from 2015 until 2018. By doing so, intra-yearly variabilities could be observed and the risk of inaccurate results through one extreme year (abnormal weather condition) could be mitigated. The supply profiles consist of hourly capacity factors, which were then multiplied with the installed VRES capacity. Current installed VRES capacities in 2018 were based on country-specific data, whereas the development of installed capacities in 2030 and 2050 are regional-specific for Egypt and Singapore due to lack of data. In the case of the Netherlands and Italy, country-specific data was available for future installed VRES capacity.

The preceding step of the research methodology includes the analysis of the variability of current and future grids per each examined country. The hourly residual power load was calculated, which subsequently was analysed for power and electric energy variabilities on different time-cycles with the aid of a power frequency spectrum analysis (see Figure 6). In addition, the RLDC was created to observe peaking hourly power productions and annual VRES surplus power.

In the following analysis section, this paper's methodology will be expanded upon with the applied equations, assumptions, and parameters.

3. ANALYSIS OF METHODOLOGY

In the following paragraphs, the analysis of the novel research methodology applied in this study gets elaborated more in detail. Thereby, the analysis is divided into the demand and supply side of the power system as well as the analysis of the final grid variability based on the residual power load. The detailed explanations of all analysis are explained in the following paragraphs.

3.1 Demand Side Analysis

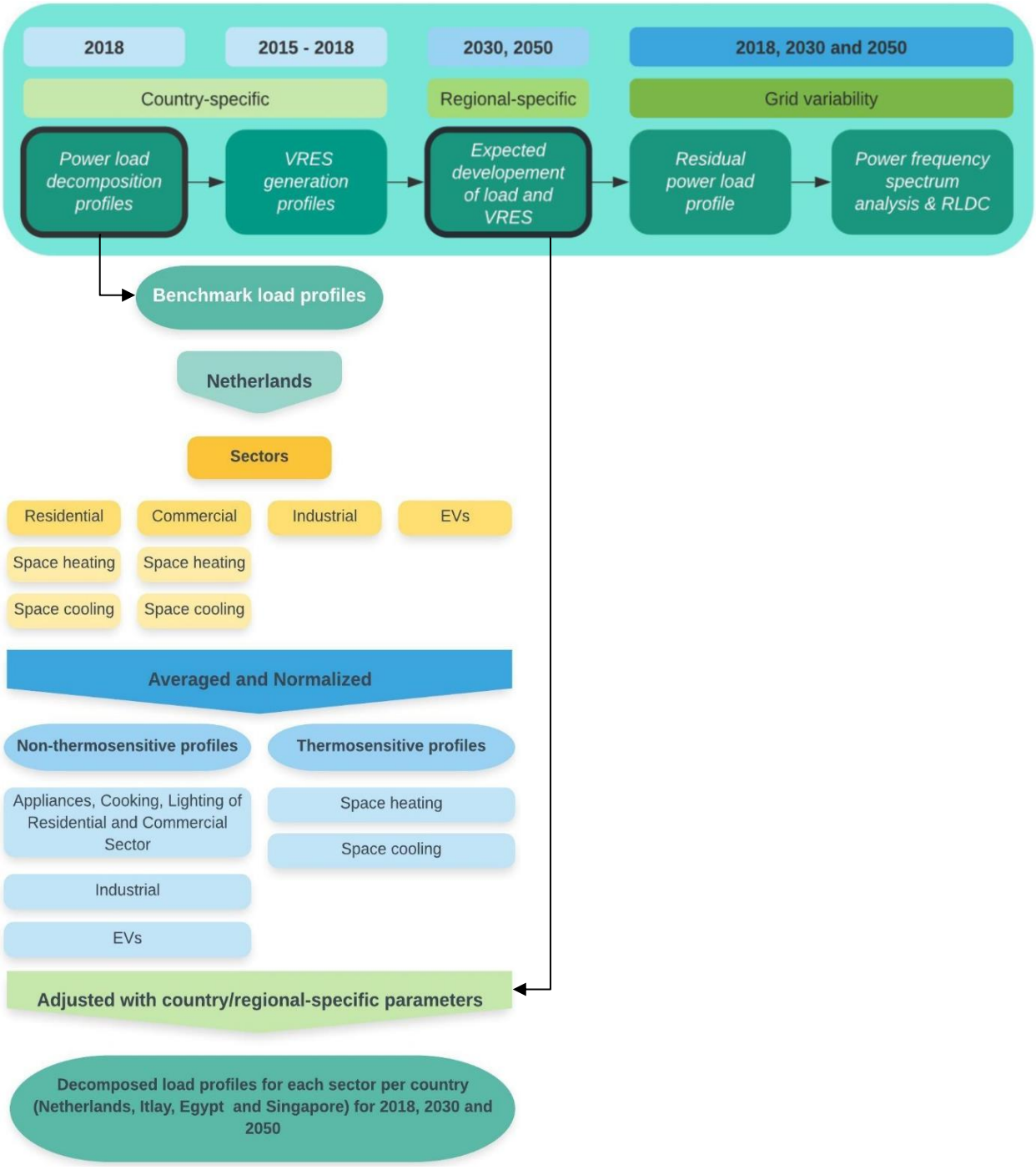

Figure 7: Research design of the demand side including the load decomposition based on the Netherlands as benchmark country. (RLDC = residual load duration curve)

To examine the growth factor of each sector (residential, commercial, and industrial) per examined country, an approach was designed to decompose the total power load into profiles for the various sectors. In addition, annual load profiles for space heating and space cooling were generated to analyse the expected growth in the adoption rate of heat pumps and AC systems in the residential and commercial sectors. Due to simplification and lack of data, annual load profiles for the different sectors were based on the Netherlands. These load profiles served as benchmarks to generate the corresponding load profiles for the other examined countries after they were corrected with country-specific parameters (see Figure 7).

In the first step, the total Dutch power load was disaggregated or decomposed. It is crucial to note the decomposition of an existing load profile cannot be disaggregated into as many end-consumer profiles as possible. Three significant aspects constrain the possibilities of disaggregating opportunities of certain power end-consumers (European Comission, 2018):

1. First, detailed information about the hourly load profile of the end-consumer is required. Additionally, the expectation for changes in the future annual demand of this specific end-consumer must be known or assumed based on certain country-specific parameters and presumptions. Issues with data access about certain end-consumers may emerge.
2. Secondly, it is impossible to completely decompose the load profile into all its parts and sub-end-consumers, due to limited data availability. Nevertheless, the decomposition should consider the most relevant end-consumers to generate an explicit representation of the total load profile. The end-consumers considered in this research can be retrieved from Figure 7. The remaining power demand (e.g. agriculture and fisheries) can be considered as an aggregated remainder, represented by the difference between the retrieved total power load profile per country and the summed-up power load profile of the residential, commercial, industrial sector as well as EVs consumption. Thus, decomposing the load profile could be described as a partial decomposition (European Comission, 2018).
3. Thirdly, the load profiles can also be divided into thermosensitive and non-thermosensitive demands (see Figure 7). This enables the examination of what sectors are dependent or correlated with ambient temperatures. The thermosensitive part depends on the outside temperature (e.g. heat pumps, AC) whereas the non-thermosensitive component is independent of the ambient temperature, illustrated by electric appliances, EVs, or industries (European Comission, 2018). As previously mentioned, the impact of day-length seasonality on power consumption for lighting is neglected. This analysis considers that the residential and commercial sectors both include thermosensitive behaviour by the power demand in space heating and space cooling.

In the second step, once the total load profile was decomposed, the load profiles of the sectors containing thermosensitive behaviours (residential and commercial) were averaged and normalized. This was done so they could be adjusted with country-specific parameters to generate the load profiles for the other examined countries (see Figure 7). By doing so, the current annual power profile for space heating and space cooling in the Netherlands was subtracted from the total power profile for the corresponding sectors. This resulted in the only non-thermosensitive part of the load profile for the residential and commercial sectors. Also, in the second step, two alternative methods were applied to average the Dutch profiles for the remaining countries. For Italy, the annual non-thermosensitive profiles of both sectors (residential and commercial) were averaged over the entire year and served as a base profile. Due to the significantly warmer climates in Egypt and Singapore, only the summer months of June – August, and May – September were averaged over the year for the residential and commercial sectors, respectively. The reason for the larger period considered for the commercial sector is, to limit the effect of the Dutch summer holiday dip in power demand (see Appendix I; Figure 41). The same normalized load profiles for the non-thermosensitive sectors (industrial sector and EVs) were applied among all examined countries.

In the last step, the distinct sectoral and country-specific load profiles were projected into the future (2030 and 2050), based on expected growth rates in future power demands given by regional parameters. These forecasted power demands were retrieved from DNV GLs ETO report and are, among others, influenced by the region's gross domestic product (GDP), population growth rate (demographics), human development index, and an expected increase in EVs (DNV GL, 2019). To create the total future power load profile, all projected power profile loads of the sectors and the remainder must be summed up to generate the new aggregated total load profile for the year 2030 and 2050 for each country. These newly generated load profiles are likely to display different behaviour and variability than the initial one (European Comission, 2018).

In the following sections, the analysis of the demand side and considered power sectors are explained more thoroughly, including the relevant equations and assumptions.

3.1.1 Total Power Load Decomposition (Netherlands as Benchmark Country)

The annual load profiles of the residential, commercial, and industrial sectors were generated with the aid of the Dutch power profiles retrieved from NEDU. There are ten different power profiles with distinct characteristics, as illustrated in Table 1 (NEDU, 2018). The number of connections and averaged annual consumption per power profile is based on the year 2018. The E1, E2, and E3 profiles represent small, medium, and large end-consumers, respectively. E4A is a separate profile and consists of public lighting up to 100 kW. All NEDU profiles are annually normalized and thus, must be multiplied with the number of connections and annual consumption per profile to generate the total annual power demand per profile. Since power profiles are in 15 minutes interval, a transformation to hourly data was applied.

Table 1: NEDU power profile categories with grid connection capacity ouputs and number of connections (NEDU, Verbruiksprofile, 2018). (OT = annual operation time)

Power Profile	Grid connection capacity	Description	Connections (* 10^3)	Averaged annual consumption [kWh]
E1A	≤ 3 x 25 A	Single tariff	1,496	2,584
E1B	≤ 3 x 25 A	Night tariff	4,879	3,097
E1C	≤ 3 x 25 A	Evening tariff	1,608	3,396
E2A	> 3 x 25 A & ≤ 3 x 80 A	Single tariff	42	20,180
E2B	> 3 x 25 A & ≤ 3 x 80 A	Double tariff	323	25,650
E3A	> 3 x 80 A & < 100 kW	OT ≤ 2000 h	14	70,026
E3B	> 3 x 80 A & < 100 kW	OT 2,000 – 3,000 h	6	118,508
E3C	> 3 x 80 A & < 100 kW	OT 3,000 – 5,000 h	2	165,359
E3D	> 3 x 80 A & < 100 kW	OT ≥ 5,000 h	0.2	183,017
E4A	> 3 x 80 A & < 100 kW	Public lighting	24	18,950

The power profiles from NEDU also include information about the number of connections per profile (see Table 1). Accordingly, the aggregated NEDU connections of E1, E2, E3, and E4 are given in Table 2 (NEDU, 2018). The number of NEDU connections can be compared to the final stock (e.g. number of dwellings) for the residential, commercial, and industrial sectors in the Netherlands for the year 2018, illustrated in Table 2 (CBS 2, 2018). The following paragraphs describe how the load profile for each sector was created based on these NEDU profiles.

Table 2: Number of connections per sector (CBS 2, 2018; NEDU, Verbruiksprofile, 2018)

Sector	**Residential**	**Commercial**	**Industrial**		**Total**
Final Stock (CBS)	7,814,912	942,026	194,977		8,951,915
Power Profile	**E1**	**E2**	**E3**	**E4**	**Total**
Connections (NEDU)	7,983,000	365,000	22,200	24,000	8,394,200

3.1.2 Residential Sector

According to CBS, the final stock in the residential sector for the year 2018 resulted in 7,814,919 dwellings (see Table 2). Since the NEDU power profile E1 for the same year equalled to 7,983,000 connections and was only 2% higher than the CBS value, the aggregated E1 power profile was used for the residential sector. The remaining 168,088 connections were assumed to belong to the small businesses from the commercial sector. Thereby, the annual demand profiles of E1A, E1B, and E1C were generated, according to their number of connections and annual consumption. The final demand profiles were then summed up and normalized representing the annual profile of the residential sector (see Figure 8 (weekly profile) and Appendix I; Figure 40 (annual profile)).

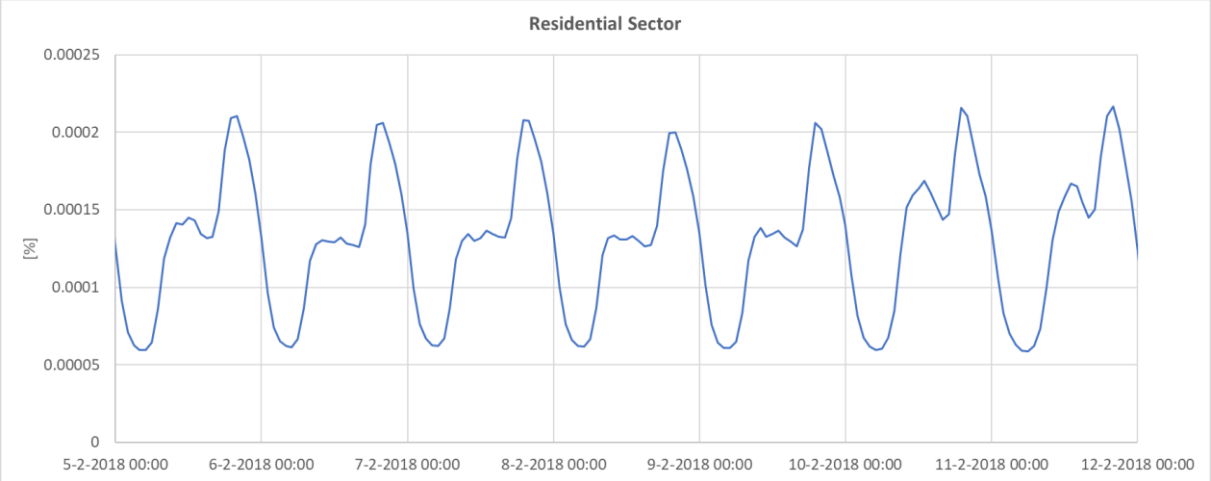

Figure 8: The normalized load profile of the residential sector in 2018, on a weekly time scale in February, representing the aggregated E1A NEDU profiles (NEDU, Verbruiksprofile, 2018).

3.1.3 Commercial Sector

According to CBS, the commercial sector entailed 942,026 buildings in 2018, which represents around 2.6 times more connections than buildings are equipped with E2 grid access (only 365,000 connections) (see Table 2). Thus, the remaining 577,026 commercial building connections must display E1, E3, and E4 power profile behaviours. Table 3 illustrates the exact profile-decomposition, applied in this study, of the commercial sector into distinct NEDU power profiles. Since the residential sector does not make use of all connections from the E1 power profiles (see Table 2), the remaining 168,088 connections are assumed to belong to medium consumers and were counted towards the commercial sector. The power profiles of E3 combined only add 22,200 connections (see Table 3). The public lightning (E4), resulting in 24,000 connections, was also allocated to the commercial sector since it was claimed to be a public service. The applied methodology equals 579,288 building connections and thus, the remaining 367,738 are assumed to be equipped with E3C grid-connection. Many large consumers have their own telemetry and thus, do not demand the allocation of consumption profiles by the grid operators since they can precisely track and forecast their consumption (Energiemanager, 2018). As a direct consequence, a sizeable share of large consumers in the commercial sectors and the industrial sector are excluded from the numbers indicated by NEDU because they do not need forecast consumption profiles. Therefore, it is assumed that the remaining buildings of the commercial sector are large consumers like the E3C power profile, due to its high number of operation hours (see Table 1). The power profile of E3D displays even higher numbers of operation hours and is assumed to mimic the industrial sector. The final load profile of the commercial sector is the result of the combination of the previously mentioned NEDU power profiles, based on their specific contribution [%] to the final profile (see Table 3). Subsequently, the final profile was normalized over the year on an hourly basis. The weekly load profile of the commercial sector is illustrated in Figure 9 and the annual profile can be retrieved from Appendix I in Figure 41.

Table 3: NEDU Power Profile decomposition, resulting in the load profile of the commercial sector (NEDU, Verbruiksprofile, 2018).

Sector	From E1 to E2	From E2 to E2	From E3 to E2	From E4 to E2	Total	Remaining from E3C	Total
Commercial	168,088	365,000	22,200	24,000	579,288	362,738	942,026
[%]	0.18	0.02	0.39	0.03		0.38	

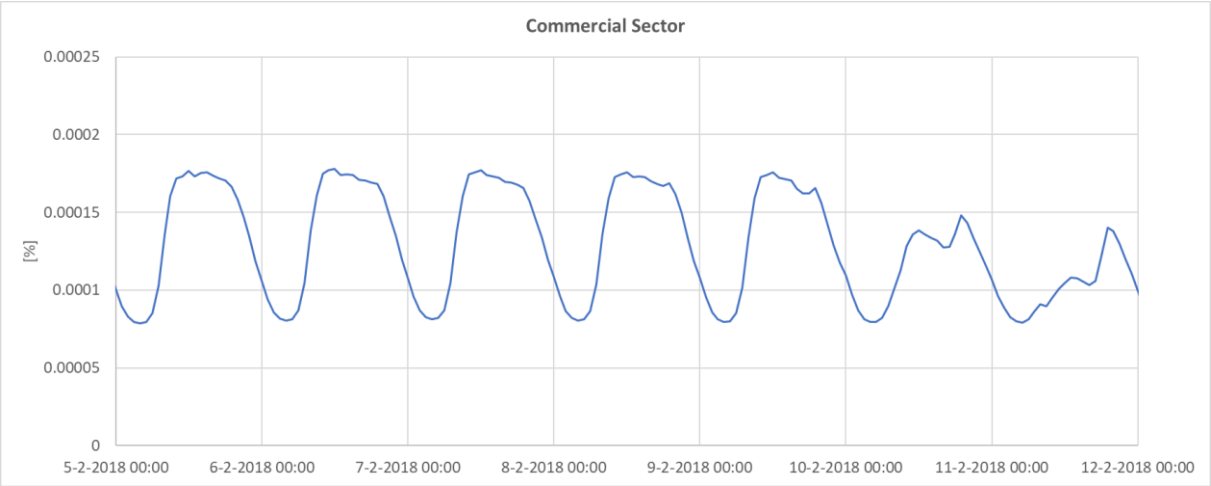

Figure 9: The normalized load profile of the commercial sector in 2018, on an weekly time scale in February, representing the combination of different NEDU profiles (NEDU, Verbruiksprofile, 2018).

3.1.4 Industrial Sector

As previously mentioned, it is challenging to retrieve forecast load profiles of large power consumers because of their ability to accurately monitor and forecast their demand with the aid of smart metering applications. As a result, these large power consumers do not require the NEDU power profiles for demand estimations of grid and transmission operators (Energiemanager, 2018). In addition, literature and data-access on detailed power consumption on the industry-level are very limited (Cialani & Mortazavi, 2018). Thus, it was assumed that the large power consumers of the industrial sector are displaying an annual load profile equivalent to the E3D NEDU power profile (see Table 1). The very high operation time of more than 5,000 hours per year illustrates a realist value for the industrial sector because an analysis of a chemical manufacturing company showed on average a planned production time of 8,304 hours per year (Mwanza & Mbohwa, 2015).

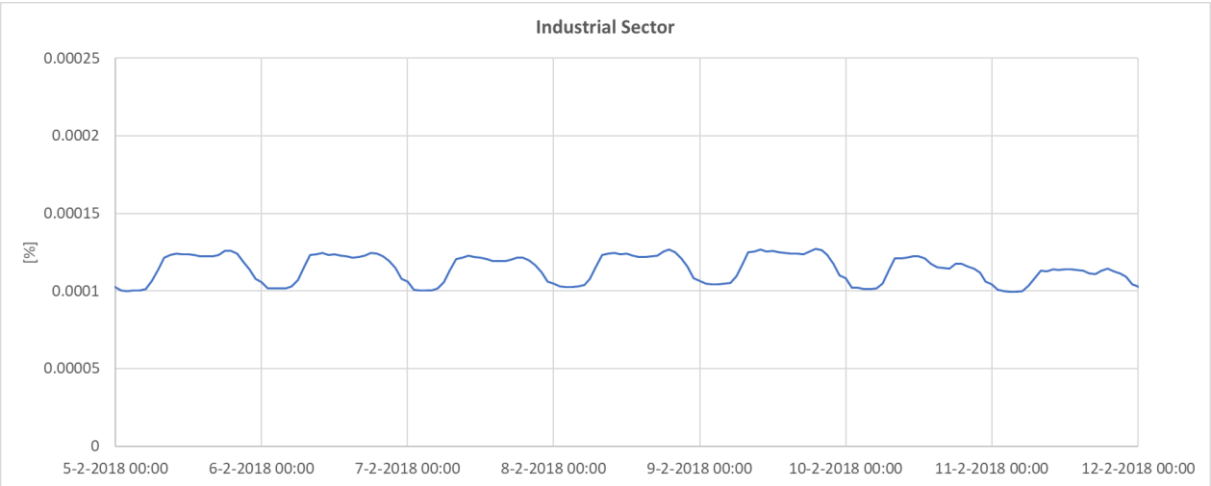

Figure 10: The normalized load profile of the industrial sector in 2018, on an weekly time scale in February, representing the aggregated E3D NEDU profiles (NEDU, Verbruiksprofile, 2018).

The industrial profile pattern is more balanced with a lower daily power variability in comparison to the residential and commercial sectors (see Figure 8, Figure 9, and Figure 10). Due to its more constant production-process, the daily power profile of industrial end-consumers is much flatter compared to the other sectors which, again, is most aligned with the E3D NEDU power profile (Granell, Axon, Wallom, & Layberry, 2015).

3.1.5 Space Heating and Domestic Hot Water (DHW)

To simulate the effect of the electrification of heating technologies responsible for space heating and domestic hot water (DHW) in the residential and commercial sector, annual power consumption profiles for heating purposes are required. In 2016, 98% of the total natural gas demand in the Dutch residential sector was used for space heating and DHW (CBS 1, 2018). Therefore, the natural gas profiles retrieved from NEDU were employed and assumed to mimic the annual behaviour demand profile for heating purposes (see Table 4). This assumption is also supported by a study that states that 96% of the total gas consumption in dwellings is used for space heating purposes (Majcen , Itard, & Visscher, 2013). Further, also another study calculated and estimated heat pump power demands based on natural gas consumption profiles (Veldman, Gaillard, Gibescu, Slootweg, & Kling, 2010). It is worth mentioning that gas profile G2A and G2C have the same values and G2B is unavailable in the dataset which thus, results in only one usable consumption profile for the G2 gas profile.

Table 4: NEDU natural gas profile categories, grid connection capacity and additional describitions (NEDU, Verbruiksprofile, 2018)[1] (NEDU, Verbruiksprofile, 2020)[2] (OT = operation time).

Gas Profile	Grid connection capacity (annual consumption)	Description
G1A[1]	< 5,000 m^3	
G2A[1]	≥ 5,000 m^3 & < 170,000 m^3	OT < 750 h
G2B[1]	≥ 5,000 m^3 & < 170,000 m^3	OT 750 – 1,500 h
G2C[1]	≥ 5,000 m^3 & < 170,000 m^3	OT ≥ 1,500 h
GXX[2]	≥ 170,000 m^3 & < 1,000,000 m^3	

The NEDU natural gas profiles are divided into three distinctive profile parameters. First, the heating temperatures (HT) represent the threshold temperatures when space heating is required, thus, when the outside temperature falls below these values the profile expects energy input to the system to achieve the desired indoor temperatures. As expected, the HT numbers exhibit diurnal behaviour with greater values during the day and decreased ones at night when residents are asleep. Second, the regression coefficient (RER) illustrates the temperature-dependent parameter and is responsible for calculating the energy demand for space heating according to the relation between outside temperature and the respective heating temperature (HT). And lastly, the temperature-independent parameter (TIP) which calculates the energy consumption for DHW and is assumed to be not dependent on the outside temperature (Energiemanager, 2018; NEDU, Verbruiksprofile, 2018). The final consumption profiles of the distinct gas profiles (see Table 4), are calculated according to the following two equations (Equation 1 and Equation 2), both requiring the input of country-specific outside temperatures (T_{out}) on an hourly basis. The NEDU document also includes averaged standard outside temperatures (SOT) and if one would use them as the T_{out} the sum of the final consumption profile would equal 1. Nevertheless, since this methodology must include outdoor conditions from several countries in separate regions, actual measured outside temperatures for four consecutive years (2015-2018) were retrieved from the data webpage Renewables.Ninja, averaged over one year and applied as the true outside temperature (Pfenninger & Staffell, 2020). Thus, the final profile had to be normalized to generate usable time series.

*If T_{out} ≤ HT: FPF = (HT - T_{out}) * RER + TIP* *Equation 1*
If T_{out} > HT: FPF = TIP *Equation 2*

T_{out} = outside temperature [°C]
HT = heating temperature [°C]
RER = regression coefficient, temperature-dependent parameter
TIP = temperature-independent parameter
FPF = final profile factor per hour

In the residential sector, the gas profile G1A was applied because it represents the only profile simulating an annual gas consumption rate lower than 5,000 m^3. The Dutch average gas consumption in 2016 for dwellings in the residential sector resulted in 1,300 m^3 and thus, justifying the selected gas profile (CBS 3, 2018). The G1A profile distinguishes between the heating season (October – April) and the non-heating season (May – September) with adjusted values for the above-mentioned profile-specific parameters (HT, RER, and TIP). The generic model applies the methodology of heating-degree-days (HDD) to determine if the profile of the heating season or non-heating season serves as a basis (van Breukelen, 2019):

$$HDD = \frac{1}{24} \times \sum_{i=1}^{24} (T_{base} - T_i)^+ \qquad \textit{Equation 3}$$

HDD = heating-degree-days, daily
T_{base} = base temperature [°C]
T_i = outside temperature of hour i [°C]
$^+$ = only positive values considered

For all examined countries, a base temperature of 15.5 °C was applied to indicate the threshold outside temperature. If the outside temperature is below 15.5 °C space heating is expected (European Environment Agency, 2019). The desired indoor temperature for all countries is assumed to be the same and thus, not a variable in the HDD equation. The resulting hourly HDDs were summed up daily (sum of 24 hours) to generate the daily HDD values. It was assumed that the heating season had daily HDD values higher than 4 °C and the non-heating season had anything below this value or zero HDD. Figure 11 illustrates the load profile for heating in the residential sector, based on the measured outside temperature in the Netherlands (averaged 2015 – 2018) during the heating season (5 February – 12 February). The morning and evening heating peaks are apparent as well as the dip during the day when people are out at work or school and during the night when people are asleep.

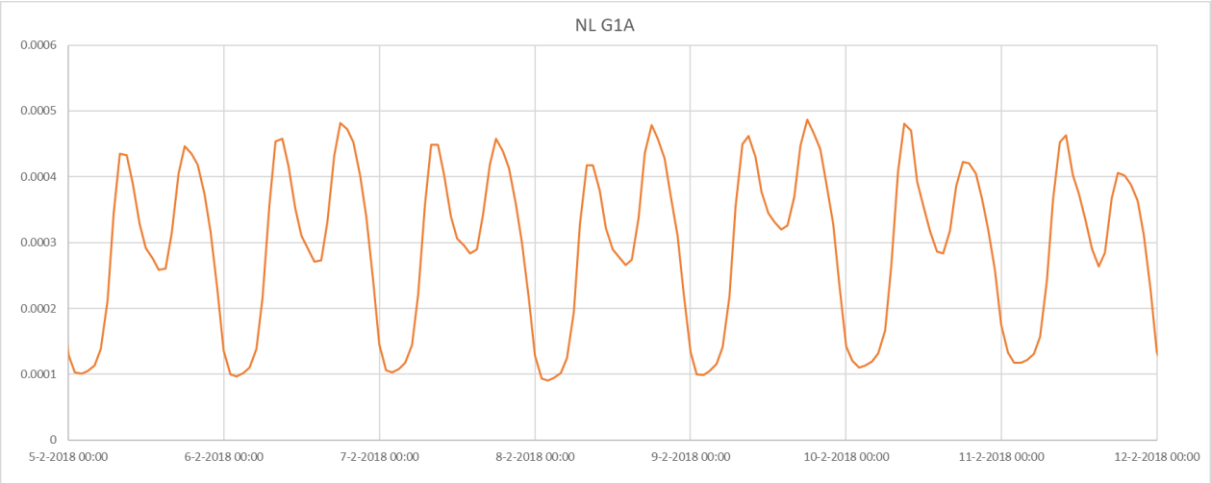

Figure 11: G1A gas profile mimicking the heating demand for the residential sector based on averaged outside temperature from 2015-2018 in the Netherlands (NEDU, 2018; Pfenninger & Staffell, 2020).

For heating purposes in the commercial sector, the GXX NEDU gas profile was used (NEDU, 2020). Although the capacity of the grid connection is fairly high (see Table 4), the pattern of this gas profile fits the electrical energy consumption of the commercial sector best because of the clear weekly variations (weekdays and weekends) which the other profiles (G2A, G2B, and G2C) show to a lesser extent. Furthermore, the temperature-independent parameters (TIP) of the GXX have a peak throughout the day, whereas the other profiles (G2A and G2C) have a strong and significant morning peak and lesser evening peaks (see Figure 12). This is less realistic for businesses in the commercial sector where working people are often present during the day, increasing the demand for comfortable inside temperature.

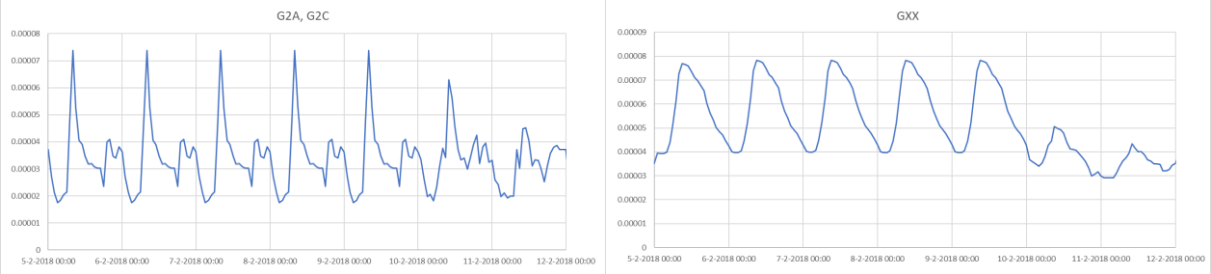

Figure 12: Temperature-independent parameter (TIP) of the G2A, G2C and GXX NEDU gas profile (NEDU, Verbruiksprofile, 2018; NEDU, Verbruiksprofile, 2020)

Figure 13 illustrates the load profile for heating purposes in the commercial sector, based on the measured outside temperature in the Netherlands (averaged 2015 – 2018) during the heating season (5 February – 12 February). A morning peak is still visible, but to a lesser extent in comparison with the residential sector profile (see Figure 11). Further, the power demand prolongs throughout the day and is overall more constant. The profile also clearly demonstrates the weekly cycles with higher power demands during the week and lower power demands over the weekend when people are not working.

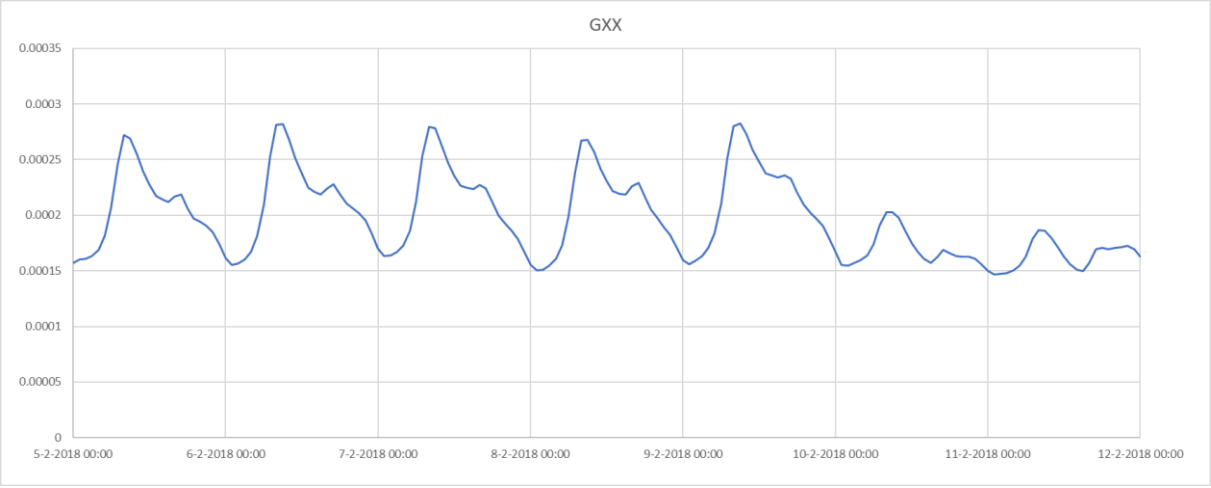

Figure 13: GXX gas profile mimicking the heating demand for the commercial sector based on averaged outside temperature from 2015-2018 in the Netherlands (NEDU, Verbruiksprofile, 2020; Pfenninger & Staffell, 2020).

The final country-specific load profiles of space heating for the residential and commercial sector, depending on the local outside temperature, were added to the total power load of the corresponding sector according to the expected shares of space heating and DHW from the total power demand for current and future (2030 and 2050) scenarios. The shares of heating purposes from the total power demand are related to the region and differ between geographic locations. Values were retrieved from ETO database (see Appendix II; Table 10, Table 11, Table 12 and Table 13) (DNV GL, 2019).

3.1.6 Space Cooling

The power consumption profile for space cooling, based on AC, is based on research conducted for Gujarat, India (Garg, Maheshwari, & Upadhyay, 2010; McNeil, Karali, & Letschert, 2019). These reports differentiate between residential and commercial space cooling as well as between peak and off-peak cooling hours. To generate the weekly demand pattern, two parameter values were applied to translate the retrieved daily profile into a weekday and a weekend profile for either peak and off-peak hours for both sectors, residential and commercial. Combined there are four distinct annual consumption profiles for space cooling (see Figure 14). The parameters applied to transform the profile pattern from weekdays into weekends were calculated by using the previously mentioned NEDU power consumption profile from the residential and commercial sectors (see the power profiles in Figure 8 and Figure 9). Thereby, all weekdays and weekends were averaged separately and the variance among them represented the transforming-parameter from weekdays to the weekend. By doing so, the original space cooling profile was multiplied with the calculated transforming-parameter for weekends in both sectors. The transforming-parameters are 1.032 and 0.8 for the residential and commercial sector, respectively, which leads to slightly higher power demand for space cooling during the weekend in the case of residential dwellings and significantly lower values for space cooling among businesses in the commercial sector on weekends (see Figure 15). Most space cooling in the residential sector is demanded during the evening and morning peak-hours and nearly disappears during the daytime when people are outside of the home. The commercial sector, on the other hand, displays a strong peak throughout the day and significantly reduces during night-time, aligning with standard working hours. However, space cooling profiles for other regions may differ as these profiles were based on Gujarat, India.

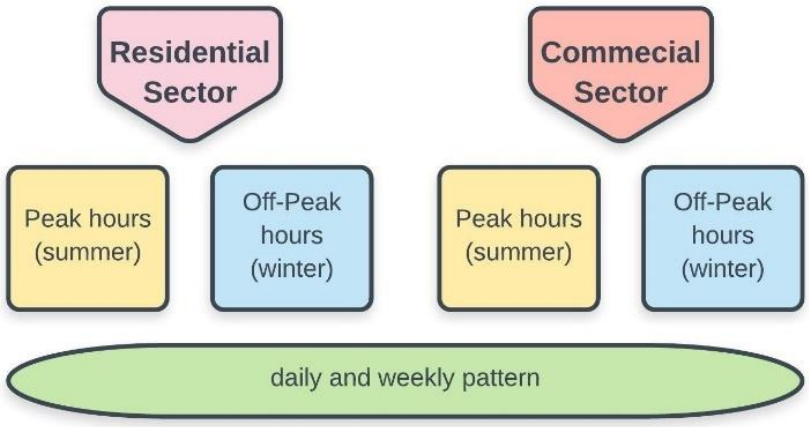

Figure 14: The space cooling consumption profiles for the residential and commercial sector, split up into peak and off-peak hours for the summer and winter seasons, respectively. All profile patterns were transformed into a weekly pattern in addition to the daily pattern.

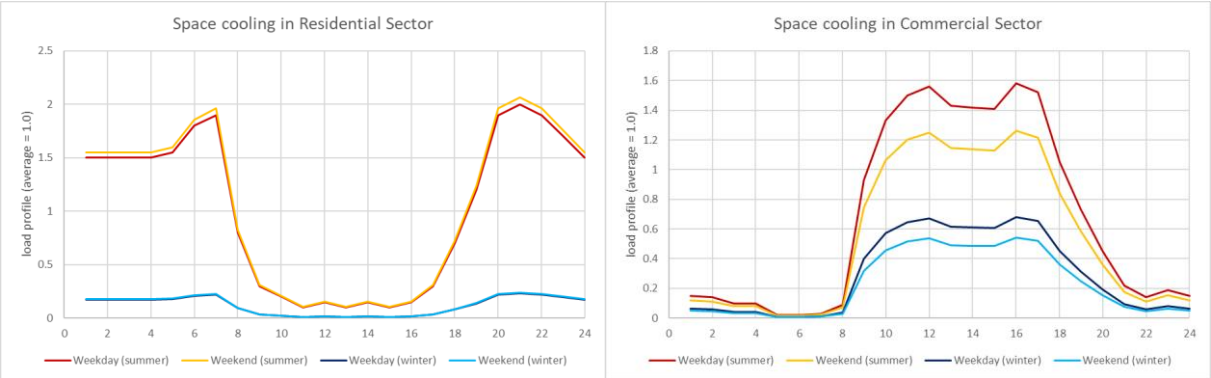

Figure 15: Consumption profile pattern for space cooling in the residential and commercial sector, split up into weekdays, weekends, summer (peak hours) and winter (off-peak hours) (Garg, Maheshwari, & Upadhyay, 2010; Gelaro, et al., 2017).

The off-peak profiles (winter) in the residential sector are almost zero whereas the off-peak profiles for the commercial sector continue to demand power for space cooling (e.g. hotels, data centre cooling system) (see Figure 15). To create power consumption profiles for all considered regions separately, the original space cooling profiles were corrected by applying the cooling-degrees-days (CDD) methodology. A similar approach to generate the country-specific annual outside temperature for the space heating power demand was used, resulting in hourly values averaged for one year based on four consecutive years between 2015 – 2018 (Pfenninger & Staffell, 2020). Due to hourly frequency temperature data, the hourly method for CDD calculations was applied as followed (van Breukelen, 2019):

$$CDD = \frac{1}{24} \times \sum_{i=1}^{24} (T_i - T_{base})^+ \qquad \textit{Equation 4}$$

CDD = cooling-degree-days, daily
T_i = outside temperature of hour i [°C]
T_{base} = base temperature [°C]
$^+$ = only positive values considered

For all examined countries, a base temperature of 22 °C was used as a threshold for outside temperature, and for anything above this, space cooling was expected to be needed (European Environment Agency, 2019). The resulting hourly CDD were summed up daily (sum of 24 hours) and then divided again equally among the 24 hours of the day. By doing so the daily CDD values can be multiplied with the corresponding cooling profile. The final consumption profile patterns for each region's residential and commercial sector were calculated by making the following two equations:

If $CDD_{daily} > 0$: $FPF = CDD_{daily} * PPSC$ *Equation 5*
If $CDD_{daily} \leq 0$: $FPF = OPPSC$ *Equation 6*

CDD_{daily} = daily cooling-degree-days
PPSC = peak profile space cooling
OPPSC = off-peak profile space cooling
FPF = final profile factor per hour

The final country-specific load profile for space cooling, depending on the local weather-condition, was added to the total power load of the corresponding sector according to the expected shares of space cooling of the total power demand, for current and future (2030 and 2050) scenarios. The shares of space cooling are related to the region and values were retrieved from the ETO database (see Appendix II; Table 10, Table 11, Table 12 and Table 13) (DNV GL, 2019).

3.1.7 Electric Vehicles (EVs)

The impact of EVs on this research only considered plug-in vehicles (PEVs) of battery electric vehicles (BEVs) and neglect plug-in hybrid vehicles (PHEVs). PHEVs were excluded from the system boundary because the DNV GL ETO report suggests that PHEVs should only be seen as a bridging technology until the range of BEVs is sufficient enough, which is expected to be achieved in the near future (DNV GL, 2019). In addition, PHEVs display very high purchase prices and expensive operational costs, which will ultimately lead to the phase-out of PHEVs in the future transportation system (see Figure 16). Hydrogen-powered fuel-cell electric vehicles (FCEVs) are not assumed to be used in the future for the passenger (light-vehicle) road transport due to their low energy efficiency (half of BEVs), significant electricity loss when converting electricity to hydrogen (electrolysis), and higher cost of the more complicated propulsion technology FCEVs (DNV GL, 2019).

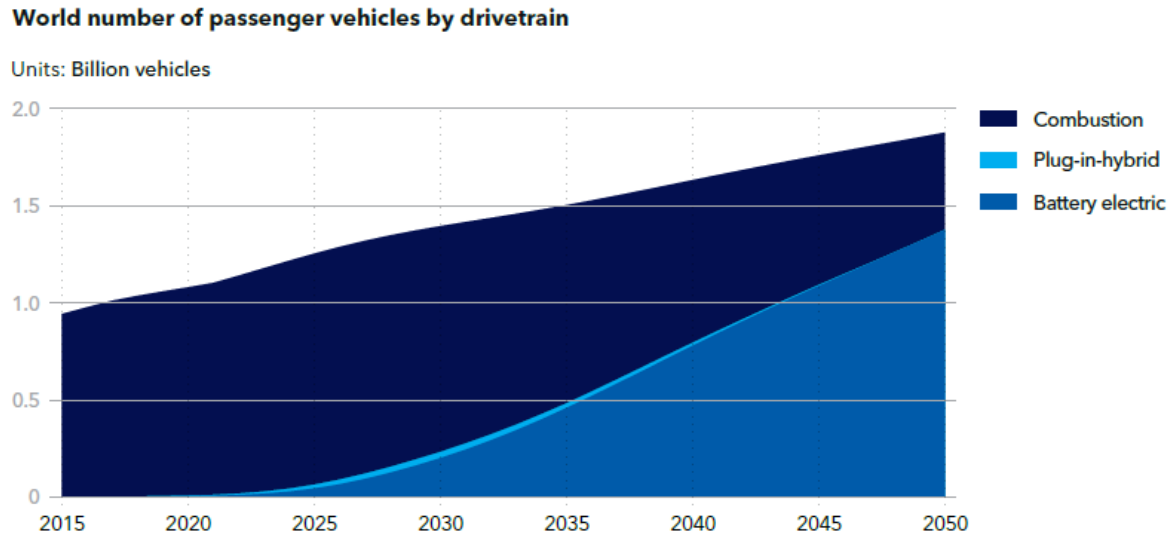

Figure 16: Future dynamic of passenger vehicles in the transportation sector. PHEVs will slowly phase-out and BEVs will become the dominant and only type of EV (DNV GL, 2019).

The annual power load profile of BEVs was retrieved internally from DNV GL (DNV GL, EV hourly capacity profile). The profile has the characteristics of the hourly capacity of BEV over the year, with daily and weekly variations (see Figure 17). By hourly capacity, the profile owner refers to the car's availability per hour for charging or vehicle-to-grid (V2G) purposes, represented as the percentage of cars connected to the grid but are not necessarily actively charging. The profile allows researchers to calculate flexibility services through smart charging. Nevertheless, this report only evaluates the variability and not flexibility measures. The profile still illustrates the activity or charging behaviour of EVs, enabling it to nevertheless be used but must be normalized over the year. In the next step, the normalized profile was scaled-up by multiplying it with the average annual power consumption of all combined BEV existing in the corresponding country. The total annual power consumption of all BEV was calculated according to the following equation:

$$P_{cons.} = Eff._{bat.} * VKT * nr._{BEV} \qquad \textit{Equation 7}$$

$P_{cons.}$ = annual power consumption of total BEV stock [kWh]
$Eff._{bat.}$ = Efficiency consumption value of BEV battery [kWh/km]
VKT = country-specific annual vehicle kilometre travelled [km]
$nr._{BEV}$ = total stock of BEV

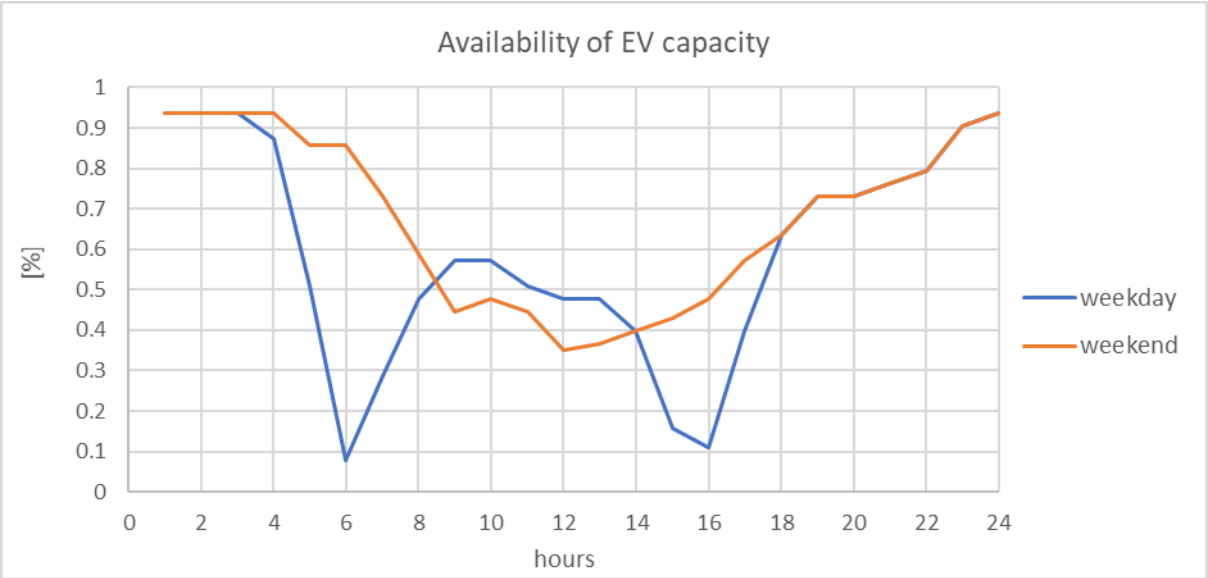

Figure 17: Availability of EV capacity on weekdays and weekends, based on the "hourly capacity profile" from DNV GL (DNV GL, EV hourly capacity profile).

It is assumed that the current (2018) power consumption of full-electric passenger vehicles, such as BEVs, have an averaged demand of 0.189 kWh per kilometre travelled (see Table 5) (ev-database, 2020). This value was retrieved from a database which considers a selection of 93 fully electric vehicles, emphasizing the reliability and data integrity (ev-database, 2020). According to a study conducted in Germany, Sweden, Canada, and the USA, the mean daily vehicle kilometres travelled (VKT) by passenger vehicles is 47.8 km, resulting in an annual travelled distance of 17,447 km (Plötz, Jakobsson, & Sprei, 2017). This amount lies within the range of 15,000 km – 25,000 km travelled, which was the assumed global distance mentioned in the DNV GL report (DNV GL, 2019). Nevertheless, the report by Plötz et al. 2017 emphasizes the high variance of VKT among demographically and geographically distinct regions, which range from 33 km to 57 km of daily VKT. Thus, the current analysis distinguishes VKT between the examined countries (see Table 5). The VKT for the future scenarios (2030 and 2050) is assumed to remain constant, whereas the overall efficiency of a BEV (battery and power train) is expected to marginally increase. Compared to 2018, the average power consumption per BEV is expected to decrease by 6% and 17% for 2030 and 2050, respectively (DNV GL, 2019). This assumption results in average power demand of 0.178 kWh and 0.157 kWh per kilometre travelled for a BEV passenger car in 2030 and 2050, respectively (see Table 5). The total stock of BEV cars varies per country and future expected shares of BEV from the total nation stock of passenger vehicles is based on the region's development according to the ETO database (see Appendix II; Table 10, Table 11, Table 12 and Table 13) (DNV GL, 2019).

Table 5: Characteristation parameters applied in this analsysis of current and future scenarios (2030 and 2050), regarding battery electric vehicle (BEV) and their battery efficiency. The annual vehicle kilometers driven (VKT) varies for each country. (DNV GL, 2019)[1] (ev-database, 2020)[2] (Odyssee-mure, 2020)[3] (iea, 2009)[4] (data.gov.sg, 2018)[5]

Scenario		**2018**	**2030**	**2050**
Battery efficiency [kWh/km]		0.189[2]	0.178[1]	0.157[1]
Country	**Netherlands**	**Italy**	**Egypt**	**Singapore**
VKT [km]	13,024[3]	8,127[3]	24,000[4]	17,500[5]

3.1.8 Generating the Country-specific Decomposed Power Loads

To compose the country-specific annual power load profiles for the three sectors and BEV, the decomposed load profiles have to be adjusted and scaled up with country-specific parameters (see Appendix II; Table 10, Table 11, Table 12 and Table 13). Whereas the same normalized annual load profile for the industrial sector and EVs was used among all countries, the baseload profile for the residential and commercial sector retrieved from Netherlands had to be adjusted to serve as a basis for the other examined countries. Most values for the future scenarios (2030 and 2050) were calculated according to the expected increase or decrease of power demand, according to the regional development retrieved from the ETO database (DNV GL, 2019). The percentages for space heating and space cooling, by heat pumps and AC, correspond to the share values from the total power demand per sector (in 2030: 34% of 37 TWh is used for space heating in the Dutch residential sector, see Appendix II; Table 10). The consumption of power producers and transmission system operators (TSOs) for 2018 was calculated as the difference between the total measured power demand of each country, retrieved from different sources (see Chapter 3.4; data collection), minus the power demand of all sectors. The generated amount was transformed into a percentage of relations from the total power demand of the sectors and used to calculate the power consumption in 2030 and 2050. These percentages of the consumption of power producers and TSOs from the total power demand equal to 6.1%, 1.5%, 13.6%, and 1.9% for Netherlands, Italy, Egypt, and Singapore, respectively.

To create the total power load for 2018, 2030, and 2050, the decomposed profiles were adjusted with the country-specific values for space heating and space cooling for the residential and commercial sectors. The profile of the industrial sector is assumed to remain constant since the variability of the profile is much smaller, compared to the residential and commercial sectors. Nevertheless, the electrification of the industrial and manufacturing process in the future was considered with an increased power demand in 2030 and 2050. The stochastically remainder, defined as total power load per country minus all examined sectors, was used as the load profile for the remaining sectors, such as agriculture and fisheries, and the consumption of power producers and TSOs. Expected future growth factors per each considered sector are based on the ETO report and linked to the region's development and thus, differences among the future power demand between countries can be observed (DNV GL, 2019). Thereby, Italy and Netherlands are based on the European (EU), Egypt on the Middle East and North Africa (MEA) and Singapore on the South East Asia (SEA) expected growth factors. The space heating values for Egypt were averaged between the values of MEA and Sub-Saharan Africa (SSA), because they appeared to be more realistic for Egypt due to its higher average outside temperature than other countries in the MEA region. For example, the average annual temperature in Egypt is 25 °C, compared to the average in the Middle East, which is 20.3 °C (USAID, 2015; AverageWeather, 2020).

The baseload profiles for Egypt and Singapore had to be corrected for daylight-savings time (25.3.2018) because of their constant time zone over the year. Also, a correction factor for differences in the weekend days between Egypt and the other examined countries was applied because the Egyptian weekend is from Friday to Saturday.

3.2 Supply Side Analysis

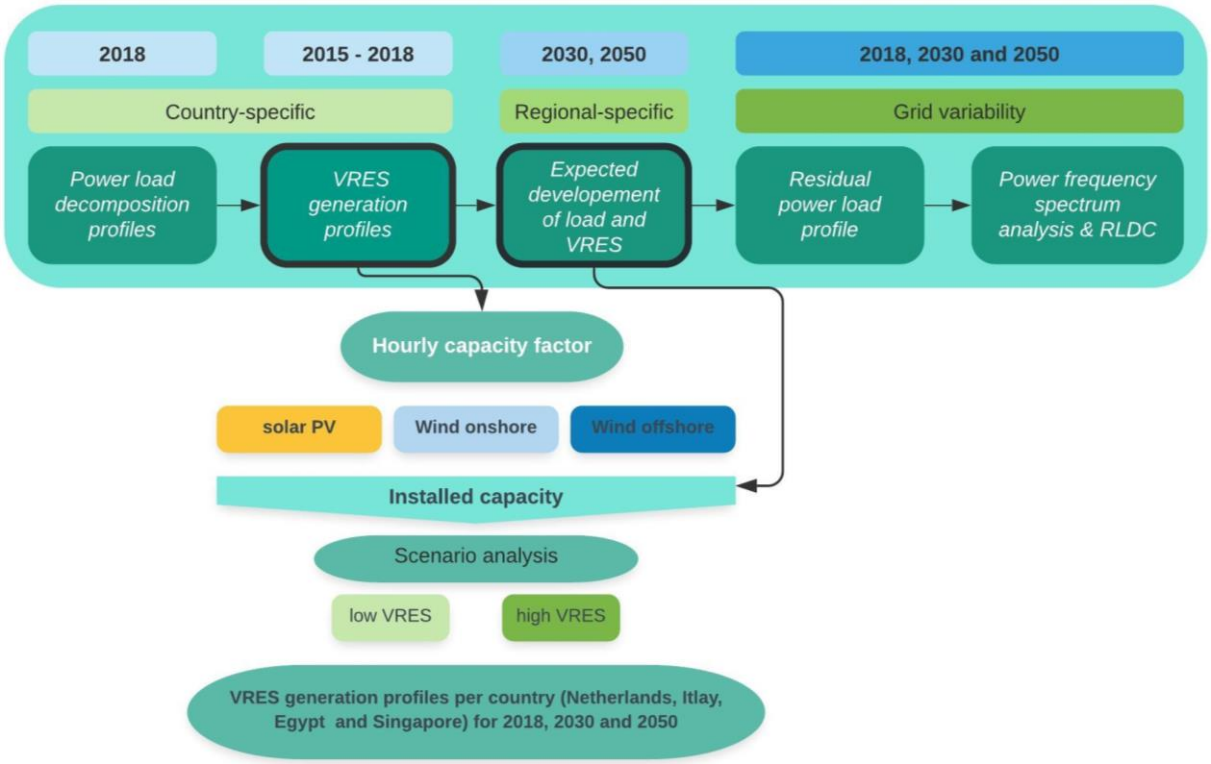

Figure 18: Overview of the supply side analysis including VRES technologies and their hourly capacity factor. (RLDC = residual load duration curve)

Solar PV, onshore, and offshore wind were used as variable renewable energy sources (VRES) in this analysis and represent the supply side of the created model (see
Figure 18). Spatially and geographically distinct regions display vast differences in their solar irradiance and wind speed. Therefore, different supply profiles were generated for each benchmark country of their corresponding region. The hourly supply profiles were retrieved from Renewables.Ninja database and are prolonged over four consecutive years (2015 – 2018) to also include inter-annual variabilities (Pfenninger & Staffell, 2020). The profiles include capacity factors, which are based on local solar irradiance, wind speed, and temperatures. The profiles for the future scenario 2030 and 2050 are also based on the environmental conditions from 2015 -2018 but differ in their capacity factors due to the expected increase in efficiency of the technology.

The database includes more detailed data for European countries and therefore, the capacity factors of VRES for 2018 could directly be retrieved for the Netherlands and Italy. In the case of Egypt and Singapore, the capacity factors can also be generated but one can only select one specific point on the country perimeter (per point function in Renewables.Ninja).

The hourly capacity factors for the scenario 2030 and 2050 for all benchmark countries calculated with the per point function in Renewables.Ninja, because it is assumed that the efficiency of technology will increase making the original existing profiles for Netherlands and Italy irrelevant. The country-specific installed capacity for each scenario, description of the used benchmark solar PV and wind farms (or region), and corresponding averaged capacity factor per technology are illustrated in Appendix II; Table 14, Table 15, Table 16 and Table 17. For the Netherlands and Italy, more country-specific data was available and thus, the 100% RES scenario from e-Highway 2050 served as a database for the 2030 and

2050 scenarios (entsoe, 2013). For Egypt and Singapore, the regional development (MEA and SEA) was used as the expected growth of VRES installed capacity (DNV GL, 2019).

3.2.1 Solar PV

For the 2030 scenario, it is assumed that all solar PV installed power plants are equipped with a one-axis tracking system (azimuth) and display the most suitable country-specific tilt which was retrieved from the Jacobson and Jadhavs report (Jacobson & Jadhav, 2018). For the 2050 scenario, it is assumed that all installed solar PV power plants have an even two-axis tracking system (azimuth and tilt) making them perfectly positioned to absorbed most solar irradiation. In all scenarios, only centralized solar PV farms are considered, neglecting decentralized solar PVs installed on rooftops. It is assumed that the solar PV system losses are 10% and if no tracking or single-tracking is included, that they are always located with an azimuth angle of 180° either southwards or northwards facing for latitudes higher than zero or lower, respectively (Pfenning & Staffell, 2016).

3.2.2 Wind (Onshore and Offshore)

Onshore and offshore wind capacity factors for 2030 and 2050 were generated by assuming that the average onshore and offshore wind turbines for the corresponding scenario display the characteristics seen in Table 6. The wind turbine types selected were based on a study conducted by the Berkeley Lab, which indicates that in 2030 the average onshore wind turbine will have a hub height of 115 m and the ability to generate 3.25 MW, while the average offshore wind turbine will display a hub height of 125 m and a power generation capacity of 11 MW (Wiser, Hand, Seel, & Paulos, 2016). The Renewables.Ninja database allows a selection of different wind turbine types and the ones mentioned in Table 6 display characterizations like the above-mentioned values. The turbine with the greatest capacity that can be selected is the Vesta V164 and is lower than the expected future value.

Table 6: Characteristics of future onshore and offshore wind turbines (Pfenninger & Staffell, 2020).

Parameter	Type	Capacity [MW]	Hub Height [m]
Onshore	Vestas V112	3.3	115
Offshore	Vesta V164	9.5	125

3.2.3 VRES Scenario Analysis

While the demand side of future scenarios (2030 and 2050) was scaled up by the corresponding growth factors, the supply side also considers growth factors of the installed capacity but is divided into a low VRES and high VRES scenario (see Table 7). The values for either scenario are the percentages of the expected country-specific growth factors per VRES technology (based on regional (Egypt and Singapore) or national (Netherlands and Italy) expected development parameters), which can be retrieved from Appendix II; Table 14, Table 15, Table 16 and Table 17 (e.g. solar PV installed for low VRES scenario in NL for 2030: 0.8 * 14.4 GW = 11.5 GW).

Table 7: Characteristics of low and high VRES scenarios for 2030 and 2050, in relation to the country-specific installed capacity values.

Scenarios	Shares from country-specific installed capacity [%]
Low VRES	80
High VRES	120

3.3 Residual Power Load Analysis

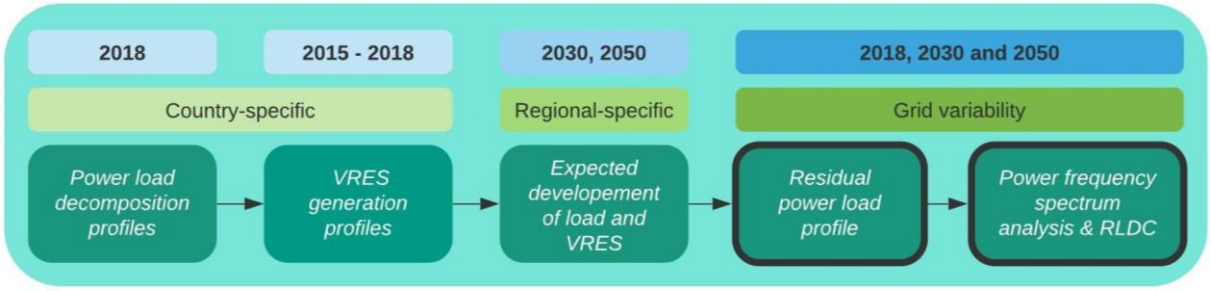

Figure 19: Overview of the residual power load analysis and the resulting examination of the current and future (2030 and 2050) grid variability. (RLDC = residual load duration curve)

Once the summed up total power load profile and VRES generation profile on an hourly basis was identified, the residual power load was calculated to analyse the grid variability of future electrical energy markets per country. The residual power load was calculated according to the following equation (Buttler, Dinkel, Franz, & Spliethoff, 2016):

$$P_{residual}(X) = P_{load}(X) - (P_{Wind}(X) + P_{solar\ PV}(X)) \qquad \textit{Equation 8}$$

$P_{residual}$ = *Residual power load of hour x, [MW]*
P_{load} = *Total power load (demand) of hour x, [MW]*
P_{Wind} = *Onshore and offshore wind generation of hour x, [MW]*
$P_{solar\ PV}$ = *solar PV generation of hour x, [MW]*

The hourly residual power load was also averaged and up-scaled to daily, weekly, and monthly residual power load values to calculate the power and electrical energy variability on different time-cycles (see Figure 20Figure 21).

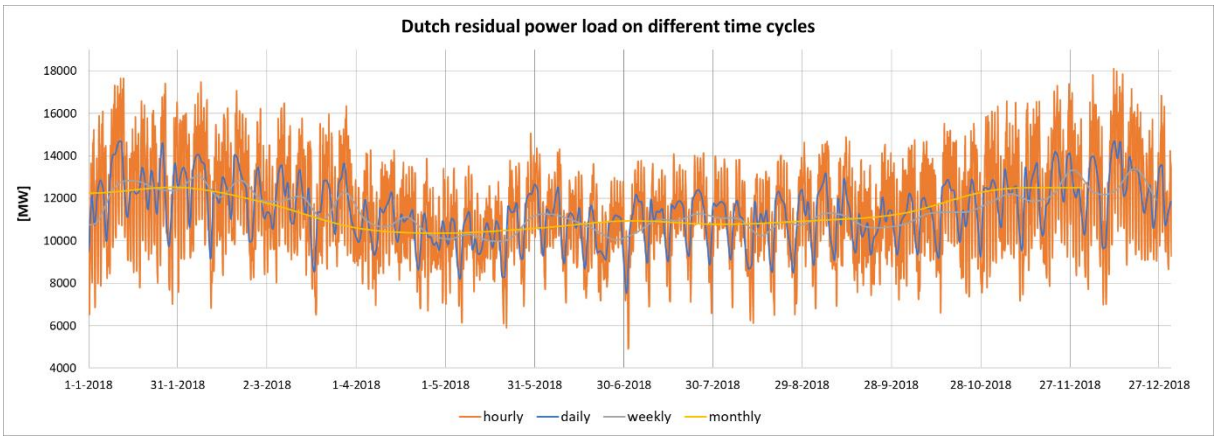

Figure 20: The Dutch residual power load in 2018 on different time-cycles (hourly, daily, weekly and monthly).

3.3.1 Power Frequency Spectrum Analysis

Once the residual power loads for each scenario and benchmark country were realized, with the aid of the generic model, the variability of this residual power load among different time-cycles, by a so-called power frequency spectrum analysis like a Fast-Fourier-Transformation (FFT). Because the time series are discrete, a standard discrete (FFT) method can be applied to examine hourly, daily-, weekly-

and seasonal- cycles in VRES power production, in the power demand and in the corresponding residual load (Gerwen, Eijgelaar, & Bosma, 2020).

In total 17 different time-cycles were considered (see Table 8) and defined as intra-daily (24 hours), weekly (7 days – 10 days), monthly (4 weeks), seasonal (6 – 12 months), and intra-yearly (2 years). The generated model makes use, depending on the analysed time-cycle, of either the hourly, daily, weekly, monthly, or yearly averaged value of the corresponding residual power load (see Table 8). For each time-cycle, the maximum power to be delivered to balance the residual power load (amplitude of a time-cycle) was calculated as well as the total amount of electrical energy which must be charged or discharged by flexibility measures, to smoothen the residual power load (see Figure 21) (Clerjon & Perdu, 2018). The final values are average over the observed time period (2015 – 2018).

Table 8: Considered time-cycles, correspond basis of the residual power load and value used in the graphs illustrated in the result paragraph.

Time-cycles	Basis of residual power load	Value used in result graphs [h]
3 hours	hourly	3
6 hours	hourly	6
12 hours	hourly	12
24 hours (intra-daily)	hourly	24
3 days	daily	72
5 days	daily	120
7 days (weekly)	daily	168
10 days (weekly)	daily	240
2 weeks	weekly	336
3 weeks	weekly	504
4 weeks (monthly)	weekly	672
2 months	monthly	1,460
3 months	monthly	2,190
4 months	monthly	2,920
6 months (seasonal)	monthly	4,380
12 months (seasonal)	monthly	8,760
2 years (intra-yearly)	yearly	17,520

3.3.1.1 Power and Electrical Energy Variability per Time-Cycle

The power and electrical energy variability of the examined time-cycles were calculated according to Equation 9 and Equation 10. It is significant to note that each of the final values are the averaged power and electrical energy variability outcomes over the observation period (2015 – 2018), thus, outliers

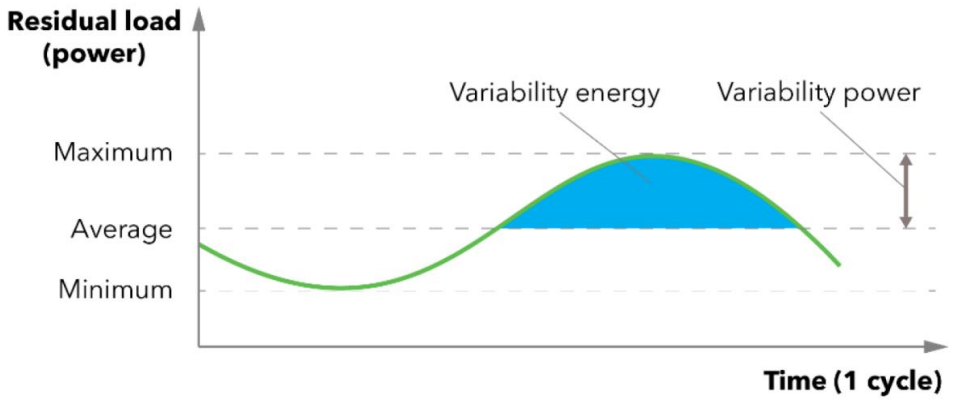

Figure 21: Visualization of the calculated maximum power and electrical energy variability of any given time-cycle (frequency interval) (ten Klooster, 2017).

could have significantly higher values when analysed individually. Nevertheless, the outcome gives a valuable understanding of the averaged variability per each time-cycle. A visualization of the methodology applied to analyse the grid variability can be observed in Figure 21. Thereby, the oscillations of different frequency intervals (examined time-cycles) of the residual power load time series were analysed by a power frequency spectrum analysis similar to a Fourier analysis (Olsen, et al., 2019). The power variability of the residual load in a given time-cycle (frequency interval) was defined as the amplitude of the cycle and calculated according to the following equation (Buttler, Dinkel, Franz, & Spliethoff, 2016):

$V_p(T_x) = (P_{max}(T_x) - P_{min}(T_x))/2$ *Equation 9*

V_p = Power variability, [MW]
P_{max} = Maximum power, [MW]
P_{min} = Minimum power [MW]
T_x = time-cycle (e.g. 7 days) [hours, days, weeks, months, years]

The electrical energy variability of the residual load for a specific time-cycle can be calculated as the inverse Discrete Fourier Transformation (iDFT) where positive. For any frequency interval (examine time-cycle) this results in an integral in units of electrical energy [MWh] which was calculated according to the following equation (Olsen, et al., 2019):

$V_E(T_x) = \sum_{Rn>\overline{Rx}}^{Tx} ((R_n - \overline{R_x}) * t)$ *Equation 10*

V_E = electrical energy variability, [MWh]
R_n = Residual power load at data point n, [MW]
$\overline{R_n}$ = Mean Residual power load over time-cycle x, [MW]
t = duration of the selected time unit (day, week, month or year) in hours [h]
T_x = time-cycle (e.g. 7 days) [hours, days, weeks, months, years]

3.3.2 Residual Load Duration Curve (RLDC)

The previously mentioned power and electrical energy variability equals the value needed to balance the supply and demand, thus flattening the residual power load. This variability does not apply if the amount must be charged or discharged (with flexibility measures) to the power grid. Nevertheless, it gives advice on the flexibility capacity needed for each time-cycle. The RLDC, on the other hand, indicates how much annual power surplus there is among each examined scenario. Thereby, the RLDC is the residual load curve sorted from highest to lowest value displaying the amount of time the residual load is positive (discharging needed from dispatchable source) or negative (charging needed in energy storage for instance). This methodology gives a broad insight into how much power generation or storage capacity is required but without including time-cycles (Gerwen, Eijgelaar, & Bosma, 2020). The RLDC also can give approximations about the required installed capacity of each dispatchable power generation technology based on the merit order system from base-generation (e.g. coal) to peaking generation (e.g. natural gas) (see Figure 22).

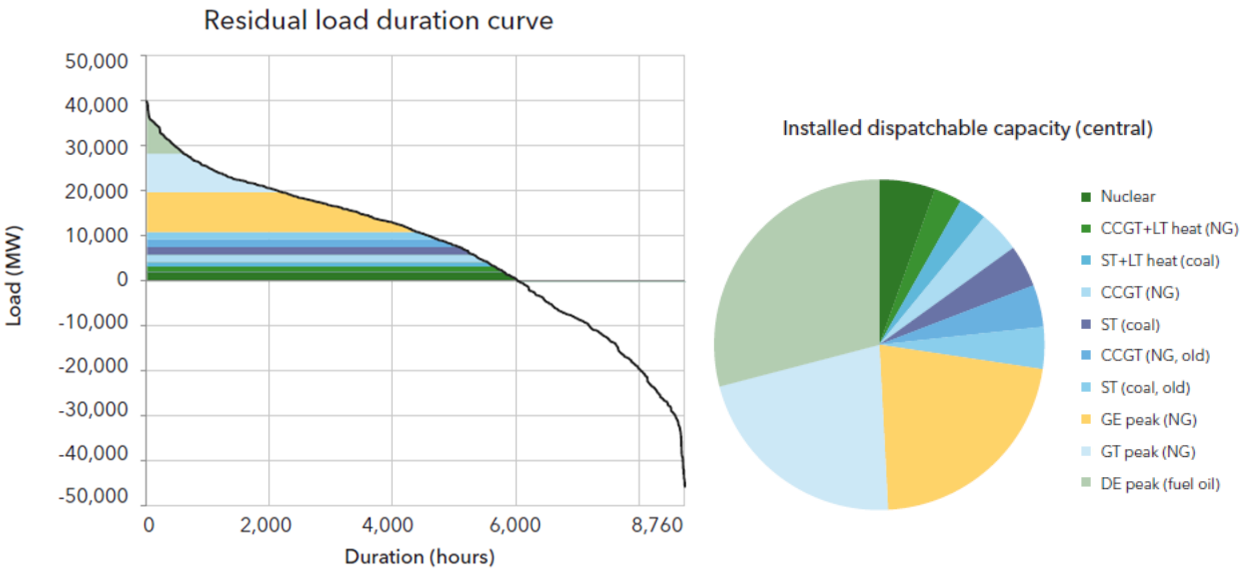

Figure 22: Residual load duration curve (RLDC) and remaining dispatchable power demand according to the merit order in a scenario for Europe in 2050 (Gerwen, Sun, Eijgelaar, Bosma, & Dugstad, 2018). (GT = gas turbine, GE = gas engine, ST = steam turbine, CCGT = combined cycle gas turbine, NG = natural gas, LT = low temperature heat generation)

3.4 Data Collection Summary

All climate-related data, such as outside temperatures, solar PV, and wind capacity factors, were retrieved from the software database Renewables.Ninja (Pfenninger & Staffell, 2020). The report of Gelaro et al. 2017 describes the methodology and structure of the database. The annual total power load for each examined country was retrieved from different sources but should represent measured and realistic hourly data. The total power load from the Netherlands and Italy was retrieved from ENTSO- E (entsoe, 2018). The total power load from Egypt was established from a DNV GL internal database (DNV GL, 2014) and the one from Singapore from an energy market company (EMC, 2018). These total power loads were used to calculate the stochastically remainder (total load minus each sector) for each benchmark country. The load profiles for the sectors residential, commercial, and industrial as well as space heating and DHW were calculated based on NEDUs forecast profiles of different connection capacities (NEDU, 2018).

4. VALIDATION

4.1.1 Demand Profile Validation

The residential and commercial load profiles are based on Dutch and Indian datas (see Chapter 3.1) but the final profiles were validated with measured load profiles in Egyptian households and Malaysian businesses for the residential and commercial sector, respectively. The industrial sector was validated with a Danish profile and the total load profile was validated for the German power market by comparing measured data with generated once (according to the methodology of this report).

4.1.1.1 Residential Sector

The residential load profile was validated based on the Egyptian profile because a report analysed daily load profiles in Egyptian households (Attia, Evrard, & Gratia , 2012). The calculated profiles and the once retrieved from the other report are visualized in Figure 23, divided into average, summer, and winter profiles. The overall profile looks similar, with a small morning peak and a significant evening peak with a gradual increase over the day. During the night the consumption is still quite high for both profiles, due to AC. Both profiles display significant differences between summer and winter months, as a result of the increased power demand for space cooling and almost no demand for space heating in hot climate regions, such as Egypt. Overall, the calculated residential profile fits quite well with the measured profile. However, the calculated summer profile displays a higher peak in the morning hours, caused by the morning peak demand for space cooling in the Indian profile (see Figure 15).

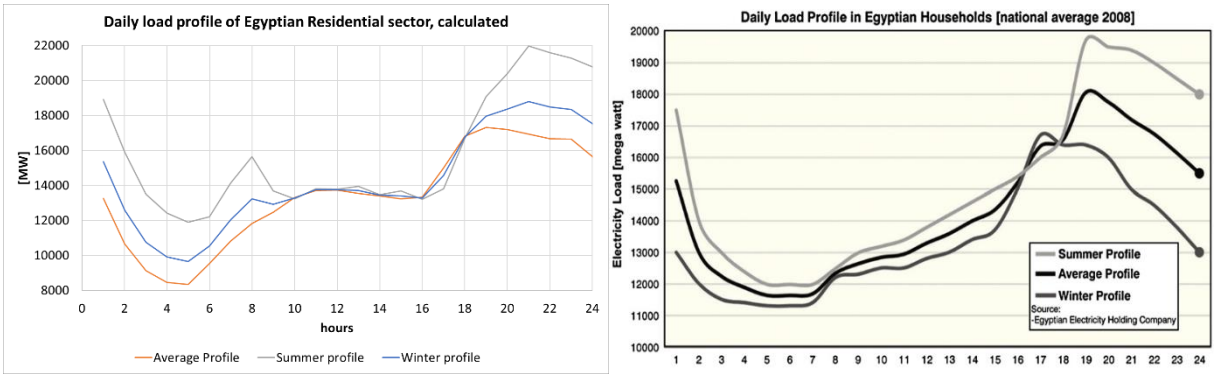

Figure 23: Validation of the residential sector, based on Egypt (Attia, Evrard, & Gratia , 2012)

4.1.1.2 Commercial Sector

The calculated profile for the commercial sector of Singapore was validated with a measured profile from the neighbouring country of Malaysia (Ponniran, Mamat, & Joret, 2012). The profile retrieved from a study is based on a single business unit that explains the low power consumption (see Figure 24). Nevertheless, the profile can be compared with the normalized calculated profile from Singapore. Both profiles display peaks during the day, when people are at work and thus, business consuming power. Before and after work hours the power consumption significantly declined for both profiles. The peak-demand is at 12:00 and 14:00 for the calculated and measured profile, respectively. The disparities could result from the measured profile, which had a considerably lower dataset (only one) and thus, could differ from the average.

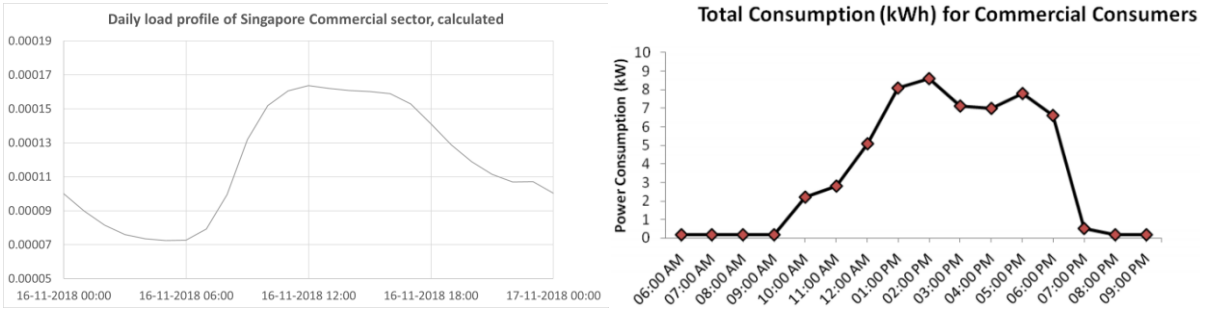

Figure 24: Validation of the commercial sector, based on Singapore (calculated profile) and Malaysia (retrieved from report) (Ponniran, Mamat, & Joret, 2012)

4.1.1.3 Industrial Sector

The Danish public enterprise Energinet, responsible for operating and developing the power transmission system, recently uploaded some hourly profiles for certain industries (energinet, 2020). The profile of the Danish chemical industry was applied to validate the calculated industrial profile from the current analysis (see Figure 25). Both profiles display significantly lower amplitude compared to the residential and commercial sectors, with smaller power peaks during daytime. In both profiles, the weekly cycles are visible. The measured profile from the Danish chemical factor does not reduce production as much during the night-time as seen in the calculated one. An explanation could be that the chemical industry has a substantially greater amount of operation hours (8,304 hours per year) compared to other businesses in the industrial sector (Mwanza & Mbohwa, 2015).

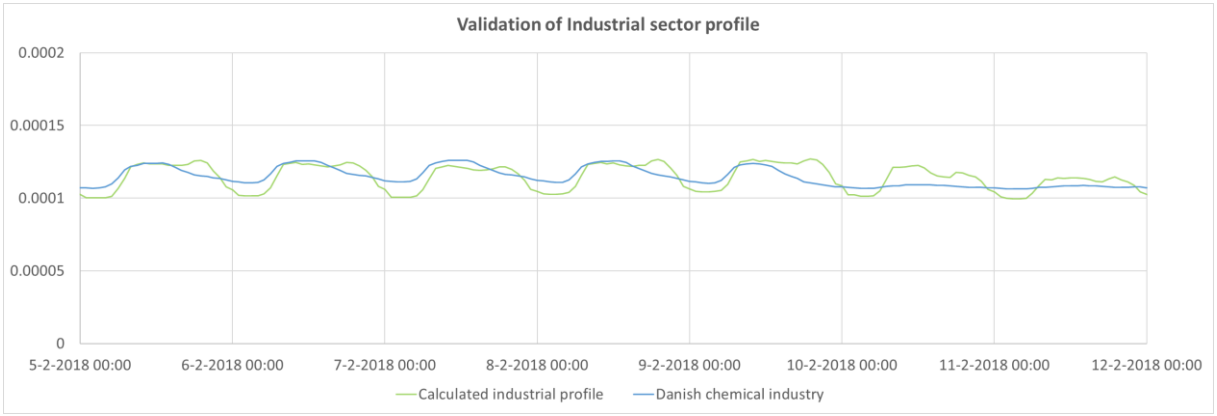

Figure 25: Validation of calculated industrial sector profile with measured profiles from the Danish chemical industry (energinet, 2020).

4.1.1.4 Total Power Load Profile

The total load profile of Germany was generated, by combining all sectors according to the methodology of the current analysis (see Chapter 3). The profile was subsequently compared with the actual measured load profile (see Figure 26), retrieved from ENTSO-E (entsoe, 2018). Both profiles have a similar daily and weekly pattern, although the calculated profiles display a slightly decreased power demand during the daytime. This could be explained by the fact that the generated model calculates the power demand profiles based on the benchmark country, the Netherlands, and thus, power consumption profiles for certain sectors (e.g. commercial) may vary for other countries.

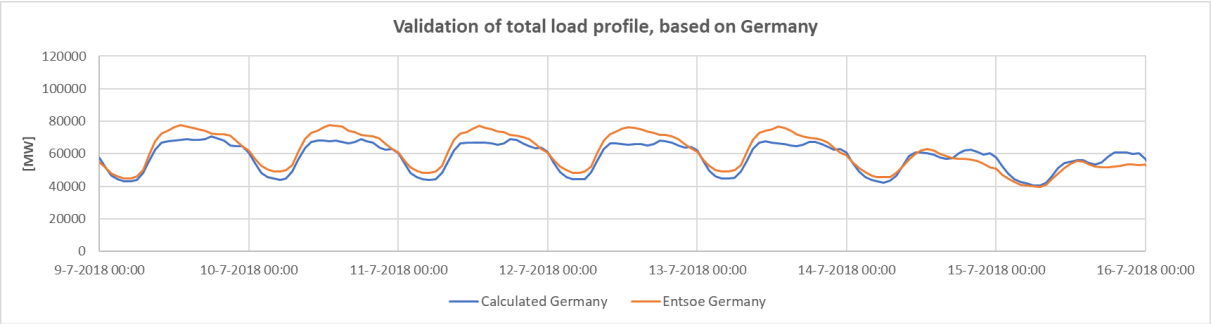

Figure 26: Validation of total load profile (demand side), based on Germany in 2018 (entsoe, 2018)

4.1.2 Power Frequency Spectrum Validation

The statistical software MATLAB was employed to validate the generic model, which analyses the power variability of residual loads, by examining its power frequency spectrum. The Fourier theory explains that even complex waveforms, such as a time series dataset (residual loads), can be described by different sinusoidal signals. This statistical test analyses the frequency and amplitude of the sines and cosines, which can have valuable insights into the fluctuation behaviour or variability of the original waveform (residual power load) (van Winden, 2018). Whereas the discrete Fourier transformation (DFT) transforms the signal into a frequency spectrum, the inverse discrete Fourier transformation (iDFT) changes the frequency domain back to a time domain, which facilitates the interpretation of the amplitude into specific time-cycles. The Fast Fourier Transformation (FFT) was performed due to the considerable amount of equations with high calculation times of the DFT (van Winden, 2018). MATLAB was used as statistical software instead of Excel which is limited to 4,096 samples for the FFT function. DNV GL used a similar methodology to examine power demand cycles by using a frequency spectrum analysis also based on FFT (Gerwen, Eijgelaar, & Bosma, 2020).

In Figure 27, the frequency spectrum analysis calculated in MATLAB and with the aid of the generated model for the current Egyptian power market are visualized based on the residual power load of 2018 (see Appendix IV; Figure 67/Figure 68 for the Netherlands and Italy). For Egypt, the same time-cycle peaks can be observed from both graphs (see Figure 27). The largest peak is exactly at 24 hours, representing the daily cycle. A second peak can be seen around hour 8,760, which illustrates the seasonal power demand cycles. Whereas the positions of the peaks correlate well with those calculated in MATLAB, the amplitudes (MW) are slightly lower when running the statistical test in MATLAB. This may have occurred because when using MATLAB, the frequency peak can leak part of its amplitude value to neighbouring frequencies, which slightly spreads the peak and thus, lowers the maximum peak. The generated model of the current analysis, examines the frequency spectrum of each time-cycle on its maximum and minimum values (see Equation 9) which can lead to higher amplitudes, especially if, for example, there are extreme values in one specific hour. Also, the plots for the Netherlands and Italy display similar time-cycles (frequencies) (see Appendix IV; Figure 67 and Figure 68). The MATLAB code can be retrieved from Appendix VI.

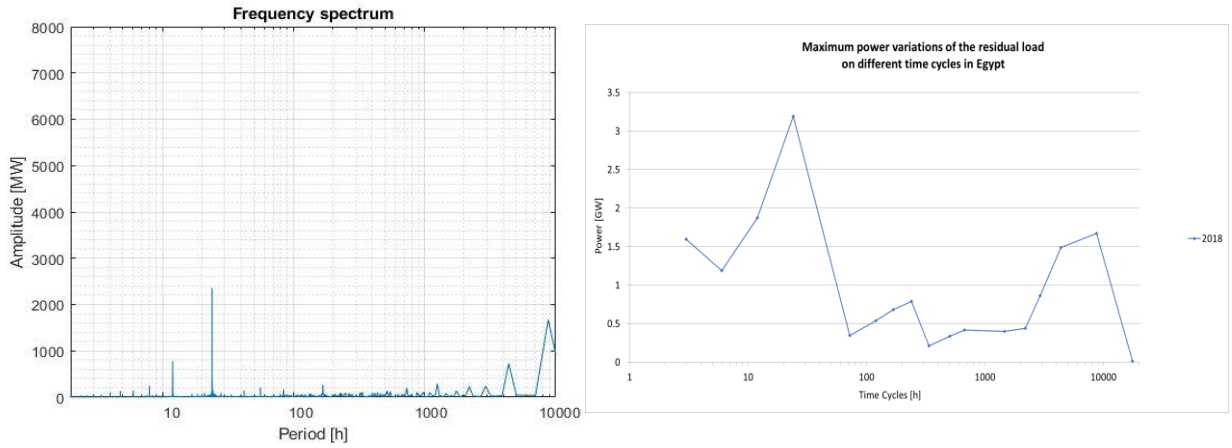

Figure 27: Power frequency spectrum calculated in MATLAB (left) and generated model (right) for Egypt in 2018.

5. RESULTS

5.1 Scenario Definition

A summary of the applied scenarios for each examined country is illustrated in Table 9. In 2030 and 2050 two scenarios were analysed, a low VRES and high VRES scenario (see Chapter 3.2.3). The low VRES scenario equals to 80% and the high VRES to 120% of the foreseen installed VRES capacity in 2030 and 2050. The demand side of the power systems is assumed to be the same for both scenarios and calculated according to the expected development of future power demand (see Appendix II; Table 9, Table 10, Table 11, Table 12 and Table 13). The following results are all based on the country-specific residual power loads in 2018 and, for the future (2030 and 2050), according to a low and high VRES scenario of each examined country (see Table 9). Thus, in total five scenarios were analysed per country.

Table 9: Overview of all scenarios included in this study for the year 2018, 2030 and 2050. Low VRES scenairo 80%/high VRES scenario 120% of anticipated installed VRES capacity in 2030 and 2050 per examined country (see Appendix II; Table 14, Table 15, Table 16 and Table 17).

Scenarios	**2018**	**2030**		**2050**	
Netherlands, Italy, Egypt and Singapore	Current installed VRES	Low VRES	High VRES	Low VRES	High VRES

5.2 Power Frequency Spectrum Analysis

5.2.1 Netherlands (Northern Europe)

The generated power frequency spectrum analysis of the Dutch residual power load, among all scenarios for high VRES and low VRES for 2030 and 2050, is illustrated in Figure 28. It is predicted that the shares of VRES in the power mix are increasing in the future and therefore the power variability of the residual load is directly affected and power variations of low and high VRES scenarios in 2030 and 2050 are significantly increased (see Figure 28). Among all scenarios, there are two peaks visible which are significantly larger than others at the intra-daily time-cycle (24 hours) and at the 10 days (240 hours) time-cycle representing the weekly cycles. The intra-daily power variability increases from 2.5 GW in 2018 to 6.4 GW and 9.8 GW for the high VRES scenario in 2030 and 2050, respectively. The weekly maximum power displays similar behaviour to the intra-daily time-cycle, inclining from 1.7 GW in 2018 to 7 GW in 2030 and 10.6 GW in 2050, for the high VRES scenario. The seasonal power variability (12-month time-cycle; 8,760 hours) increases from 1.2 GW in 2018 to 2.7 GW/3.5 GW and 3.3 GW/4.4 GW for the low and high VRES scenario in 2030 and 2050, respectively. The intra-yearly power variability (17,520 hours) is only 0.5 GW for the high VRES scenario in 2050.

Inactive sleeping hours and working vs. non-working hours can be one explanation for the variability peaks on daily and weekly time-cycles. Another explanation is, that with increasing shares of solar PV and due to its diurnal power generation cycle, the intra-daily power variations is enhanced while the increase in wind power affects the weekly and seasonal power variation more (see power frequency spectrum of VRES in the Netherlands; Appendix V; Figure 69 and Figure 70). It is foreseen that in 2030 and 2050 the installed onshore and offshore wind capacity will be larger than the installed solar PV. It is also anticipated that the VRES power supply will be dominated by wind and will also be influenced by its higher capacity factor compared to solar PV (see Appendix II; Table 14). This also explains the noticeable peaks in the power variability on weekly and seasonal time-cycles for the future scenarios 2030 and 2050, triggered by installed wind capacity (see Figure 28).

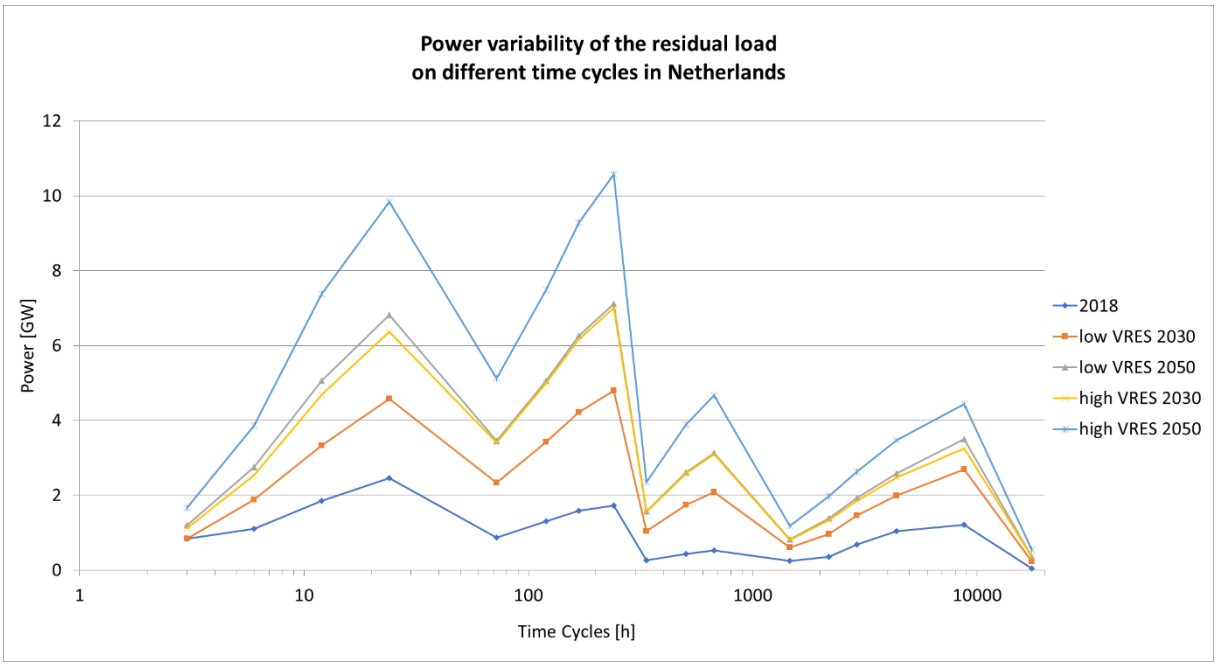

Figure 28: Power variability of the residual power load on different time-cycles in Netherlands, averaged values over the observed time-period (2015 – 2018), see Table 8 for detailed description of applied time-cycles and corresponding amount of hours on the horizontal axis.

The electrical energy variability (power over time in GWh), increases among all time-cycles because more power can be generated over a longer duration (see Figure 29). If more VRES is installed, the electrical energy variability per each time-cycle is enhanced, and thus, more charge or discharge capacity (e.g. storage) is needed to balance out the grid. The intra-daily (24 hours) flexibility capacity increases from 17 GWh in 2018 to 45 GWh and 66 GWh in 2050 for the low and high VRES scenario, respectively (see Figure 29). The flexibility required on a weekly scale result in up to 451 GWh and 673 GWh for the high VRES scenario in 2030 and 2050, respectively. The seasonal storage in 2050 for

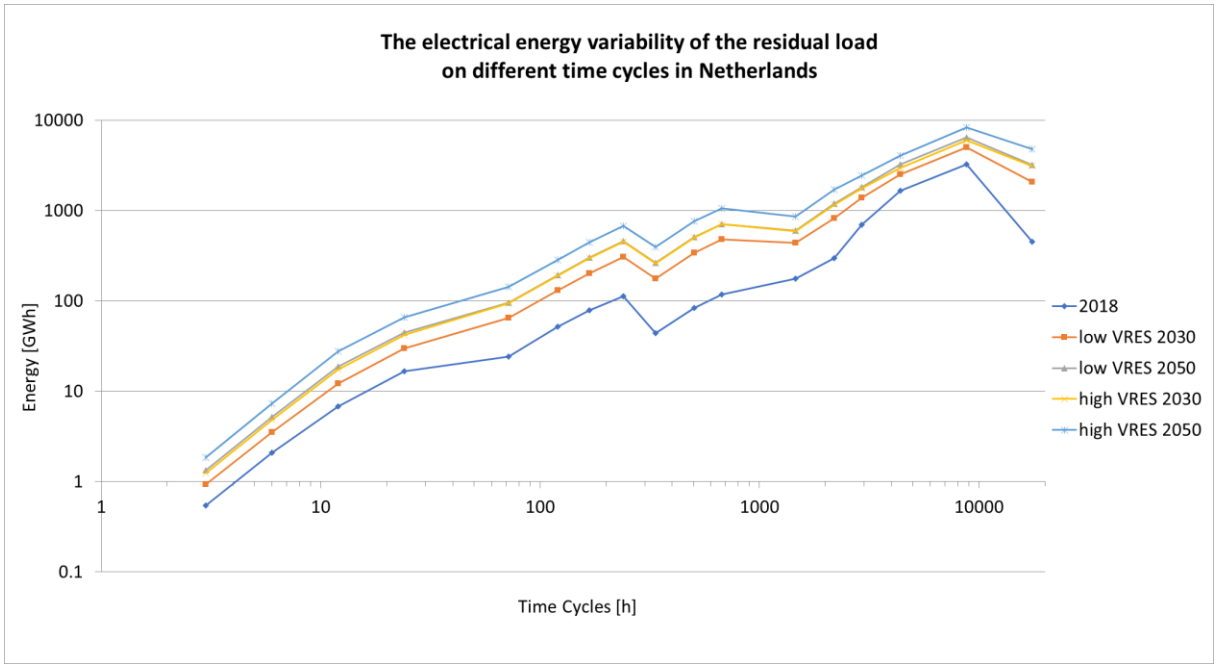

the Figure 29: Electrical energy variability of the residual power load on different time-cycles in the Netherlands, averaged values over the observed time-period (2015 – 2018), see Table 8 for detailed description of applied time-cycles and corresponding amount of hours on the horizontal axis.

high VRES scenario in Netherlands requires a capacity of 8,271 GWh, in case no other storage or flexibility measures are applied to smaller time-cycles. The intra-yearly (17,520 hours) electrical energy variability is smaller than the seasonal variation among all scenarios with a required electrical energy capacity of 4,769 GWh for the high VRES scenario in 2050.

5.2.2 Italy (Southern Europe)

The intra-daily power variability of the residual power load in Italy displays the highest peaks among all time-cycles, with up to 40 GW for the high VRES scenario in 2050. Expectations for the Italian power market predict that installed VRES capacity will be dominated by solar over wind (see Appendix II; Table 15), causing the large values for intra-daily power variability of up to 40 GW for the high VRES scenario in 2050 (see Appendix V; Figure 72). The weekly variation has a maximum power value of 13 GW and 20 GW (at time-cycle 10 days) in the high VRES scenario in 2030 and 2050, respectively (see Figure 30). The time-cycles based on weekly averages demonstrate the overall second smallest, after intra-yearly, power variability of only 6.4 GW for the high VRES scenario in 2050 based on a 3-week time-cycle (see Figure 30). The seasonal power variability (12-month time-cycle; 8,760 hours) increases from 3.5 GW in 2018 to 7.9 GW and 11.3 GW for the high VRES scenario in 2030 and 2050, respectively. The intra-yearly power variability is only 1.7 GW for the high VRES scenario in 2050.

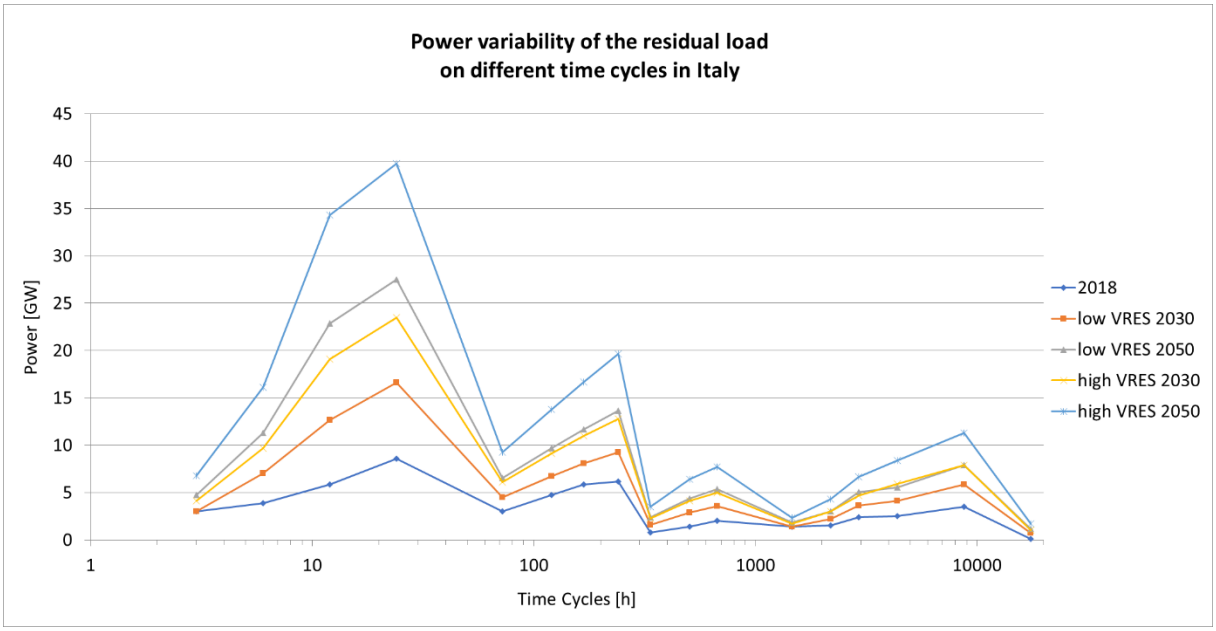

Figure 30: Power variability of the residual power load on different time-cycles in Italy, averaged values over the observed time-period (2015 – 2018), see Table 8 for detailed description of applied time-cycles and corresponding amount of hours on the horizontal axis.

The charge or discharge flexibility capacity required in the future power grid of Italy is illustrated in Figure 31. A gradual increase in electrical energy variability among larger time-cycles can be observed and the highest variation occurs on the 12-month time-cycles (8,760 hours), of 25,464 GWh for the high VRES scenario in 2050, which represents the seasonal differences of the residual power load. The intra-daily (24 hours) flexibility capacity increases from 54 GWh in 2018 to 205 GWh and 310 GWh in 2050 for the low and high VRES scenario, respectively (see Figure 31). The flexibility electrical energy required to balance the grid on a weekly scale result, in 778 GWh and 1,181 GWh for the high VRES scenario in 2030 and 2050, respectively. Again, the intra-yearly (17,520 hours) electrical energy variability is smaller than the seasonal variation among all scenarios.

The daily electrical energy variability of the residual power load for the high VRES scenario in 2050 results in 4.6-times higher variation (310 GWh) compared to the Netherlands, influenced by 2.7-times more installed non-dispatchable VRES capacity which is dominated by solar PV (101 GW solar PV; 41 wind; see Appendix II; Table 15).

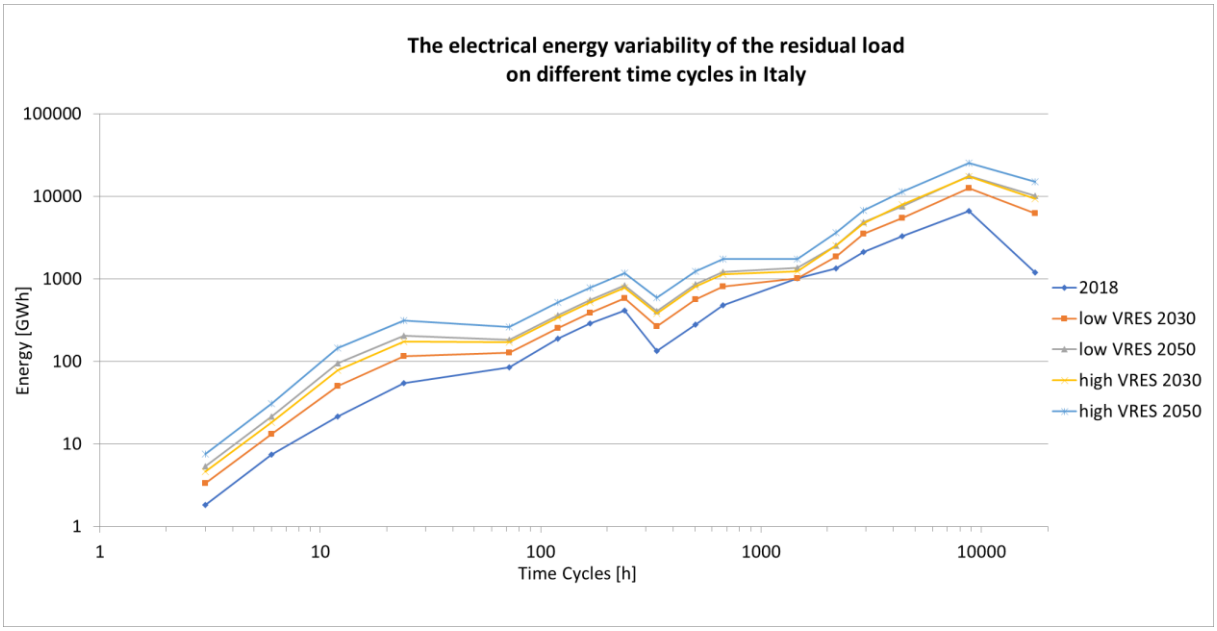

Figure 31: Electrical energy variability of the residual power load on different time-cycles in Italy, averaged values over the observed time-period (2015 – 2018), see Table 8 for detailed description of applied time-cycles and corresponding amount of hours on the horizontal axis.

5.2.3 Egypt (Middle East and North Africa MEA)

The power frequency spectrum analysis of Egypt with power variability and electrical energy variability is illustrated in Figure 32 and Figure 33. The intra-daily power variability (time-cycle of 24 hours) dominates with 28 GW and 40 GW for the low and high VRES scenario in 2050, respectively. The weekly and seasonal power variability, on the other hand, display significantly smaller values (see Figure 32). The weekly variation has its highest peak at the 10-day time-cycle (240 hours) ranging from 0.7 GW in 2018 to 6.7 GW and 9.7 GW in 2050 for the low and high VRES scenario, respectively. The seasonal power variability (12-month time-cycle; 8,760 hours) increases from 1.7 GW in 2018 to 3.2 GW and 5.3 GW for the high VRES scenario in 2030 and 2050, respectively. The intra-yearly power variability represents the overall smallest power variability with only 0.4 GW for the high VRES scenario in 2050. Further, the time-cycles based on weekly averages demonstrate the second smallest power variability ranging from 0.3 GW in 2018 to 3.5 GW in 2050 for the high VRES scenario, based on a 3-week time-cycle.

Overall, there is a significant gap between the scenarios from 2030 and 2050, especially on intra-daily power variability (see Figure 32). The reason for this phenomenon could be explained by the fact that the Egyptian total power demand in 2050 is anticipated to increase 2.4-fold compared to 2018. Simultaneously, predictions regarding VRES generation foresee a significant increase from 9.7% to 55.8% of the total power generation in 2030 and 2050, respectively (DNV GL, 2019). As a direct consequence, the power grid for 2050 has significantly higher installed capacity of VRES (see Appendix II; Table 16) and thus, adds more variability to the power system. An explanation of the dominant variability peak on intra-daily time-cycle is that in 2050 the installed capacity of solar PV in Egypt is expected to be 2.6 times larger than installed wind, both onshore and offshore combined, 75 GW and 29 GW, respectively. Considering that the capacity factors of both VRES technologies differ, the shares from the total

power generation equal to 31% and 25% for solar PV and wind, onshore and offshore, respectively (DNV GL, 2019). The daily maximum power generation variability of solar PV is significantly higher (32 GW: high VRES 2050) in comparison to the maximum power generation variability for wind which displays peaks on weekly and seasonal time-cycles (range of 1.8 – 8.5 GW: high VRES 2050) (see Appendix V; Figure 73 and Figure 74). Whereas the solar PV generation in the Netherlands and Italy, aside from the dominant daily cycles, shows a seasonal cycle in the power variation, the Egyptian solar PV production does not have significant seasonality (see Appendix V; Figure 70, Figure 72, and Figure 74). As a result of the aforementioned factors, the weekly and seasonal variations are significantly smaller than the intra-daily variations.

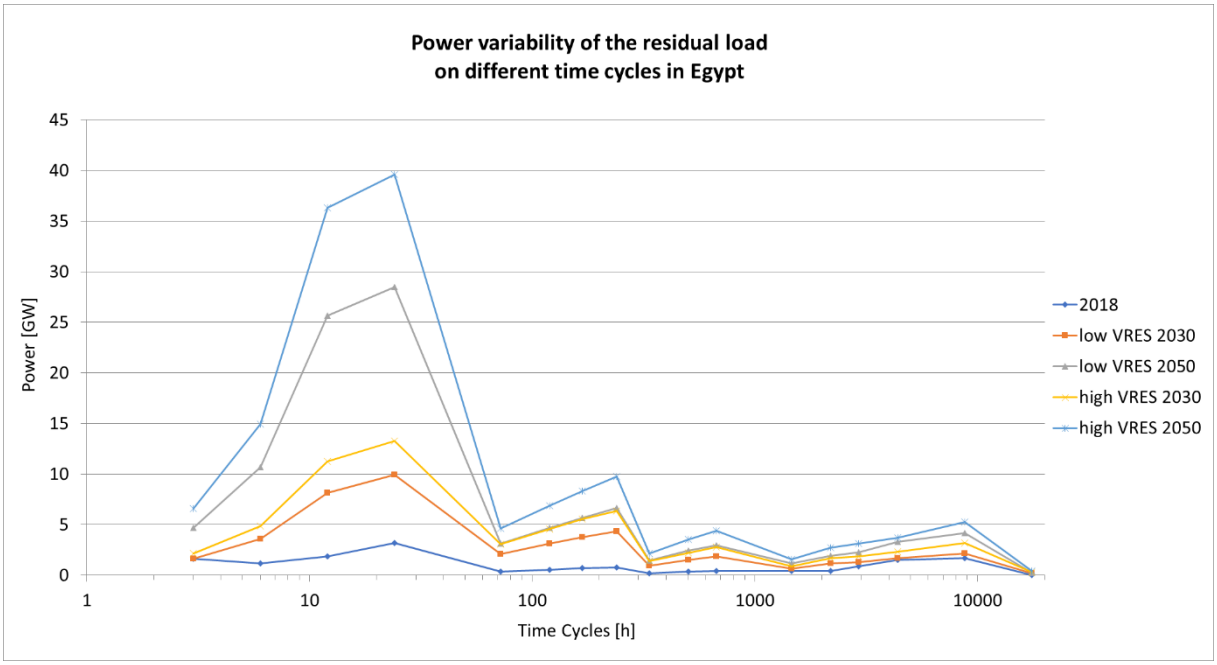

Figure 32: Power variability of the residual power load on different time-cycles in Egypt, averaged values over the observed time-period (2015 – 2018), see Table 8 for detailed description of applied time-cycles and corresponding amount of hours on the horizontal axis.

The power variation output over time, defined as electrical energy variability, among all scenarios regarding the Egyptian power market is illustrated in Figure 33. The intra-daily variation of the Egyptian power market in 2050 requires 249 GWh and 357 GWh as flexibility capacity to balance out the variability below a time-cycle of one day, considering the low and high VRES scenarios, respectively. In 2030 the electrical energy variability is decreased, resulting in 75 GWh and 105 GWh for low and high VRES scenarios. All future scenarios display significantly larger intra-daily values than the current one (2018) of 19 GWh which is equal to only 5% of the electrical energy variability in 2050 for the high VRES scenario. The seasonal electrical energy variability illustrates smaller discrepancy compare to the intra-daily and weekly time-cycle variation, among all future scenarios (see Figure 33). The seasonal variation ranging from 5,222 GWh in 2018 to 9,721 GWh in 2050 for the high VRES scenario. Further, the intra-yearly (17,520 hours) electrical energy variability is smaller than the seasonal variation among all future scenarios (low and high VRES in 2030/2050).

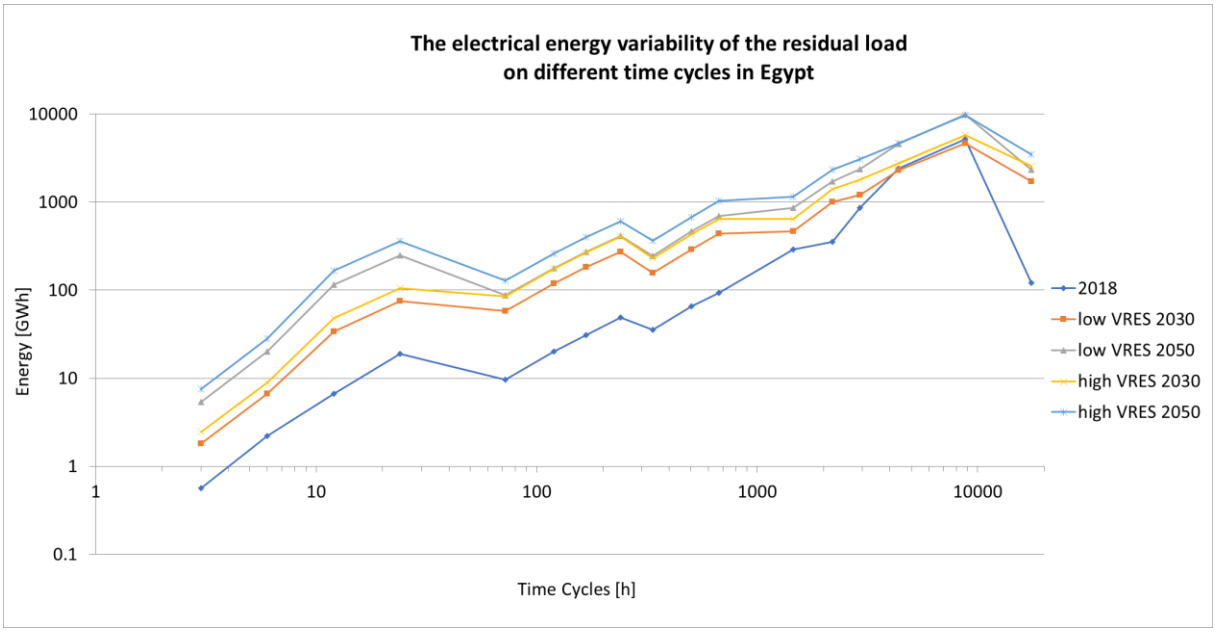

Figure 33: Electrical energy variability of the residual power load on different time-cycles in Egypt, averaged values over the observed time-period (2015 – 2018), see Table 8 for detailed description of applied time-cycles and corresponding amount of hours on the horizontal axis

5.2.4 Singapore (South East Asia SEA)

The power frequency spectrum analysis of the Singaporean power market divided into power variability and electrical energy variability is visualised in Figure 34 and Figure 35. Overall, the power variability of the Singaporean residual load is significantly larger in 2050 compared to 2030 for the low and the high VRES scenario. Again, this discrepancy is triggered by the expected regional development in the SEA region, which suggests that the shares of non-dispatchable VRES form the total power supply will increase significantly from 6.6% in 2030 to 55.7% in 2050. Concurrently, the total power demand is anticipated to increase by 3.2-fold between 2018 and 2050 (DNV GL, 2019). The peak power variability occurs at intra-daily time-cycles (24 hours) with values of 8.3 GW and 11 GW in 2050 for the low and high VRES scenario, respectively (see Figure 34). This is influenced by the fact that solar PV is expected to be the dominant VRES power source in SEA with a share of 35% from the total power supply whereas the combined wind power, onshore and offshore, is expected to contribute 20% to the power supply (DNV GL, 2019).

The weekly power variability displays the highest peaks at the 10-day time-cycle (240 hours) with a range from 0.3 GW in 2018 to 2.5 GW and 3.5 GW in 2050 for the low and high VRES scenario, respectively. While the variation based on weekly averages results in smaller values compared to intra-daily and weekly time-cycles, the seasonal power variability (12-month time-cycle; 8,760 hours) equals to higher power variation than on a weekly time-cycle with a peak value of 4.2 GW in 2050 for the high VRES scenario (see Figure 34). The fairly high seasonality is a different behaviour than observed in the Dutch, Italian, or Egyptian future power systems (see Figure 28, Figure 30, Figure 32, and Figure 34). Whereas the power supply profile of wind for the Netherlands, Italy, and Egypt display their largest variability peaks on weekly time-cycles, the Singaporean wind generation curve results in a larger variation on seasonal time-cycles (see Appendix V; Figure 69, Figure 71, Figure 73, and Figure 75). This explains the overall higher variation of the residual power load of seasonal over weekly time-cycles in the future power market of Singapore (see Figure 34). Like the previously examined country-specific power frequency spectrum analysis, the intra-yearly (17,520 hours) power variability represents the overall smallest power variability with only 0.3 GW for the high VRES scenario in 2050.

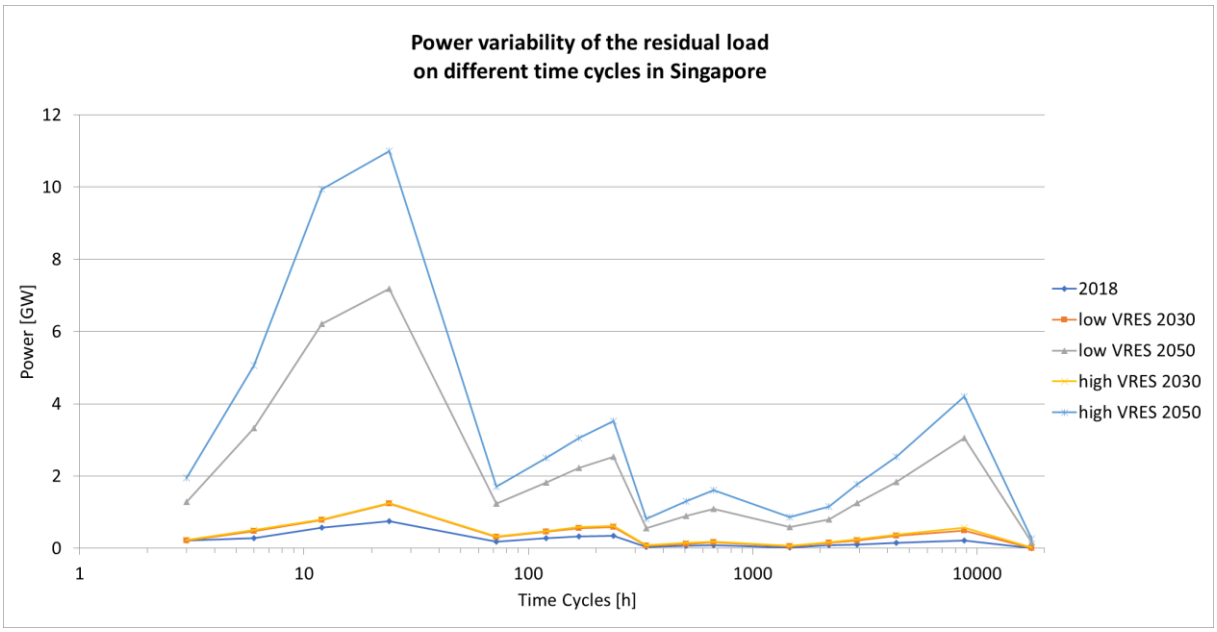

Figure 34: Power variability of the residual power load on different time-cycles in Singapore, averaged values over the observed time-period (2015 – 2018), see Table 8 for detailed description of applied time-cycles and corresponding amount of hours on the horizontal axis.

Like the power variation, the electrical energy variability of the Egyptian power market displays significantly different values between the year of 2030 and 2050 for either scenario, the low and high VRES (see Figure 35). On 24 hours' time-cycle (intra-daily), the flexibility electrical energy capacity required for the low and high VRES scenario in 2050 results in 48 GWh and 77 GWh, respectively, whereas the low and high VRES scenarios in 2030 lead to an electrical energy variability of 8.3 GWh for either scenario. The weekly electrical energy variability ranges from 153 to 214 GWh for the same scenarios. The flexibility electrical energy required to balance the power grid on a weekly time-cycle result, in 41 GWh and 147 GWh for the high VRES scenario in 2030 and 2050, respectively. The electrical energy variability on a seasonal scale (12-month time-cycle; 8,760 hours) equals to a range from 505 GWh in 2018 to

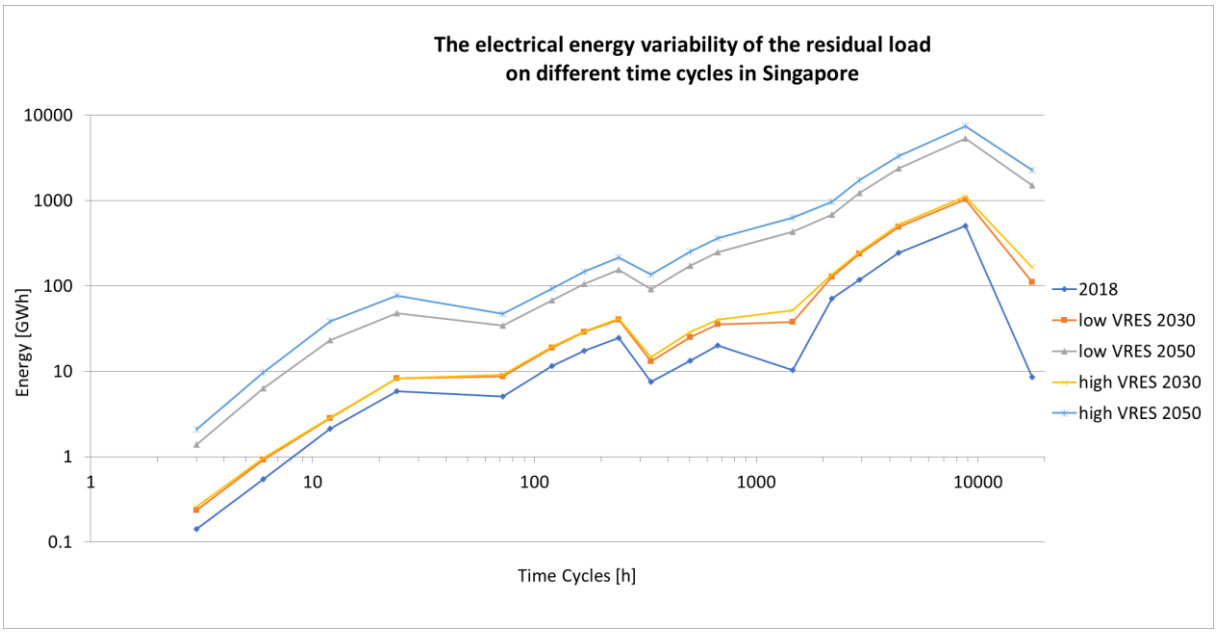

Figure 35: Electrical energy variability of the residual power load on different time-cycles in Singapore averaged values over the observed time-period (2015 – 2018), see Table 8 for detailed description of applied time-cycles and corresponding amount of hours on the horizontal axis.

7,468 GWh in 2050 for the high VRES scenario. Lastly, the intra-yearly (17,520 hours) electrical energy variability has significantly smaller values than the seasonal variation among all scenarios, ranging from 8.5 GWh in 2018 to 2,262 GWh in 2050 for the high VRES scenario (see Figure 35).

5.3 Residual load duration curve (RLDC)

5.3.1 Netherlands (Northern Europe)

The residual load duration curve (RLDC) of the Netherlands with all scenarios is illustrated in Figure 36. The power generation hours of peaking demand remain constant between 2018, 2030, and 2050 among all scenarios. The overall power demand of the Netherlands is only expected to grow 14% between 2018 and 2050, triggered by electrification and increased efficiency among all sectors, which explains the fairly constant peaking demand hours (DNV GL, 2019). The current (2018) RLDC displays a flatter decline compared to the other scenarios due to significate lower shares of VRES in the power mix. The low VRES scenarios produce 1,816 hours and 4,323 hours surplus power with a maximum surplus VRES generation of 12,313 MW and 23,945 MW, for 2030 and 2050, respectively (see Figure 36). The negative part of the RLDC for the scenarios high VRES 2030 and 2050 is predominant over the positive values (4,750 in 2030; 6,448 in 2050), thus, there are more hours of the year where VRES generates more power than demand, in case no flexibility measures are implemented. For the high

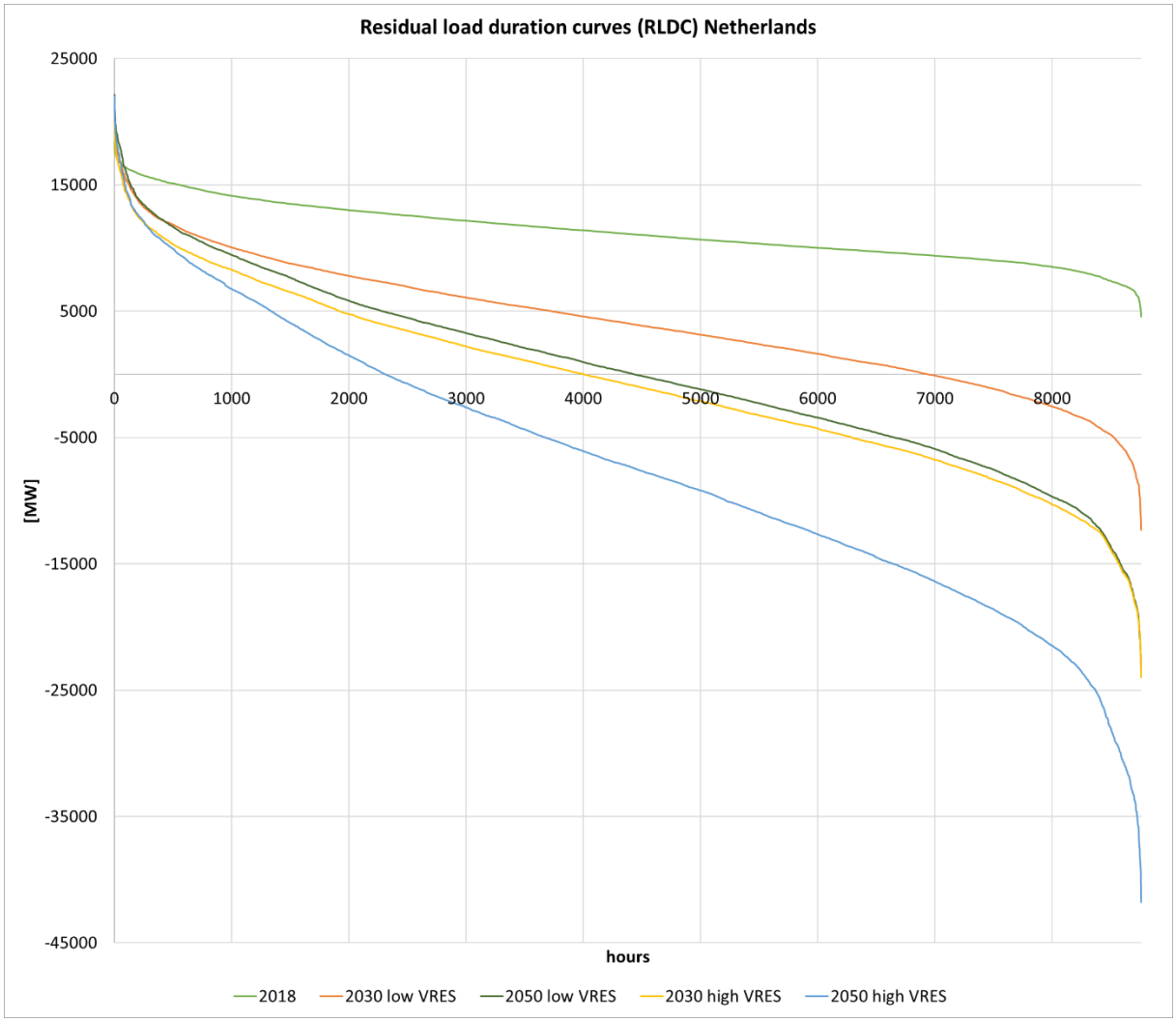

Figure 36: Residual load duration curve (RLDC) for current and future scenarios in the Netherlands, with VRES supply based on year 2015.

VRES scenario in 2050, dispatchable power sources (e.g. coal/natural gas) can only operate for 2,312 hours of the year, while the remaining hour's curtailment or energy storage is needed, due to VRES surplus generation (see Figure 36). The largest surplus in the high VRES scenario is 23,968 MW and 41,781 MW in 2030 and 2050, respectively. The cumulative annual power surplus increases from 4.7 TWh for the low VRES scenario in 2030 up to 77.3 TWh for the high VRES scenario in 2050.

5.3.2 Italy (Southern Europe)

The RLDC of Italy is illustrated in Figure 37 including the current and future scenarios for low and high VRES. The hours of peaking power demand are, like the Dutch RLDC, very equal among all examined scenarios and only differ in their value because the overall power demand for Italy is significantly larger than the one for the Netherlands. The total power demand is expected to only increase 16% from 2018 until 2050 and thus, the peak demand of dispatchable power source only inclines slightly. The high VRES scenario will generate 2,414 hours and 3,484 hours surplus power production with a maximum surplus power value of 52,355 MW and 104,668 MW in 2030 and 2050, respectively. In comparison, the low VRES scenario produces 758 hours and 2,538 hours surplus power production with a maximum surplus power value of 24,241 MW and 58,690 MW in 2030 and 2050, respectively. The cumulative annual power surplus increases from 4.7 TWh for the low VRES scenario in 2030 up to 125.7 TWh for the high VRES scenario in 2050.

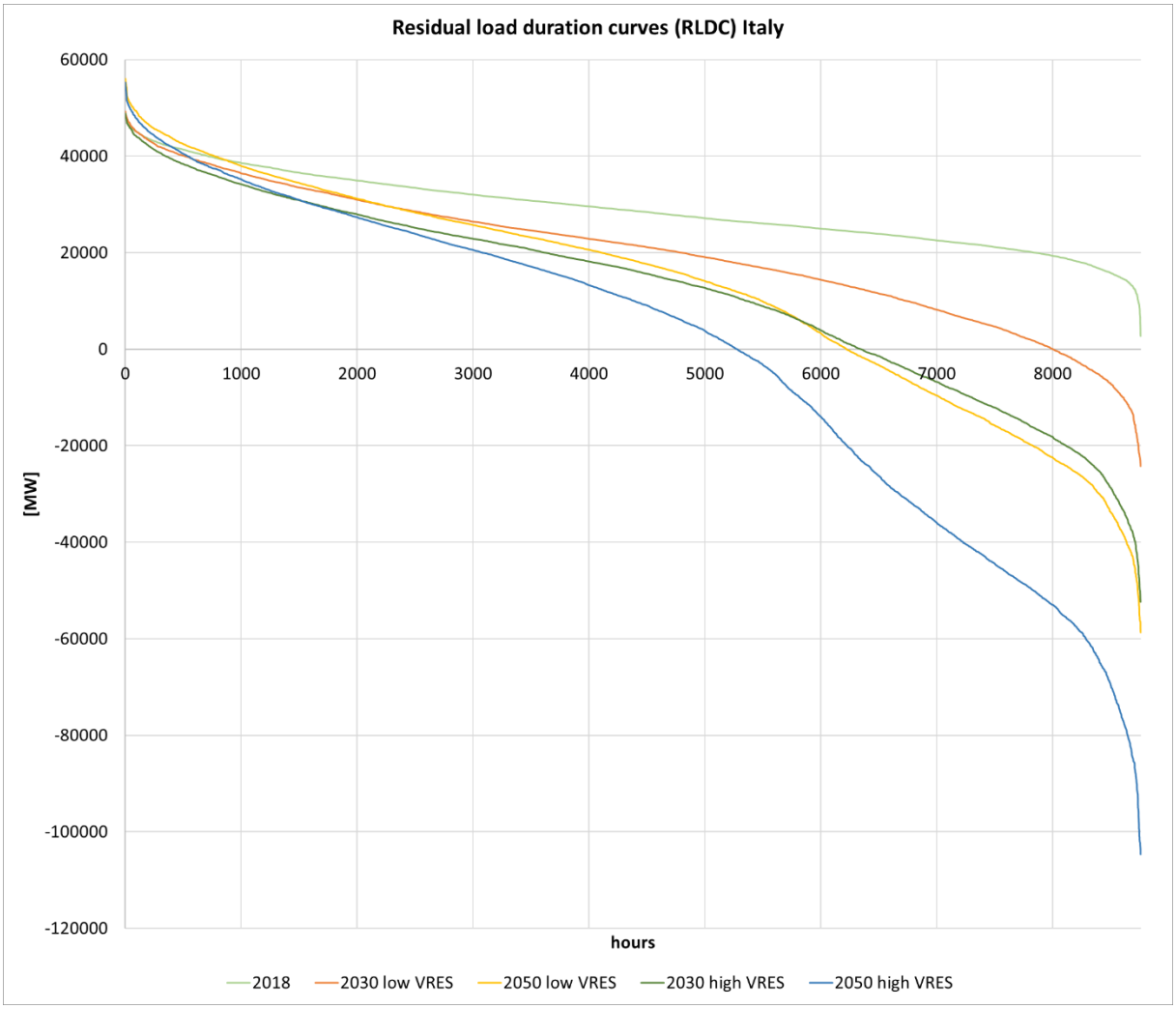

Figure 37: Residual load duration curve (RLDC) for current and future scenarios in the Italy, with VRES supply based on year 2015.

5.3.3 Egypt (Middle East and North Africa MEA)

The peaking load power generation displays differences between the future scenario 2030 and 2050 for the Egyptian power market, as visualized by the RLDCs in Figure 38. An explanation for this phenomena is because the total power demand among all sectors is expected to increase by 40% and 260% between 2018 – 2030 and 2018 – 2050, respectively (DNV GL, 2019). This has a direct consequence on the discrepancy between the values for peaking power production in 2030 and 2050. Both VRES scenarios (low and high) for the year 2050 result in significantly higher values of peaking power demand compared to the year 2030, with values of 61,739 – 63,567 MW and 32,925 – 33,726 MW, respectively (see Figure 38). The low VRES scenario generates only 167 hours and 1,992 hours surplus power production with maximum overproduction values of 8,438 MW and 32,458 MW in 2030 and 2050, respectively. The high VRES scenario produces 2,148 hours and 3,636 hours surplus power production with maximum overproduction values of 24,130 MW and 69,554 MW in 2030 and 2050, respectively. The cumulative annual power surplus increases from 0.3 TWh for the low VRES scenario in 2030 up to 15.1 TWh and 97.8 TWh for the low and high VRES scenario in 2050.

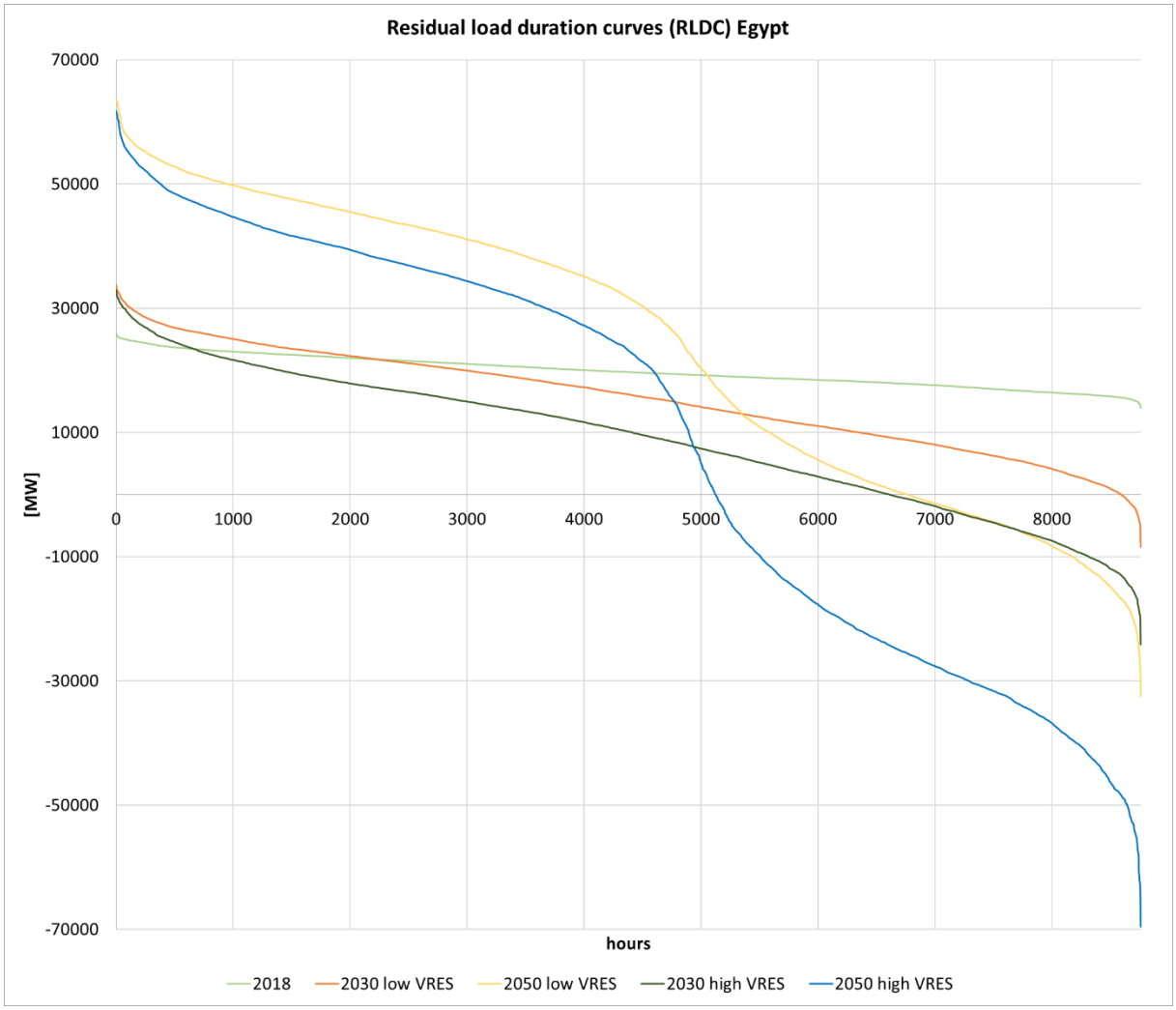

Figure 38: Residual load duration curve (RLDC) for current and future scenarios in Egypt, with VRES supply based on year 2015.

Whereas the RLDC profiles in 2030 show a gradual decline, the scenarios in 2050 display an almost S- shaped curve with a sharper decline around hour 4,500 (see Figure 39). It is expected that the installed capacity of solar PV will be 2.6-times higher than installed wind by 2050 (DNV GL, 2019). As a

result, there will be a strong fluctuation of VRES production of day/night cycles. In addition, the capacity factor calculated for the solar PV power generation in Egypt is on average 29.7% in 2050, whereas the ones for Singapore, the Netherlands, and Italy are significantly lower with values of 14.2%, 16.7%, and 22%, respectively. The combination of the large share of installed solar PV and the high capacity factor can be an explanation for a strong diurnal difference of VRES power generation along the entire year. This triggers the sharp decline at hour 4,500 in the RLDC of the Egyptian power system in 2050 (for low and high VRES scenarios).

5.3.4 Singapore (South East Asia SEA)

Like the Egyptian RLDC pattern, the peaking demand of dispatchable power generation is significantly larger in 2050 compared to 2030 (see Figure 39), caused by an expected power demand increases by 71% and 333% between 2018 – 2030 and 2018 – 2050, respectively (DNV GL, 2019). Whereas the maximum peak generation demands results in 22,477 – 22,587 MW for low and high VRES scenario in 2050, the same values in 2030 lead to 11,725 – 11,801 MW. Additionally, both VRES scenarios in 2030 result in no surplus generation of VRES and display a similar RLDC pattern compared to the current (2018) situation (see Figure 39). The reason for this observation is that the predicted installed capacity of VRES in 2030 covers only 6.6% of the total power demand (DNV GL, 2019). In 2050 the low and the high VRES scenario generate 352 hours and 1,339 hours surplus power production with maximum overproduction values of 10,657 MW and 25,209 MW, respectively. The cumulative annual power surplus equals 1.1 TWh and 9.8 TWh for the low and high VRES scenario in 2050.

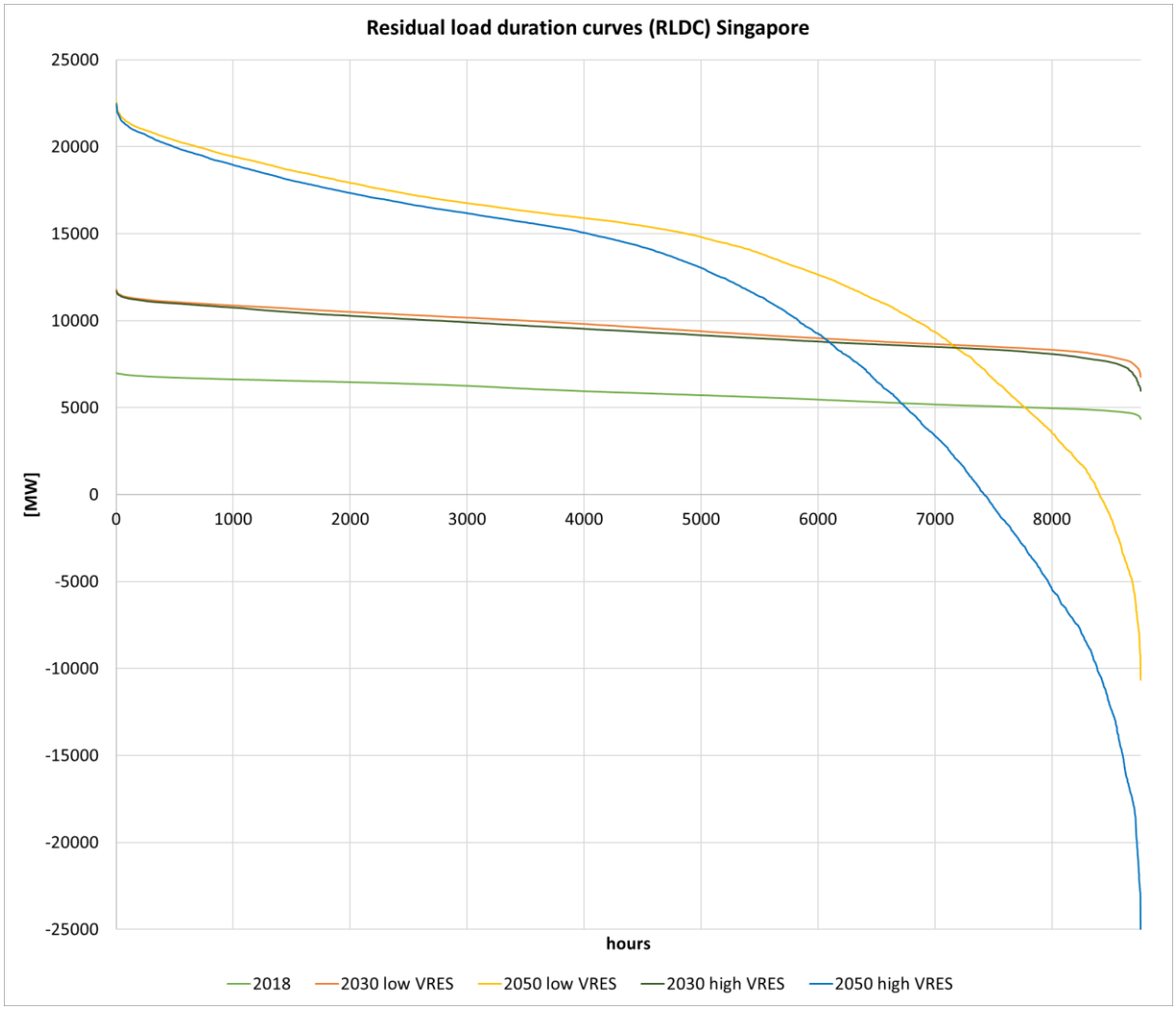

Figure 39: Residual load duration curve (RLDC) for current and future scenarios in Singapore, with VRES supply based on year 2015.

6. DISCUSSION

6.1 Methodology

The new approach developed in this research allows for the observation of differences in current and future grid variabilities with just a few parameters. Nevertheless, some simplification and assumptions had to be done, which could have had an impact on the accuracy of the outcome values. All end-consumers within the power sector among all examined countries are assumed to behave according to the proposed benchmark load profiles of the Netherlands. Additionally, the space cooling profile to illustrate the AC power consumption was based on a report conducted in India. This does not represent reality because the behaviour of some individual end-consumers can be very subjective and might differ among geographically and demographically distinct countries. Additionally, the daily heating profile of heat pumps might display a different, more constant, behaviour than a heating profile of a gas boiler which was used in this study. This is because heat pumps have a slower heating up time and thus, require more time to supply the energy demanded for a comfortable indoor temperature (Love , Oikonomou, Gleeson, & Chiu , 2017). The daytime length was not considered as a variable but could have an impact on the power consumption of lighting appliances since the length of days differs per latitude, seasonality, and thus, country. Also, public holidays were excluded in this study, which could have an impact on the seasonal power variability. The reason for the exclusion was because the holiday period is not the same for each region, and thus, it was difficult to introduce this variable in the generic model. The methodology assumes the same approach for space heating and space cooling for all examined countries and neglects differences in desired indoor temperatures. Behaviours are very subjective, and the heating or cooling profile could differ among geographical and demographical regions.

Furthermore, emerging issues of VRES technologies with different grid voltage frequencies than the traditional 50 Hz and transformation issues from direct current (DC) to alternating current (AC) on the power system were neglected although they could represent a technical hurdle to introduce more VRES in future power systems (Gerwen, Sun, Eijgelaar, Bosma, & Dugstad, 2018). Additionally, it is important to note that the methodology is neglecting the smoothening effect of VRES production, which could have an impact on the variability, especially on small time scales (intra-daily). Hourly solar PV and wind power generation values (capacity factors) are based on a specific location within the examined countries and as a result, the calculated power variabilities stated in this research might be higher compared to reality. The smoothening effect for wind power, and to a lesser extent for sola PV, can lower the overall variability by geographical region spreading and thus, decrease the cross-correlation of sites with distance. (Buttler, Dinkel, Franz, & Spliethoff, 2016). Finally, future projection on the power demand and the VRES supply for 2030 and 205 are based on expected regional development values for Egypt and Singapore. Only for the Netherlands and Italy country-specific predictions for future VRES supply could be found. To introduce accuracy, country-specific values should be considered among all examined countries.

6.2 Data Analysis

6.2.1 General

The averaged power and the electrical energy variability of the analysed time-cycles displayed different behaviours between geographically and demographically distinct regions. Nevertheless, the electrical energy variability graphs of all countries point to a steady and gradual increase along all time-cycles with higher values for future scenarios (2030 and 2050) compared to the current state (see Figure 29, Figure 31, Figure 33 and Figure 35). Greater shares of VRES and electrification of sectors, such as heat pumps and AC, constitute the reasons for larger variability values in future scenarios. As a result, more electrical energy is required to balance out the power grid by introducing flexibility measures (e.g. batteries, G2V) with charging or discharging capabilities. Consequently, more investments in energy

storage capacity are required for the future power system with increased VRES penetration rates (Olsen, et al., 2019). Overall, the power variability display peaks on intra-daily, weekly, and seasonal time-cycles with distinct values for each examined country. The intra-daily peak variation derives from diurnal cycles of power demand but also on the day vs. night fluctuation of solar PV production, and to a lesser extent, the differences in wind speed (Buttler, Dinkel, Franz, & Spliethoff, 2016; Gerwen, Eijgelaar, & Bosma, 2020). The weekly power variability of the residual power load is predominantly caused by the workday and weekend power demand cycles, and to a lesser degree are caused by weather conditions (Gerwen, Eijgelaar, & Bosma, 2020). Aside from daily cycles, the wind has a significant impact on the weekly and seasonal power variability of the residual power load. On the other hand, solar PV production has a significantly larger impact on intra-daily variabilities compared to the seasonal one, depending on the geographical region (Gerwen, Eijgelaar, & Bosma, 2020). Inter-annual variability among all countries is small, which could be explained by the fact that solar PV and wind do not display substantial variations of power generation between two consecutive years (yearly time-cycle; 17,520 hours) within the observed time-period (2015 – 2018) of all examined countries (see Appendix V; Figure 69 – Figure 76).

6.2.2 Netherlands

The power variability of the Dutch residual power load displays among all scenarios two substantial peaks in intra-daily and weekly time-cycles. Currently, the flexibility measures on an hourly basis are dominated by dispatchable power sources, such as natural gas. However, forecasted scenarios predict that in 2050 VRES curtailment and import vs. export (besides energy storage) will be the predominant measures for upward or downward flexibility on an hourly basis (Sijm, et al., 2017). Thus, it is expected that by 2050 the Netherlands will be equipped with 33 GW of interconnection capacity which could cover the intra-daily variabilities of 9.8 GW for the high VRES scenario in 2050 (Sijm, et al., 2017). Nevertheless, it is worth mentioning that the variability values stated in the current research are averaged over the observed period and extreme outliers could have significantly higher values. It is expected that in 2050 the storage capacity of EVs in the Netherlands can provide 240 GWh, which can either be charged or discharged (G2V/V2G) and could cover the averaged intra-daily electrical energy variability of 66 GWh in 2050 (high VRES scenario). It is significant to note that these values are only required to balance the residual load and do not reflect the overall energy storage demand (Gerwen, Eijgelaar, & Bosma, 2020).

In the case of the high VRES scenario, the Netherlands will generate more surplus hours per year than hours where power is required in 2030 (4,750 in 2030; 6,448 in 2050) in case no flexibility measures are implemented (see Figure 36). The expected storage capacity of 240 GWh in EVs by 2050 would only cover 0.3% of the total annual power surplus in 2050 in the high VRES scenario if no other flexibility measures or VRES curtailment have been implemented (Gerwen, Eijgelaar, & Bosma, 2020). Nevertheless, previous research has demonstrated that salt caverns and depleted gas fields can store 43 TWh and 456 TWh of hydrogen (power-to-gas (P2G)), which could be used as seasonal energy storage for the Dutch power system in the future (Juez-Larré, van Gessel, Dalman, Remmelts, & Groenenberg, 2019).

6.2.3 Italy

The power variability of the Italian residual power load displays a unique pattern among the examined time-cycles when compared to the Dutch one (see Figure 28 and Figure 30). The peak on intra-daily power variability is significantly larger for all scenarios than the weekly, monthly, and seasonal ones. Currently, Italy is equipped with 26 MW of battery storage which would not have any consequential impact on balancing the average intra-daily power variation of the residual power load in 2030 and 2050 among all scenarios (statista, 2020). Furthermore, all power variability values are significantly higher compared to the Dutch values. This disparity is the result of a generally higher power demand

for the Italian power market and thus, also more installed VRES capacity, in absolute terms, compared to the Netherlands (see Appendix II; Table 14 and Table 15).

Among all scenarios, the mid-merit and base-load power demands expand over more hours per year when compared to the Netherlands RLCDs (see Figure 36 and Figure 37). As a result, more dispatchable power sources are required. None of the examined scenarios produced more surplus hours per year than hours where demand is required. The source of this distinction between the Dutch and the Italian power surplus is caused by the high VRES scenario in 2050 the Dutch power system will generate on an annual, cumulative basis. This is 1.4 times more non-dispatchable power (VRES) than the total power demand (184 TWh VRES; 131 TWh load), whereas expectations for the Italian market foresee for the same scenario only 1.04 times more VRES generation than power demand (358 TWh VRES; 346 TWh load) (entsoe, 2013). Nevertheless, the annual, cumulative power surplus of 4.7 TWh in 2030 (low VRES scenario) cannot be covered by the current installed energy storage capacity of pumped-storage hydroelectricity (PSH) of 0.7 TWh (Colbertaldo, Guandalini, & Campanari, 2018). Thus, more flexibility measures need to be constructed or implemented in the future Italian power system, such as demand response, G2V, interconnectivity, and VRES curtailment.

6.2.4 Egypt

The power variability of the Egyptian residual load displays a distinct pattern compared to both the Dutch and Italian curves (see Figure 32). There is a substantial gap of power variation between time-cycles of 2030 and 2050 for both low and high VRES scenario, caused by a significant incline in power demand and VRES capacity between 2030 and 2050 (DNV GL, 2019). It is critical to note that the supply and demand forecasts are based on the regional development of the MEA region and are not country specific. The pumped-storage hydroelectric plant in Attaqa, which is expected to complete construction in 2022, will be equipped with a capacity of 2.4 GW that could nearly balance the residual power load on the seasonal time-cycle in 2030 for both low and high VRES scenarios (see Figure 32) (IRENA, 2018). The average intra-daily power variability dominates with up to 40 GW for the high VRES scenario in 2050. However, the weekly and seasonal power variations are small, ranging between 2 and 10 GW (see Figure 32). The adoption and instalment of concentrated solar power (CSP) with a heat buffer instead of solar PV could be a measure to, at least partially, mitigate the high intra-daily variability due to its ability to store electrical energy and dispatch it if required (de Castro & Capellan-Pérez, 2018).

6.2.5 Singapore

The Singaporean residual power load displays a considerable difference in grid variability between 2030 and 2050 (see Figure 34). Again, this is caused by the high growth-factor of total power demand and installed VRES capacity. The forecasted increase in total power demand of the Singaporean power market is expected to be even greater than that of Egypt (260% compared to 330%) between 2018 and 2050. As a result of Singapore's high Human Development Index (0.935) compared to that of its regional neighbours, the exact values for Singapore may differ because the growth factor is region-, and not country-specific (UNDP, 2019). A better benchmark country for the region should have been selected but was not possible due to the data on total power load profiles on an hourly basis being only accessible for Singapore. Such data was required to apply the methodology of this study.

Currently, Singapore is targeted to reach an electrical energy storage capacity of 200 MW beyond 2025, which could reduce costs for other required flexibility infrastructures to balance the load (energy storage, 2019). For 2030, this storage capacity would be enough due to zero VRES power surplus, but by 2050 more investment would be required due to annual cumulative power surpluses of 1.1 TWh and 9.8 TWh for the low and high VRES scenario, respectively.

7. CONCLUSION

7.1 Methodology

The objective of this research was to provide a novel methodology that analyses power grid variabilities, based on the residual power load, on different time-cycles and among geographically and demographically distinct regions. With the methodology developed in this study, this objective was achieved and required just a few country- and regional-specific parameters. This innovative approach generates, in a simple way, a general overview of the average variability values on different time-cycles of globally distinct current and future power markets.

In the first step, the total hourly power load profile was decomposed into three relevant sectors: residential, commercial, and industrial based on the Netherland as a benchmark country. Subsequently, the sectorial load profiles were corrected with country-specific parameters and finally summed up again to create, along with the power demand for EVs, the new total load profile per country in 2030 and 2050. In the second step, the annual non-dispatchable VRES power generation profile was generated for each examined country. Third, the resulting residual power load was calculated for a low and high VRES scenario in 2030 and 2050. In the last step, with the aid of a power frequency spectrum analysis, the power and electric energy variability was examined. Additionally, the country-specific residual load duration curve (RLDC) was analysed. A validation of this methodology was conducted via real measured data for the generated sectorial load profiles and via a statistical software (MATLAB) to confirm the outcome of the power frequency spectrum model.

The results of this novel approach have significant importance for the planning of future power systems, especially for power producers, utilities, and transmission system operations (TSOs). Thereby, the proposed methodology enables awareness and offers suggestions for flexibility measures to balance the grid and thereby, can assist in reducing the risks of curtailment or blackouts.

7.2 Data Analysis

Four countries from various global regions were selected and examined with this methodology: the Netherlands, Italy, Egypt, and Singapore. These countries represent the regions of Northern Europe, Southern Europe, Middle East and North Africa (MEA) and South East Asia (SEA), respectively. Significant differences between current and future power grid variability were observed among all examined countries. The average power variability of the residual load on intra-daily time-cycles varied between 9.8 GW (Netherlands) and 40 GW (Egypt and Italy) for the high VRES scenario in 2050. The Netherlands displays high power variations on weekly and seasonal time-cycles because it represents the only examined country expected to have more installed VRES capacity of wind, both onshore and offshore, than solar PV (see Appendix II; Table 14). In the case of Egypt, the future power system will be dominated by intra-daily variabilities due to a substantial amount of installed solar PV capacity, which displays high diurnal power variability (see Appendix V; Figure 74). The Singaporean power variability for 2050 is the only one resulting in higher seasonal than weekly power variability. This is caused by high seasonality on wind generation (see Appendix V; Figure 75). Overall, the electrical energy variability increased among the time-cycle because more power can be generated over longer periods. Flexibility measures, such as energy storage, will increase among all examined countries in the future for low and high VRES scenarios. The RLDC of the Netherlands results in the most hours of power surplus per year in 2050 (6,448 hours; high VRES) whereas the Singaporean power system only generates 1,339 hours of VRES surplus in 2050 for the same scenario. Nevertheless, the high VRES scenario for Italy forecasts with 125.7 TWh the largest annual power surplus in 2050 among all examined countries. This would require significant investments from Italy in energy storage infrastructures or other flexibility measures, such as hydrogen production or G2V if heavy VRES curtailment wants to be avoided.

8. RECOMMENDATIONS

It is advised that future research on power grid variabilities should consider more benchmark countries to create a better overview of other regions, in addition to the countries examined in this study. To apply this methodology, it is necessary to have current data on the total annual power load on an hourly basis. Additionally, the decomposition of the total power load profile, currently based on the Netherlands as a benchmark country, could be applied separately for each examined region or country to generate more country-specific load profiles and thus, achieving increased accuracy of the total current and future power load profile. Concerning the supply side, annual VRES generation profiles should be calculated for multiple sites within a country to include the smoothening effect of VRES, especially for wind. Furthermore, the effect of flexibility measures on the power variability, when implemented on different time-cycles, could be analysed to observe which strategies could best mitigate the variability and thereby lower power mismatches of supply and demand. Demand response (e.g. V2G or G2V), grid interconnectivity, and energy storage technologies, such as PSH and compressed hydrogen, could represent such flexibility measures.

9. REFERENCES

Attia, S., Evrard, A., & Gratia , E. (2012). Developement of benchmark models for the Egyptian residential buildings sector. *Applied Energy 94*, 270-284\.

AverageWeather. (2020). *average-weather*. Retrieved from https://www.average-weather.com/en/middle+east/?unit=metric

BudgetDirect. (2018). *budgetdirect.com.sg*. Retrieved from https://www.budgetdirect.com.sg/car-insurance/research/car-ownership-singapore

Buttler, A., Dinkel, F., Franz, S., & Spliethoff, H. (2016). Variability of wind and solar power e An assessment of the current situation in the European Union based on the year 2014. *Energy 106*, 147-161.

Buttler, A., Dinkel, F., Franz, S., & Spliethoff, H. (2016). Variability of wind and solar power e An assessment of the current situation in the European Union based on the year 2014. *Energy 106*, 147 - 161.

CBS 1, C. B. (2018). *Energieverbruik van particuliere huishoudens*. Retrieved from https://www.cbs.nl/nl-nl/achtergrond/2018/14/energieverbruik-van-particuliere-huishoudens

CBS 2, C. B. (2018). *CBS Open data StatLine*. Retrieved from https://opendata.cbs.nl/statline/portal.html?_la=en&_catalog=CBS&tableId=81955ENG&_theme=1073

CBS 3, C. B. (2018). *Trends in the Netherlands*. Retrieved from https://longreads.cbs.nl/trends18-eng/economy/figures/energy/#:~:text=In%202016%2C%20an%20average%20Dutch,of%20natural%20gas%20for%20heating.

CEIC. (2018). *ceicdata*. Retrieved from https://www.ceicdata.com/datapage/en/country/egypt

channelnewsasia. (2017). *channelnewsasia*. Retrieved from https://www.channelnewsasia.com/news/singapore/singapore-s-first-long-span-wind-turbine-installed-at-semakau-9327094

Cialani, C., & Mortazavi, R. (2018). Household and industrial electricity demand in Europe. *Energy Policy*, 592-600.

Clerjon, A., & Perdu, F. (2018). Matching intermittency and electricity storage characteristics through time scale analysis. An energy return on investment comparison. . *Energy & Environmental Science* , DOI: 10.1039/C8EE01940A.

Colbertaldo, P., Guandalini, G., & Campanari, S. (2018). Modelling the integrated power and transport energy system: The role of power-to-gas and hydrogen in long-term scenarios for Italy. *Energy, Volume 154*, 592-601.

data.gov.sg. (2018). *data.gov.sg*. Retrieved from https://data.gov.sg/dataset/annual-mileage-for-private-motor-vehicles

de Castro, C., & Capellan-Pérez, I. (2018). *Concentrated Solar Power: actual performance and foreseeable future in high penetration scenarios of renewable energies.* Valladolid, Spain: BioPhysical Economics and Resource Quality 3:18.

DECE. (no date). *FFT tutorial.* Rhode Island: University of Rhode Island, Department of Electrical and Computer Engineering (DECE). Retrieved from https://www.researchgate.net/file.PostFileLoader.html?id=5923adad48954c4d3440d709&assetKey=AS%3A497020986236928%401495510445504

Dittmann, F., Riviere, P., & Stabat , P. (2016). *Space Cooling Technology in Europe.* Heat Roudmap Europe 2050, European Union's Horizon 2020.

DNV GL. (2014). *Power load Egypt.*

DNV GL. (2019). *Energy Transition Outlook, A global and regional forecast to 2050.* DNV GL.

DNV GL. (n.d.). *EV hourly capacity profile.*

EMA. (2018). *ema.gov.sg*. Retrieved from https://www.ema.gov.sg/Singapore-Energy-Statistics-2019/Ch03/index3

EMC. (2018). *Energy Market Company Singapore*. Retrieved from https://www.emcsg.com/

Energiemanager, D. (2018). *deenergiemanager*. Retrieved from http://www.deenergiemanager.nl/tools/P_elektriciteit.html

energinet. (2020). *energinet.dk*. Retrieved from https://en.energinet.dk/Electricity

energy storage. (2019). *energ-storage.news*. Retrieved from https://www.energy-storage.news/news/singapore-eyes-200mw-of-energy-storage-beyond-2025-minister

entsoe. (2013). *e-HIghway2050*. Retrieved from https://docs.entsoe.eu/baltic-conf/bites/www.e-highway2050.eu/e-highway2050/

entsoe. (2018). *Transparency Platform Data Repository*. Retrieved from https://transparency.entsoe.eu/content/static_content/Static%20content/data%20repository/DataRepositoryGuide.html

European Comission. (2018). *METIS Technical Note T8, Demand and Heat Modules.* European Union. Directorate-Generral for Energy.

European Environment Agency, E. (2019). *Heating and cooling degree days.* Retrieved from Indicator Assessment: https://www.eea.europa.eu/data-and-maps/indicators/heating-degree-days-2/assessment

ev-database, E. V. (2020). *ev-database.* Retrieved from https://ev-database.org/cheatsheet/energy-consumption-electric-car

Garg, A., Maheshwari, J., & Upadhyay, J. (2010). Load Research for Residential and Commercial Establishments in Gujarat. *Energy Conservation and Commercialization (ECO-III)*.

Gelaro, R., McCarty, W., Suárez, M., Todling, R., Molod, A., Takacs, L., . . . Zhao, B. (2017). The Modern-Era Retrospective Analysis for Research and Application, Version 2 (MERRA-2). *Journal of Climate*, 5419-5454.

Gerwen, R. v., Eijgelaar, M., & Bosma, T. (2020). *The promise of seasonal storage.* Arnhem: DNV GL. Group Technology & Research, Position Paper.

Gerwen, R. v., Sun, Y., Eijgelaar, M., Bosma, T., & Dugstad, E. (2018). *Future-proof Renewables. Implications of a high percentage of solar and wind in the power system.* Arnehm: DNV GL. Group Technology & Research, White paper.

global wind atlas. (2020). *energydata.infos*. Retrieved from https://globalwindatlas.info/

Granell, R., Axon, C., Wallom, D., & Layberry, R. (2015). Power-use profile analysis of non-domestic consumers for electricity tariff switching. *Energy Efficiency*, 825-841.

Guozden, T. P., Carbajal, J. P., Bianchi, E., & Solarte, A. (2020). *Optimized Balance Between Electricity Load and Wind-Solar Energy Production.* Frontiers in Energy Research, 8. doi: 10.3389/fenrg.2020.00016.

iea. (2009). *Transport, Energy and CO2.* International Energy Agency.

iea. (2019). *International Energy Agency*. Retrieved from https://www.iea.org/data-and-statistics?country=WORLD&fuel=Energy%20consumption&indicator=Electricity%20final%20consumption%20by%20sector

IRENA. (2018). *International Renewable Energy Agency*. Retrieved from https://www.irena.org/Statistics/View-Data-by-Topic/Capacity-and-Generation/Technologies

IRENA. (2018). *Renewable Energy Outlook EGYPT.* Abu Dhabi: International Renewable Energy Agency.

IRENA. (2019). *Global energy transformation: A roadmap to 2050 (2019 edition).* Abu Dhabi: International Renewable Energy Agency.

Jacobson, M., & Jadhav, V. (2018). World estimates of PV optimal tilt angles and ratios of sunlight incident upon tilted and tracked PV panels relative to horizontal panels. *Solar Energy* , 55-66.

Jakubcionis, M., & Carlsson, J. (2018). Estimation of European Union service sector space cooling potential. *Energy Policy Volume 113*, 223-231.

Juez-Larré, J., van Gessel, S., Dalman, R., Remmelts, G., & Groenenberg, R. (2019). Assessment of underground energy storage potential to support the energy transition in the Netherlands. *First Break Volume 37*, 57-66.

Klein, K., Killinger, S., Fischer , D., Streuling, C., Salom, J., & Cubi, E. (2016). *Comparison of the Past and Future Residual Load in Fifteen Countries and Requirements to Grid-Supportive Building Operation.* Proceedings of EuroSun. ISES, International Solar Energy Society. doi: 10.18086/eurosun.2016.09.07.

Li, P.-H., & Pye, S. (2018). *Assessing the benefits of demand-side flexibility in residential and transport.* Applied Energy, 228, 965–979. doi: 10.1016/j.apenergy.2018.06.153.

Love , J., Oikonomou, E., Gleeson, C., & Chiu , L. (2017). *The addition of heat pump electricity load profiles to GB electricity demand: Evidence from a heat pump field triep.* London: Applied Energy 204, 332-342.

Mahdy, M., & Bahaj, A. (2018). Multi criteria decision analysis for offshore wind energy potential in Egypt. *Renewable Energy 118*, 278-289.

Majcen , D., Itard, L., & Visscher, H. (2013). Theoretical vs. actual energy consumption of labelled dwellings in the Netherlands: Discrepancies and policy implications. *Energy Policy*, 125-136.

McNeil, M., Karali, N., & Letschert, V. (2019). Forecasting Indonesia's electricity load through 2030 and peak demand reductions from appliance and lighting efficiency. *Energy for Sustainable Developmnet 49*, 65-77.

Mwanza, B., & Mbohwa, C. (2015). Design of a total productive maintenance model for effective implementation: Case study of a chemical manufacturing company. *Procedia Manufacturing 4*, 461-470.

NEDU. (2018). *Verbruiksprofile*. Retrieved from https://www.nedu.nl/documenten/verbruiksprofielen/

NEDU. (2020). *Verbruiksprofile*. Retrieved from https://www.nedu.nl/documenten/verbruiksprofielen/

Netherlands Enterprise Agency. (2019). *Statistics Electric Vehicles in the Netherlands.* Ministry of Infrastructure and Water Management.

Odyssee-mure. (2020). *indicators.odysse-mure*. Retrieved from https://www.indicators.odyssee-mure.eu/energy-efficiency-database.html

Olsen, K., Zong , Y., You, S., Bindner, H., Koivisto, M., & Gea-Bermudez, J. (2019). Multi-timescale data-driven method identifying flexibility requirements for scenarios with high penetration of renewables. *Applied Energy Special Issues*.

Persson , U., & Werner , S. (2015). *Quantifying the Heating and Cooling Demand in Europe.* Halmstad: Halmstad University, Intelligent Energy Europe .

Pfenning, S., & Staffell, I. (2016). Long-term patterns of European PV output using 30 years of validated hourly reanalysis and satellite data. *Energy* , 1251-1265.

Pfenninger, S., & Staffell, L. (2020, 4 20). *Renewables.ninja*. Retrieved from www.renewables.ninja

Plötz, P., Jakobsson, N., & Sprei, F. (2017). On the distribution of individual daily driving distances. *Trasnportation Research Part B: Methodological*, 213-227.

Ponniran, A., Mamat, N., & Joret, A. (2012). Electricity Profile Study for Domestic and Commercial Sectors. *International Journal of Integrated Engineering Vol. 4. No.3*, 8-12.

power-technology. (2019). *power technology*. Retrieved from https://www.power-technology.com/projects/ras-ghareb-windfarm/

recharge. (2019). *Global news and intelligence for the Energy Transition*. Retrieved from https://www.rechargenews.com/wind/italy-on-pole-in-race-for-first-mediterranean-offshore-wind/2-1-552007

Sijm, J., Gockel, P., van Hout, M., Özdemir , Ö., van Stralen, J., Smekens, K., . . . Musterd, M. (2017). *The supply of flexibility for the power system in the Netherlands, 2015 - 2050.* alliander, ECN.

solarplaza. (2018). *Top 25 solar PV project in the Netherlands*. Retrieved from https://www.solarplaza.com/channels/top-10s/11770/top-25-solar-pv-project-netherlands/

statista. (2020). *statista.com*. Retrieved from Italy: energy storage capacity 2017, by technology type: https://www.statista.com/statistics/830894/energy-storage-capacity-by-technology-type-in-italy/

ten Klooster, W. (2017). *The Feasibility and Conceptualization of a Multifunctional Artificial Pumped Hydro Storage Island in the North Sea.* Twente: Unviersity of Twente.

The straitstimes. (2020). *straitstimes SINGAPORE*. Retrieved from https://www.straitstimes.com/singapore/environment/sembcorp-to-build-singapores-largest-floating-solar-farm-covering-45-football

Ueckerdt, F., Brecha, R., Luderer, G., Sullivan, P., Schmid, E., Bauer, N., . . . Pietzcker , R. (2015). Representing power sector variability and the integration of variable renewables in long-term energy-economy models using residual load duration curves. *Energy 90*, 1799 - 1814.

UNDP. (2019). *Human Development Reports*. Retrieved from hdr.undp.org: http://hdr.undp.org/en/content/2019-human-development-index-ranking

USAID. (2015). *Climate Change Information Fact Sheet EGYPT.* United States Agency Internaional Development.

van Breukelen, B. (2019). *Energy demand for space cooling in the future: using refrigerant models and Cooling Degree Days to model energy demand in 2100 for Africa, India and the US.* Utrecht: Faculty of Science, Utrecht University .

van der Burgt, J., Wouters, C., van der Veen, W., & van der Wijk, P. (2017). *Flexibility in the power system.* Arnhem: DNV GL.

van Winden, J. (2018). *Spectral analysis of supply-demand matching in power systems with high levels of VRE.* Utrecht: Utrecht University .

Veldman, E., Gaillard, M., Gibescu, M., Slootweg, J., & Kling, W. (2010). Modelling Future Residential Load Profiles. *Innovation for Sustainable Production* .

Visser, R., Chang, M., Groenewoud, P., Duffhues, J., & Wolse, H. (2013). *Laadstrategie Elektrisch Wegvervoer.* Movares Nederland B.V., Netbeheer Nederland .

wikipedia. (2019). *wikipedia*. Retrieved from https://en.wikipedia.org/wiki/Montalto_di_Castro_Photovoltaic_Power_Station

wikipedia. (2020). *Wind power in the Netherlands*. Retrieved from https://en.wikipedia.org/wiki/Wind_power_in_the_Netherlands

windpower. (2020). *the wind power*. Retrieved from https://www.thewindpower.net/zones_en_7_943.php

Wiser, R., Hand, M., Seel, J., & Paulos, B. (2016). *Reducing Wind Energy Costs through Increased Turbine Size: Is the Sky the Limit?* Berkeley Lab.

10. APPENDICES

10.1 Appendix I

10.1.1 Residential annual load profile (NL benchmark country)

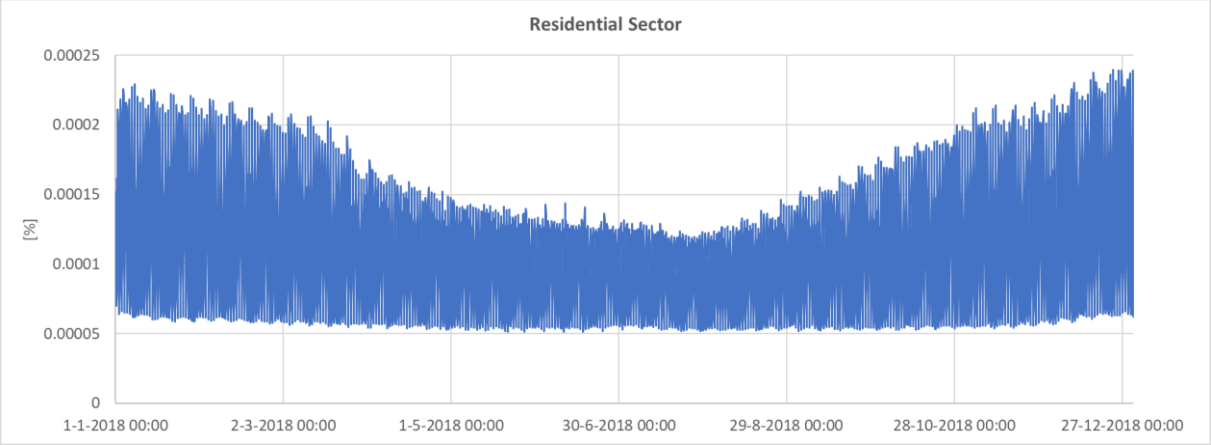

Figure 40: The normalized load profile of the residential sector in 2018, representing the aggregated E1A NEDU profiles (NEDU, Verbruiksprofile, 2018).

10.1.2 Commercial annual load profile (NL benchmark country)

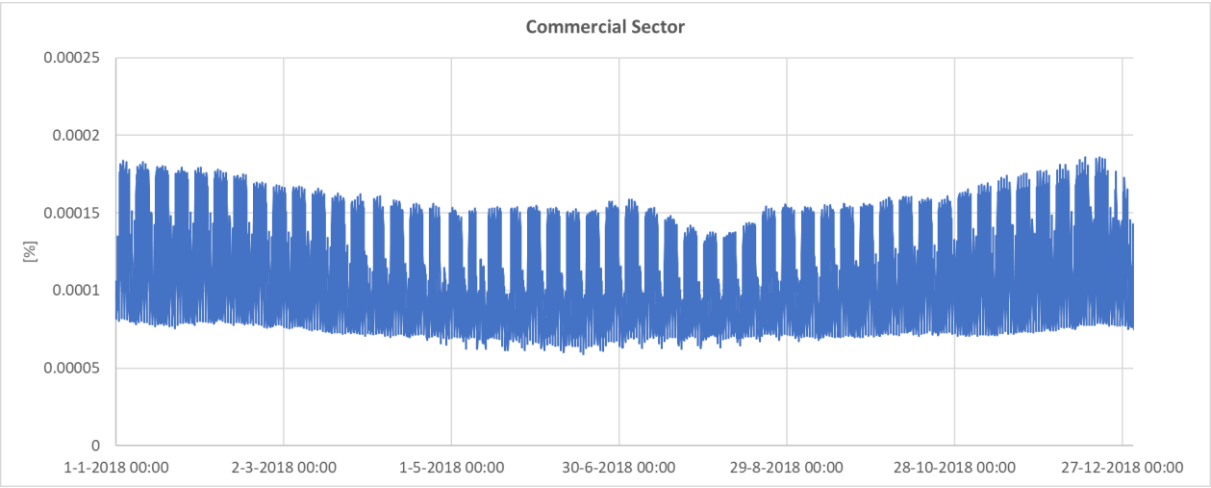

Figure 41: The normalized load profile of the commercial sector in 2018, representing the combination of different NEDU profiles (NEDU, Verbruiksprofile, 2018).

10.1.3 Industrial annual load profile (NL benchmark country)

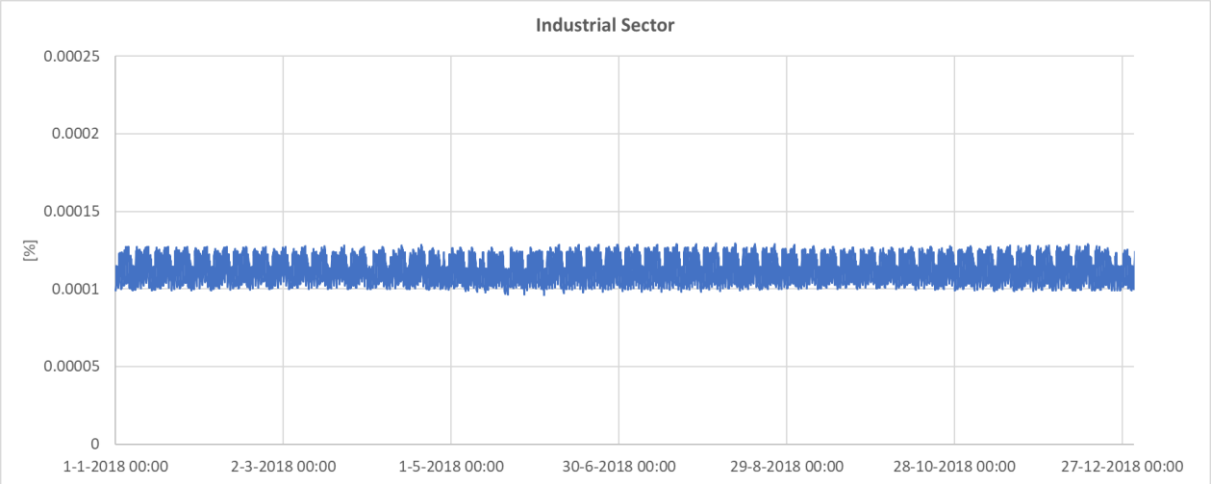

Figure 42: The normalized load profile of the industrial sector in 2018, representing the aggregated E3D NEDU profiles (NEDU, Verbruiksprofile, 2018).

10.2Appendix II

10.2.1 Country-specific Power Demand Characteristics and regional development

10.2.1.1 Netherlands (Northern Europe)

Table 10: Parameter for Netherlands, serving as input values for the demand side of the generic model (DNV GL, 2019)[1] (CBS 2, 2018)[2] (Odyssee-mure, 2020)[3] (Netherlands Enterprise Agency, 2019)[4]. (TSO = Transmission system operators; BEV = Battery electric vehicle; DHW = Domestic hot water)

Parameter		2018	2030	2050
Power demand	Residential Sector [TWh]	35.86[2]	36.94[1]	31.56[1]
	Commercial Sector [TWh]	22.97[2]	25.51[1]	28.03[1]
	Industrial Sector [TWh]	37[2]	39.22[1]	45.14[1]
	Other [TWh]	12.14[2]	7.89[1]	8.01[1]
	Total Sectors [TWh]	107.97	109.55	112.74
	BEV consumption [TWh]	0.11	3.81	11.4
	Consumption of Power producers and TSOs [TWh]	6.6	6.71	6.93
	Final Demand [TWh]	114.72	120.11	131.1
Heat pump, AC	Space heating & DHW (Residential sector) [%]	10.2[3]	34[1]	37[1]
	Space heating & DHW (Commercial sector) [%]	3.1[3]	23[1]	24[1]
	Space cooling (Residential sector) [%]	0.5[3]	2.4[1]	2.6[1]
	Space cooling (Commercial sector) [%]	5.5[3]	13[1]	12[1]
BEV	Total stock of passenger cars [nr.]	8,450,000[3]	8,619,000[1]	6,337,500[1]
	Share of BEV [%]	0.53[4]	19[1]	88[1]
	Total stock of BEV [nr.]	44,984[4]	1,637,610	5,577,000

10.2.1.2 Italy (Southern Europe)

Table 11: Parameter for Italy, serving as input values for the demand side of the generic model (DNV GL, 2019)[1] (iea, 2019)[2] (Odyssee-mure, 2020)[3] (Persson & Werner , 2015)[4] (Dittmann, Riviere, & Stabat , 2016)[5] (Jakubcionis & Carlsson, 2018)[6]. (TSO = Transmission system operators; BEV = Battery electric vehicle; DHW = Domestic hot water)

Parameter		2018	2030	2050
Power demand	Residential Sector [TWh]	115.91[2]	119.38[1]	102[1]
	Commercial Sector [TWh]	65.65[2]	72.88[1]	80.1[1]
	Industrial Sector [TWh]	93.73[2]	99.35[1]	114.35[1]
	Other [TWh]	17.42[2]	11.32[1]	11.5[1]
	Total Sectors [TWh]	292.71	302.94	307.95
	BEV consumption [TWh]	0.02	10.94	32.86
	Consumption of Power producers and TSOs [TWh]	4.28	4.43	4.5
	Final Demand [TWh]	297.01	318.31	345.31
Heat pump, AC	Space heating & DHW (Residential sector) [%]	11.4[3]	11.5[1]	12.4[1]
	Space heating & DHW (Commercial sector) [%]	15[4]	15.2[1]	16.1[1]
	Space cooling (Residential sector) [%]	3.9[3]	6[5]	12.5[5]
	Space cooling (Commercial sector) [%]	19[6]	20[5]	21.9[5]
BEV	Total stock of passenger cars [nr.]	39,020,000[3]	39,800,400[1]	29,265,000[1]
	Share of BEV [%]	0.03[3]	19[1]	88[1]
	Total stock of BEV [nr.]	10,000[3]	7,562,076	25,753,200

10.2.1.3 Egypt (Middle East and North Africa MEA)

Table 12: Parameter for Egypt, serving as input values for the demand side of the generic model (DNV GL, 2019)[1] (iea, 2019)[2] (CEIC, 2018)[3]. (TSO = Transmission system operators; BEV = Battery electric vehicle; DHW = Domestic hot water)

Parameter		2018	2030	2050
Power demand	Residential Sector [TWh]	43.22[2]	59.21[1]	116.69[1]
	Commercial Sector [TWh]	66.8[2]	88.85[1]	136.95[1]
	Industrial Sector [TWh]	40.83[2]	62.47[1]	115.15[1]
	Other [TWh]	8.49[2]	10.1[1]	14.94[1]
	Total Sectors [TWh]	159.34	220.63	383.72
	BEV consumption [TWh]	0.0007	3.19	32.96
	Consumption of Power producers and TSOs [TWh]	21.66	29.99	52.15
	Final Demand [TWh]	181	253.81	468.84
Heat pump, AC	Space heating & DHW (Residential sector) [%]	23[1]	20[1]	18[1]
	Space heating & DHW (Commercial sector) [%]	21[1]	18[1]	16[1]
	Space cooling (Residential sector) [%]	18[1]	24[1]	32[1]

BEV	Space cooling (Commercial sector) [%]	10[1]	11[1]	16[1]
	Total stock of passenger cars [nr.]	4,952,734[3]	7,478,628[1]	13,669,546[1]
	Share of BEV [%]	0.003[1]	10[1]	64[1]
	Total stock of BEV [nr.]	149	747,863	8,748,509

10.2.1.4 Singapore (South East Asia SEA)

Table 13: Parameter for Singapore, serving as input values for the demand side of the generic model (DNV GL, 2019)[1] (EMA, 2018)[2] (BudgetDirect, 2018)[3]. (TSO = Transmission system operators; BEV = Battery electric vehicle; DHW = Domestic hot water)

Parameter		2018	2030	2050
Power demand	Residential Sector [TWh]	21.5[2]	36.77[1]	63.43[1]
	Commercial Sector [TWh]	7.2[2]	14.33[1]	24.7[1]
	Industrial Sector [TWh]	18.6[2]	30.32[1]	65.29[1]
	Other [TWh]	3.2[2]	4.77[1]	10.4[1]
	Total Sectors [TWh]	50.5	86.18	163.81
	BEV consumption [TWh]	0.00005	0.27	4.39
	Consumption of Power producers and TSOs [TWh]	0.96	1.63	3.1
	Final Demand [TWh]	51.46	88.08	171.3
Heat pump, AC	Space heating & DHW (Residential sector) [%]	13[1]	12[1]	11[1]
	Space heating & DHW (Commercial sector) [%]	9[1]	9[1]	9[1]
	Space cooling (Residential sector) [%]	25[1]	38[1]	45[1]
	Space cooling (Commercial sector) [%]	16[1]	21[1]	34[1]
BEV	Total stock of passenger cars [nr.]	800,147[3]	1,440,111[1]	2,801,710[1]
	Share of BEV [%]	0.002[1]	6[1]	57[1]
	Total stock of BEV [nr.]	16	86,407	1,596,975

10.2.2 Country-specific VRES Characteristics and regional development

10.2.2.1 Netherlands (Northern Europe)

Table 14: Parameter for Netherlands, serving as input values for the supply side of the generic model, values for 2030 and 2050 were retrieved from e-Highway2050 "100% RES scenario" (entsoe, e-HIghway2050, 2013)[1] (IRENA, International Renewable Energy Agency, 2018)[2] (solarplaza, 2018)[3] (Jacobson & Jadhav, 2018)[4] (wikipedia, 2020)[5] (Pfenninger & Staffell, 2020)[6].

Installed capacity		2018	2030	2050
Solar PV [MW]		4,522[2]	14,377[1]	22,247[1]
Wind	Onshore [MW]	3,436[2]	9,803[1]	14,997[1]
	Offshore [MW]	957[2]	10,531[1]	15,900[1]
Benchmark farm		**Lat**	**Long**	**Tilt**
Solar	Zonnepark Groene Hoek[3]	52.3123	4.7224	34°[4]
Wind	Onshore: Westereems Eemshaven[5]	52.7191	5.5999	-
	Offshore: Gemini[5]	54.0730	5.7418	-

Capacity factors (averaged over 2015-2018) [%]		
Solar	One-axis tracking (azimuth)	16.2[6]
	Two-axis tracking (azimuth and tilt)	16.7[6]
Wind	Onshore (Vestas V112)	36[6]
	Offshore (Vesta V164)	52.9[6]

10.2.2.2 Italy (Southern Europe)

Table 15: Parameter for Italy serving as input values for the supply side of the generic model, values for 2030 and 2050 were retrieved from e-Highway2050 "100% RES scenario" (entsoe, 2013)[1] (IRENA, International Renewable Energy Agency, 2018)[2] (wikipedia, 2019)[3] (Jacobson & Jadhav, 2018)[4] (windpower, 2020)[5] (recharge, 2019)[6] (Pfenninger & Staffell, 2020)[7].

Parameter		**2018**	**2030**	**2050**
Solar	Installed capacity [MW]	20,108[2]	61,289[1]	101,044[1]
Wind	Onshore installed capacity [MW]	10,230[2]	19,174[1]	28,903[1]
	Offshore installed capacity [MW]	0[2]	8,218[1]	12,387[1]
Benchmark farm		**Lat**	**Long**	**Tilt**
Solar	Montalto di Castro[3]	42.3813	11.5865	27°[4]
Wind	Onshore: Puglia region[5]	41.4018	15.3537	-
	Offshore: Taranto region[6]	40.3324	17.1834	-
Capacity factors (averaged over 2015-2018) [%]				
Solar	One-axis tracking (azimuth)		21.2[7]	
	Two-axis tracking (azimuth and tilt)		22[7]	
Wind	Onshore (Vestas V112)		29.6[7]	
	Offshore (Vesta V164)		26.5[7]	

10.2.2.3 Egypt (Middle East and North Africa MEA)

Table 16: Parameter for Egypt, serving as input values for the supply side of the generic model (IRENA, International Renewable Energy Agency, 2018)[1] (DNV GL, 2019)[2] (IRENA, 2018)[3] (Jacobson & Jadhav, 2018)[4] (power-technology, 2019)[5] (Mahdy & Bahaj, 2018)[6] (Pfenninger & Staffell, 2020)[7].

Parameter		**2018**	**2030**	**2050**
Solar	Installed capacity [MW]	750[1]	22,900[3]	75,138[2]
Wind	Onshore installed capacity [MW]	1,125[1]	15,000[3]	19,662[2]
	Offshore installed capacity [MW]	0[1]	5,600[3]	9,415[2]
Benchmark farm		**Lat**	**Long**	**Tilt**
Solar	Benban Solar Park[3]	24.4441	32.7243	24°[4]
Wind	Onshore: Ras Ghareb[5]	28.5260	32.9152	-
	Offshore: Southern coast of Sinai Peninsula[6]	27.7122	33.6111	-
Capacity factors (averaged over 2015-2018) [%]				
Solar	One-axis tracking (azimuth)		28.8[7]	
	Two-axis tracking (azimuth and tilt)		29.7[7]	
Wind	Onshore (Vestas V112)		52[7]	

	Offshore (Vesta V164)	45.1[7]

10.2.2.4 Singapore (South East Asia SEA)

Table 17: Parameter for Singapore, serving as input values for the supply side of the generic model[1] (IRENA, International Renewable Energy Agency, 2018)[1] (DNV GL, 2019)[2] (Jacobson & Jadhav, 2018)[3] (The straitstimes, 2020)[4] (channelnewsasia, 2017)[5] (global wind atlas, 2020)[6] (Pfenninger & Staffell, 2020)[7].

Parameter		**2018**	**2030**	**2050**
Solar	Installed capacity [MW]	160[1]	2,977[2]	39,922[2]
Wind	Onshore installed capacity [MW]	0[1]	375[2]	4,320[2]
	Offshore installed capacity [MW]	0[1]	333[2]	6,425[2]
Benchmark farm		**Lat**	**Long**	**Tilt**
Solar	Tengeh Reservoir in Tuas[4]	1.3697	103.6642	10°[3]
Wind	Onshore: Semakau Landfill[5]	1.2031	103.7729	-
	Offshore: Coast of Bandar Penawar[6]	1.5618	104.3054	-
Capacity factors (averaged over 2015-2018) [%]				
Solar	One-axis tracking (azimuth)		14.2[7]	
	Two-axis tracking (azimuth and tilt)		14.2[7]	
Wind	Onshore (Vestas V112)		12.6[7]	
	Offshore (Vesta V164)		10.6[7]	

10.3Appendix III

10.3.1 Demand side (decomposed of total power load)

10.3.1.1 Netherlands (Europe North EUN)

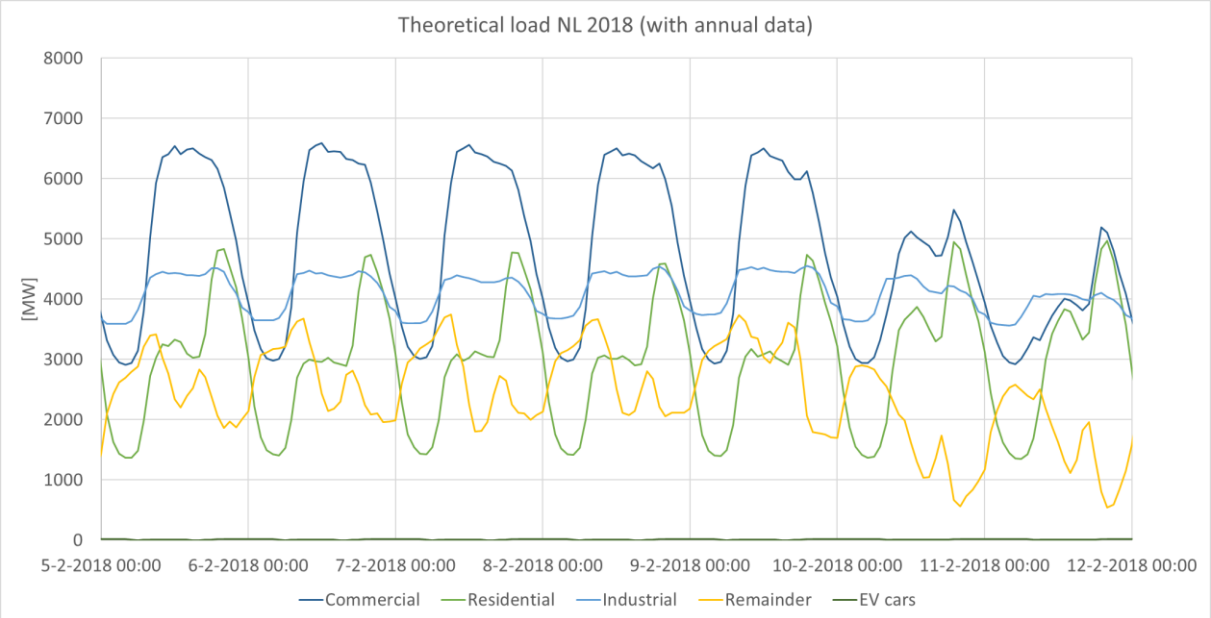

Figure 43: Decomposition of total load profile of a winter week in the Netherlands in 2018.

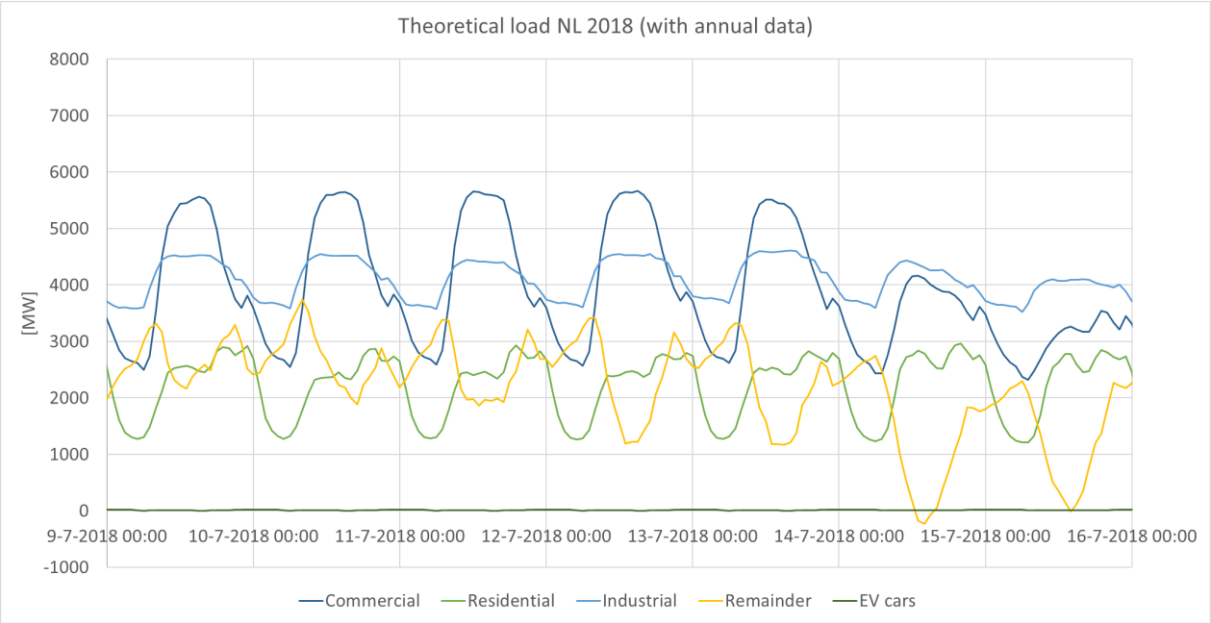

Figure 44: Decomposition of total load profile of a summer week in the Netherlands in 2018.

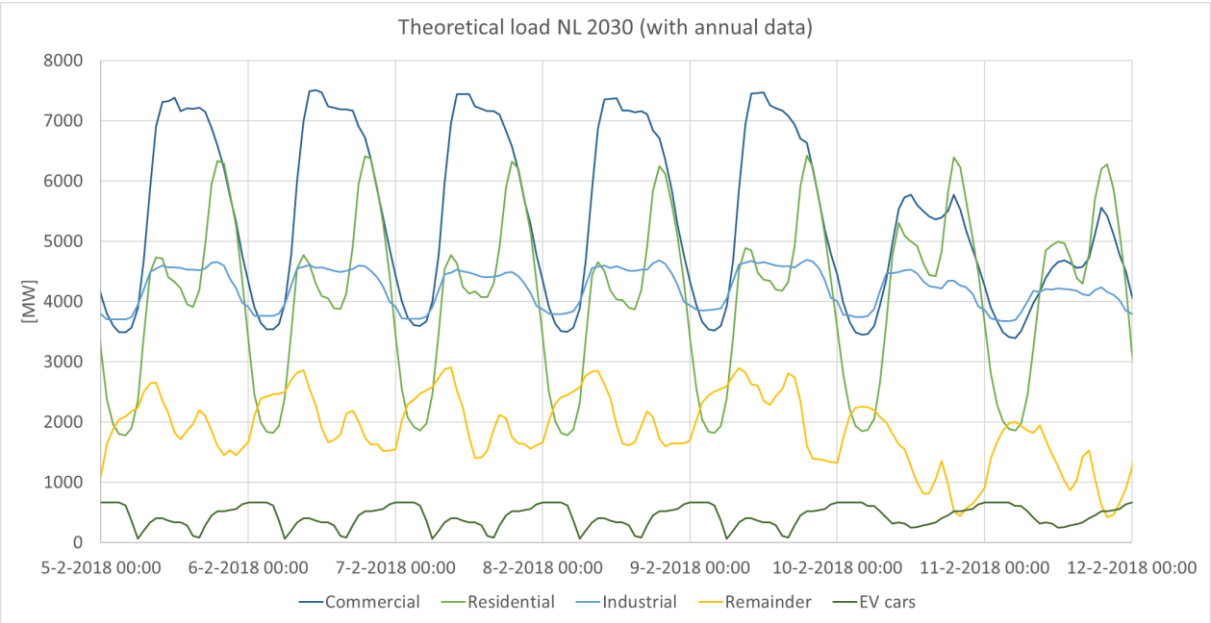

Figure 45: Decomposition of total load profile of a winter week in the Netherlands in 2030.

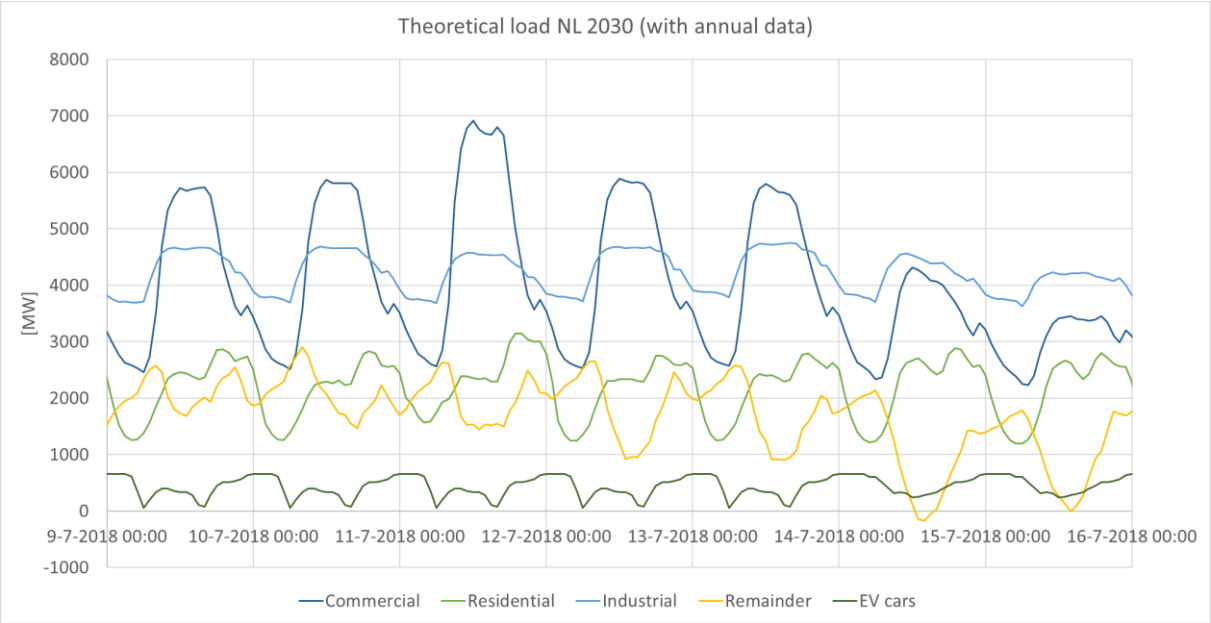

Figure 46: Decomposition of total load profile of a summer week in the Netherlands in 2050.

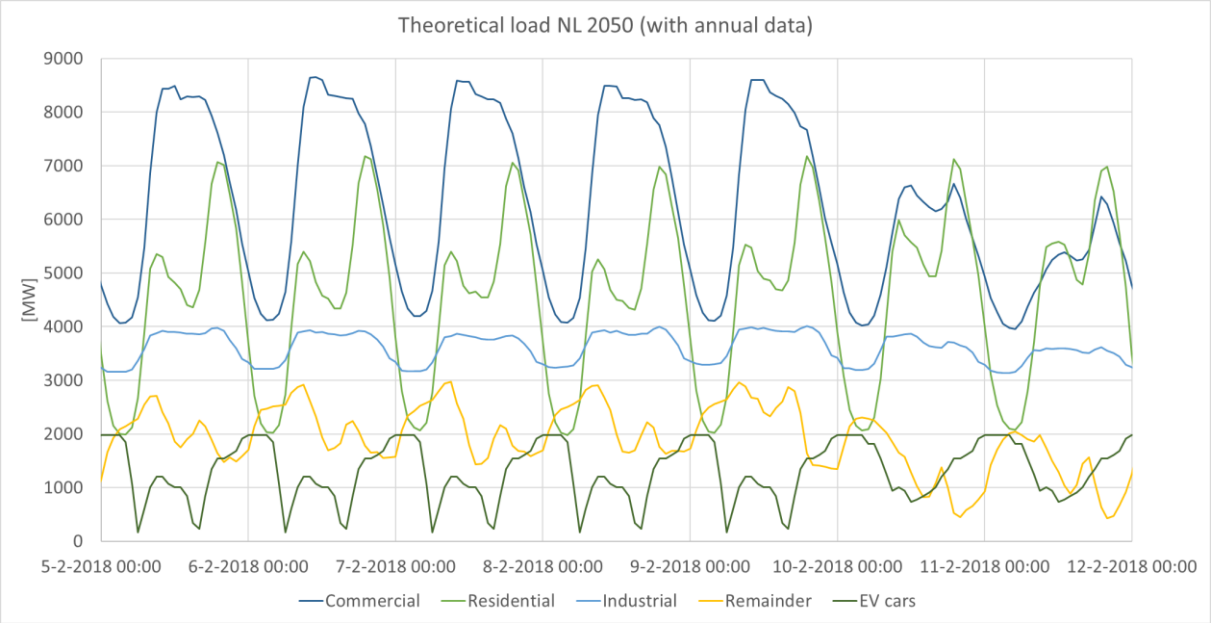

Figure 47: Decomposition of total load profile of a winter week in the Netherlands in 2050.

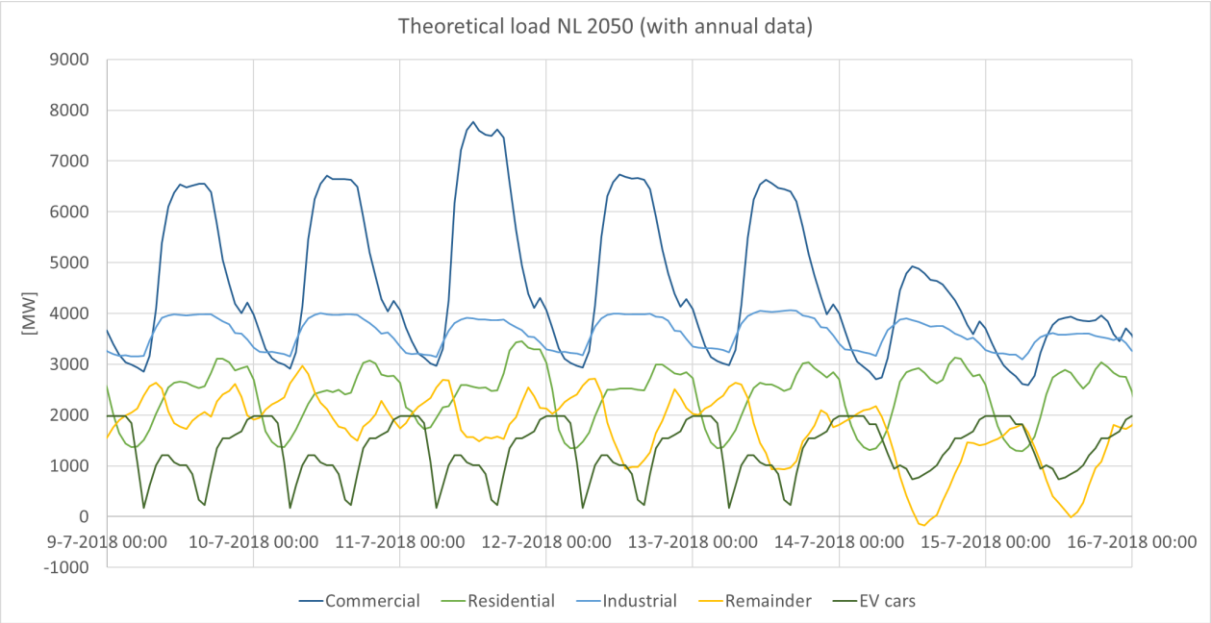

Figure 48: Decomposition of total load profile of a summer week in the Netherlands in 2050.

10.3.1.2 Italy (Europe South EUS)

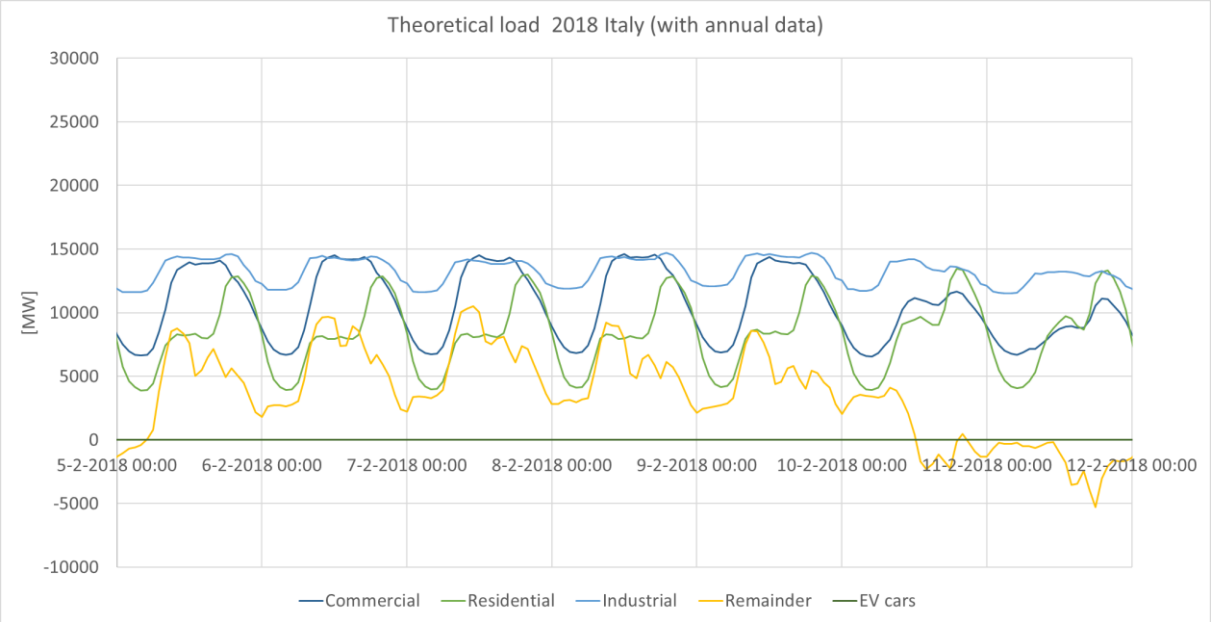

Figure 49: Decomposition of total load profile of a winter week in Italy in 2018.

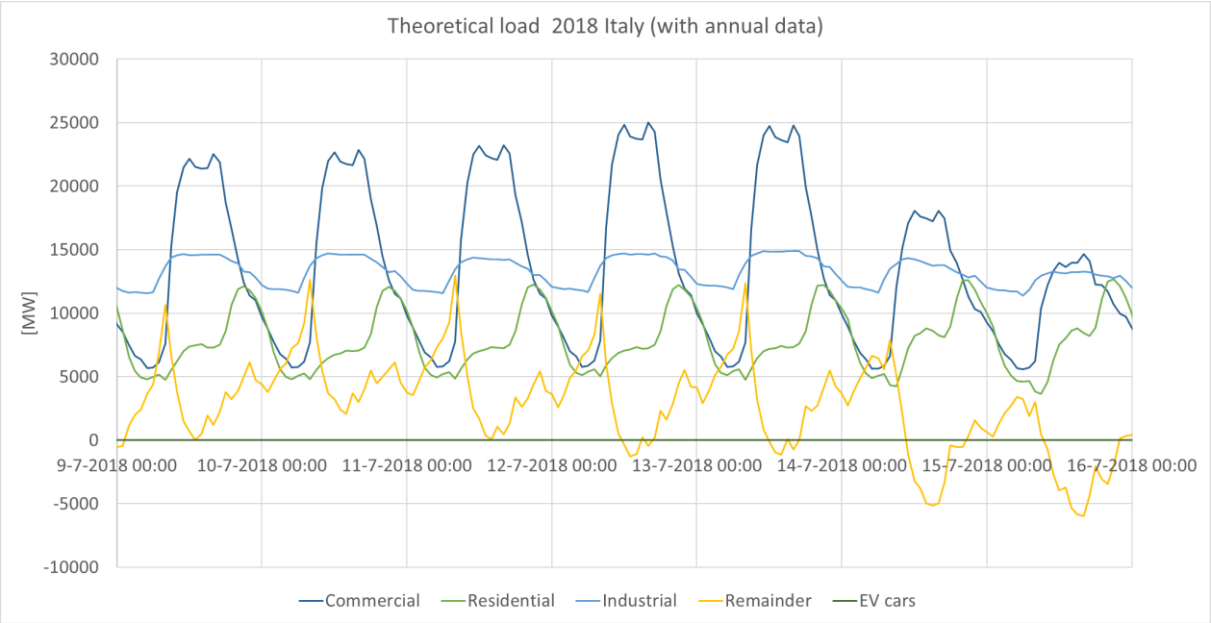

Figure 50: Decomposition of total load profile of a summer week in Italy in 2018.

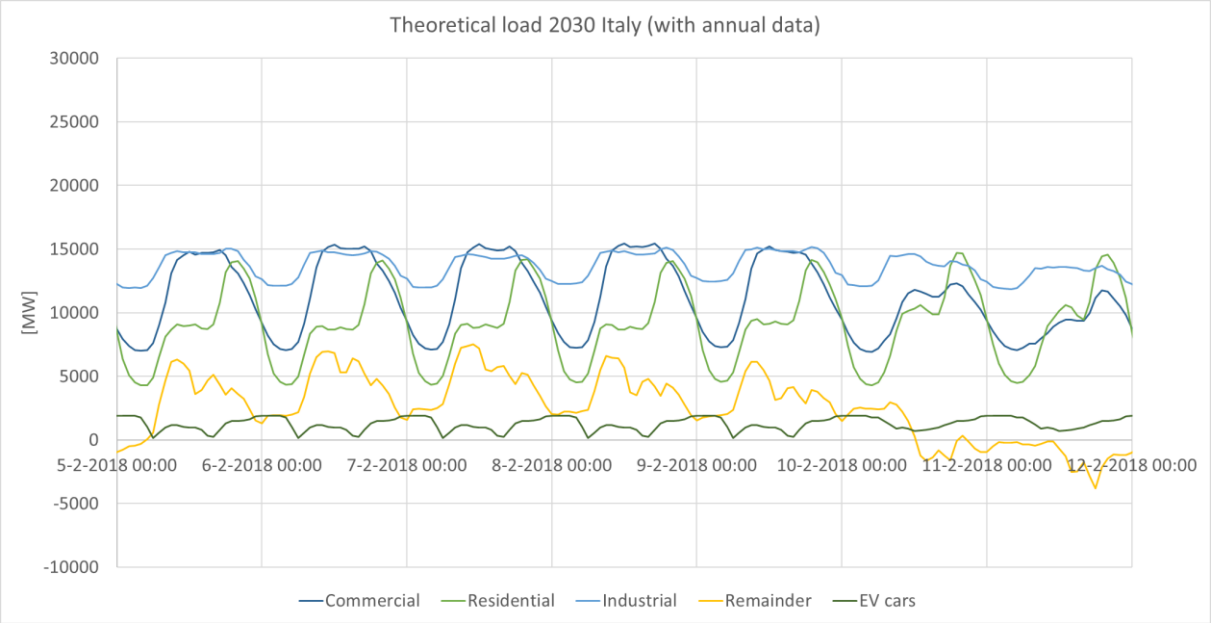

Figure 51: Decomposition of total load profile of a winter week in Italy in 2030.

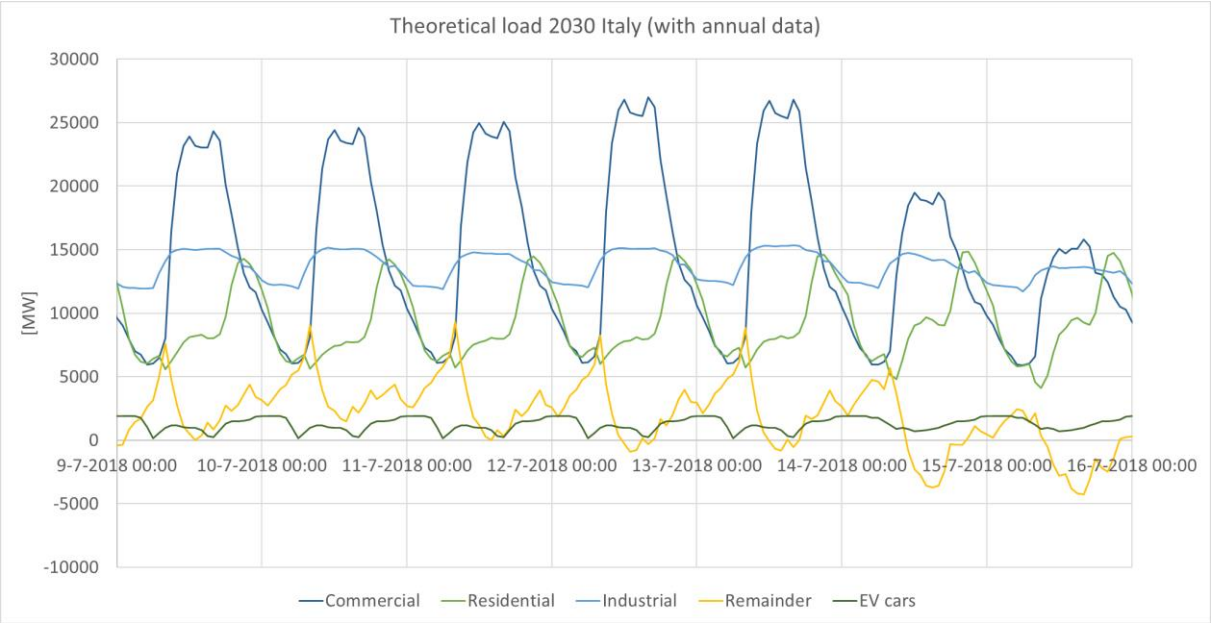

Figure 52: Decomposition of total load profile of a summer week in Italy in 2030.

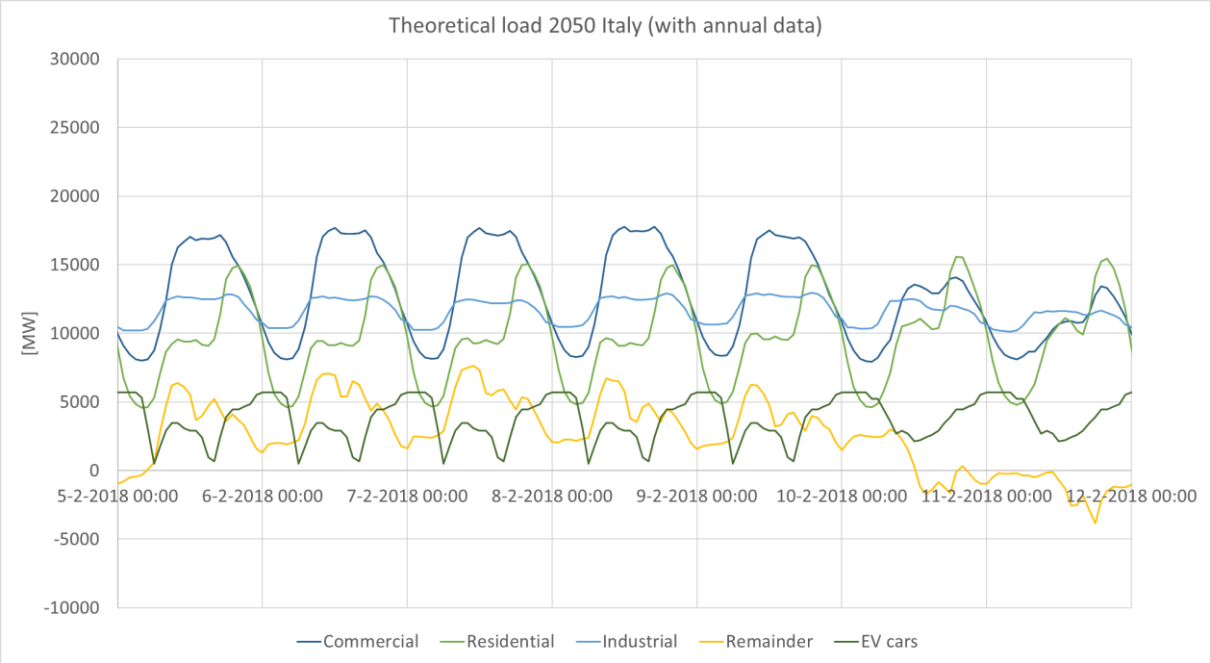

Figure 53: Decomposition of total load profile of a winter week in Italy in 2050.

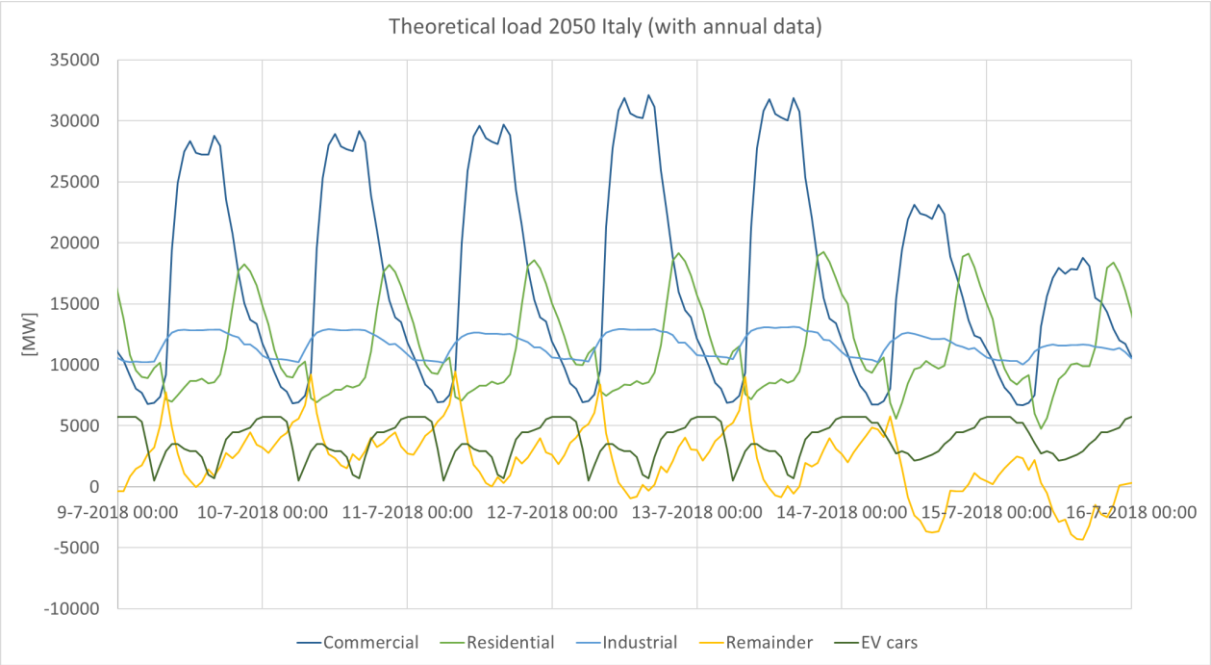

Figure 54: Decomposition of total load profile of a summer week in Italy in 2050.

10.3.1.3 Egypt (Middle East and North Africa MEA)

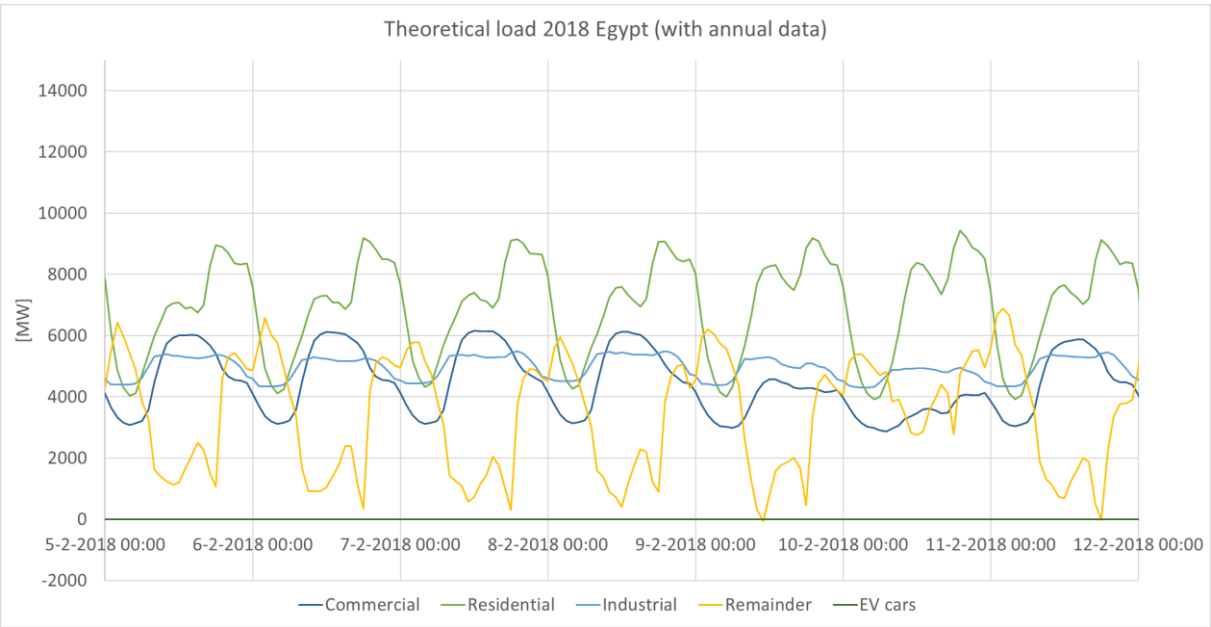

Figure 55: Decomposition of total load profile of a winter week in Egypt in 2018.

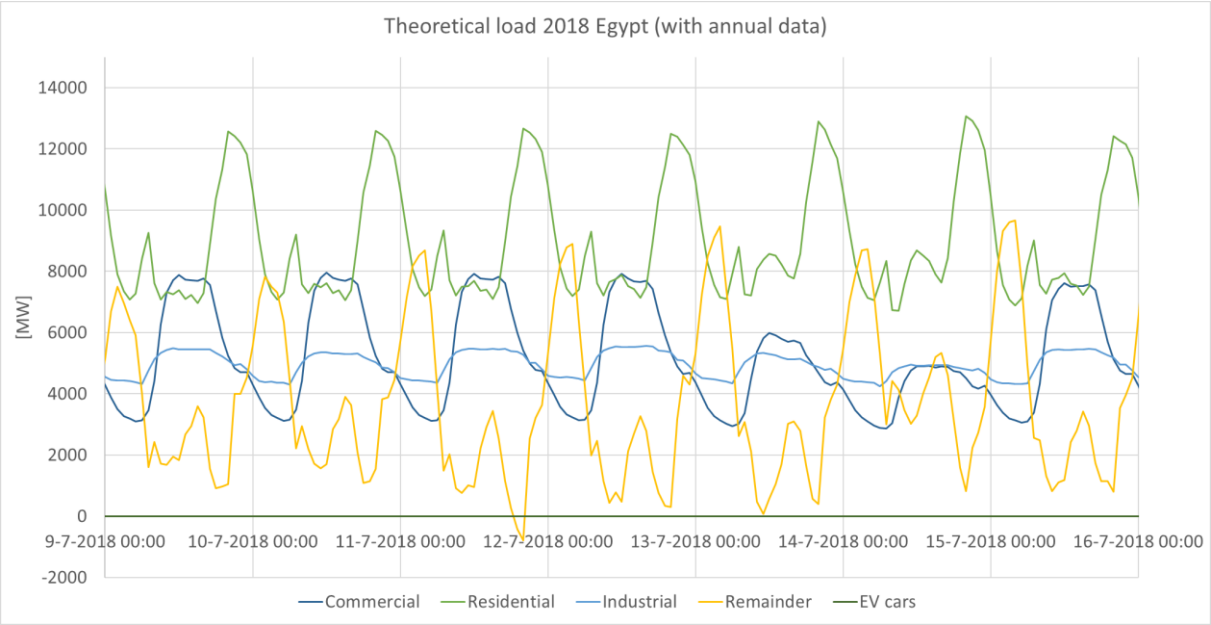

Figure 56: Decomposition of total load profile of a summer week in Egypt in 2018.

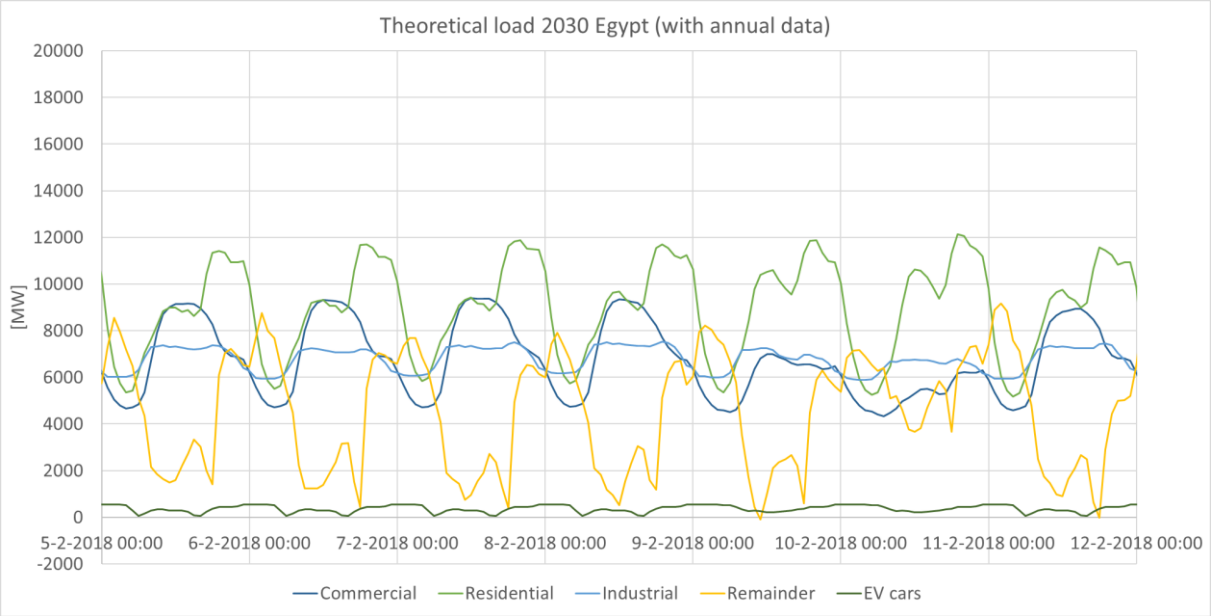

Figure 57: Decomposition of total load profile of a winter week in Egypt in 2030.

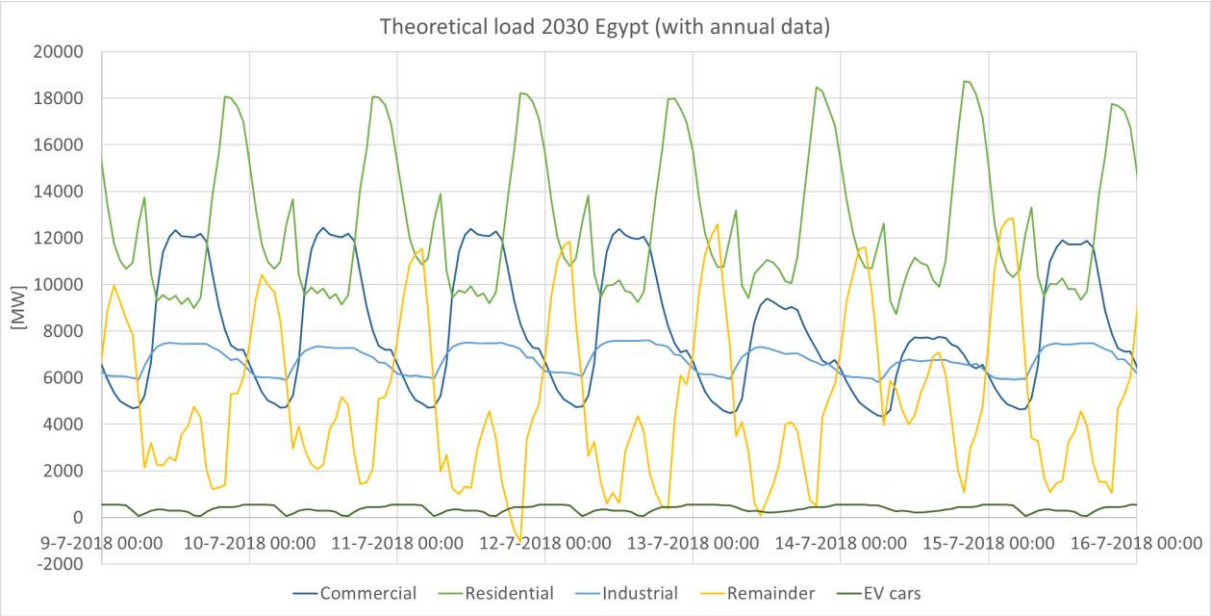

Figure 58: Decomposition of total load profile of a summer week in Egypt in 2030.

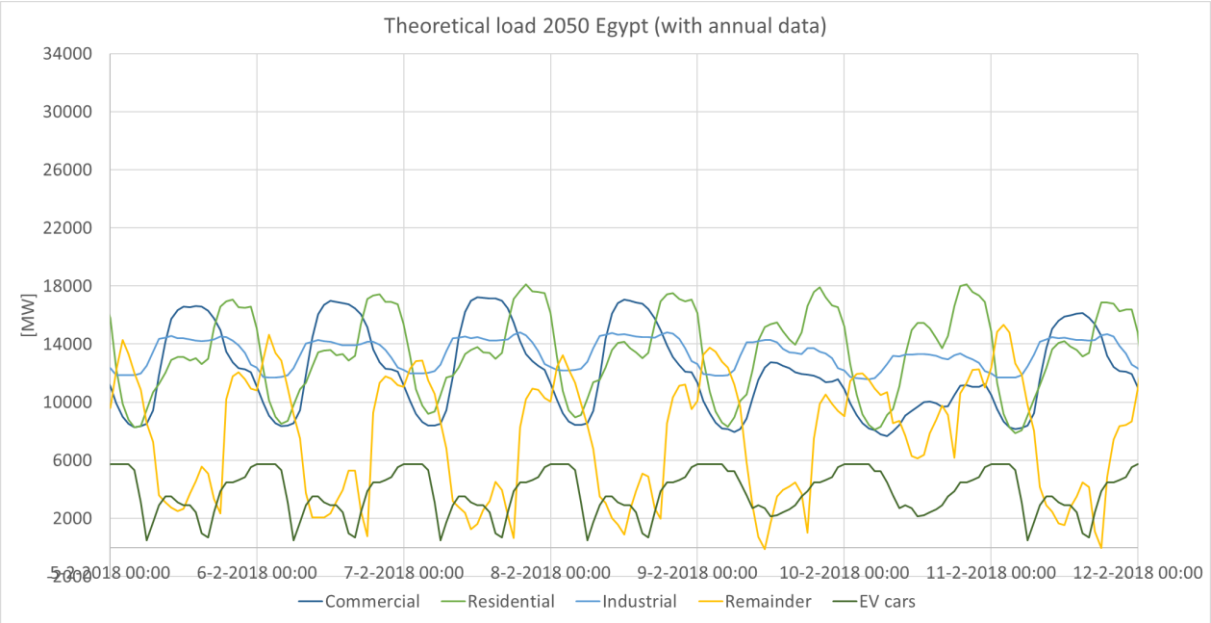

Figure 59: Decomposition of total load profile of a winter week in Egypt in 2050.

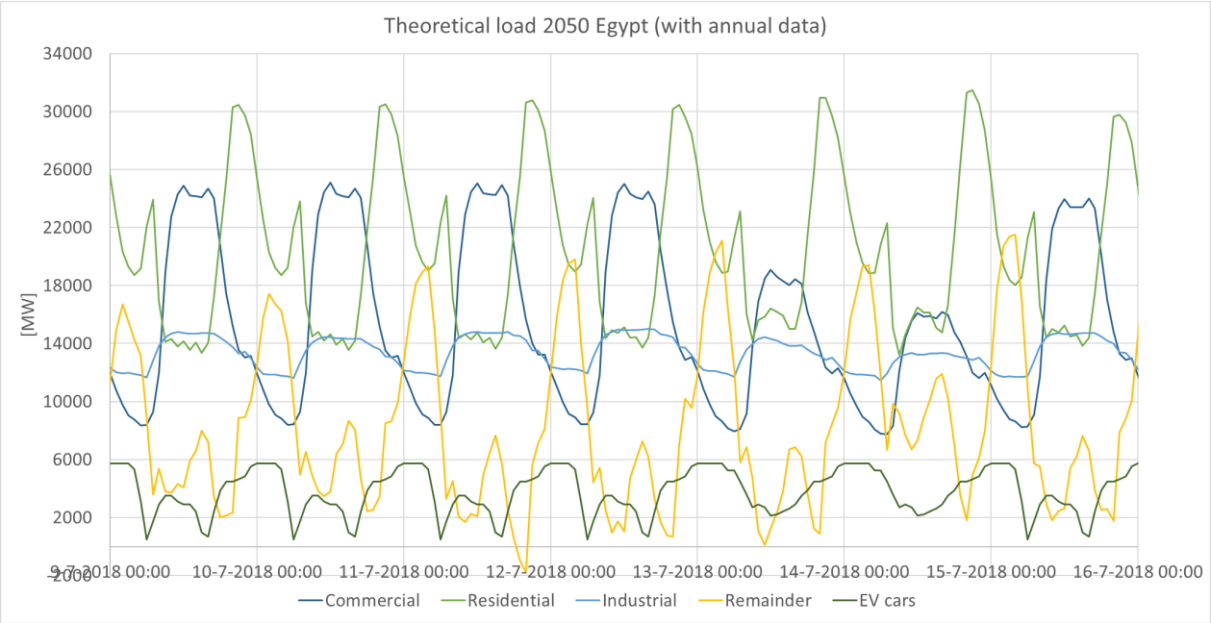

Figure 60: Decomposition of total load profile of a summer week in Egypt in 2050.

10.3.1.4 Singapore (South East Asia SEA)

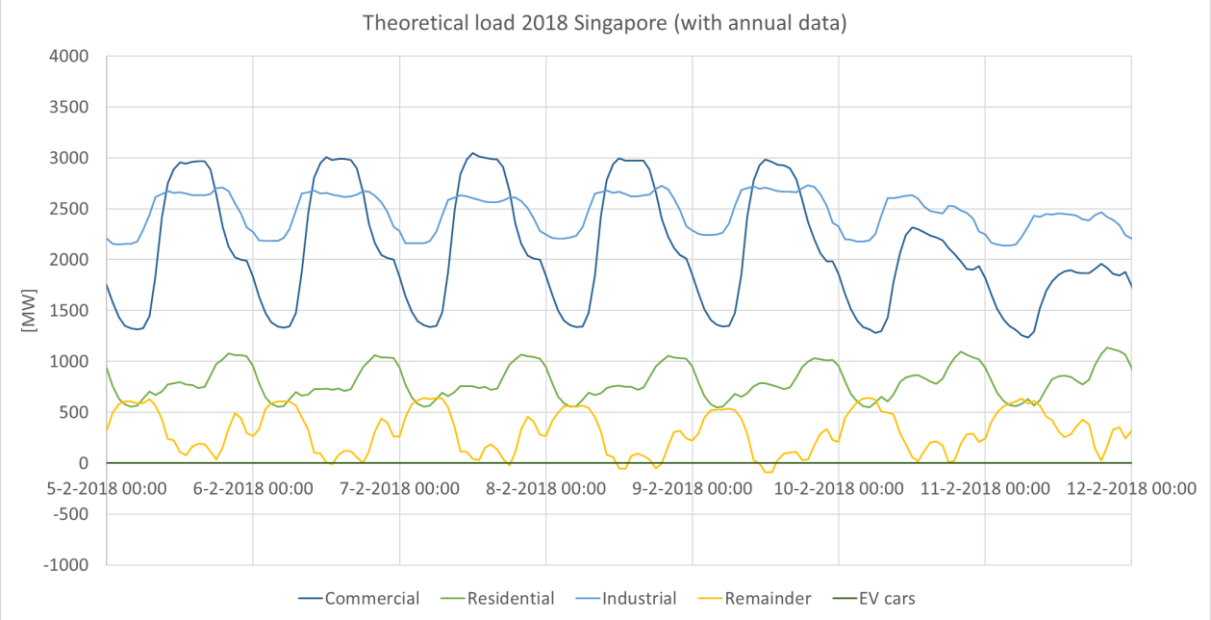

Figure 61: Decomposition of total load profile of a winter week in Singapore in 2018.

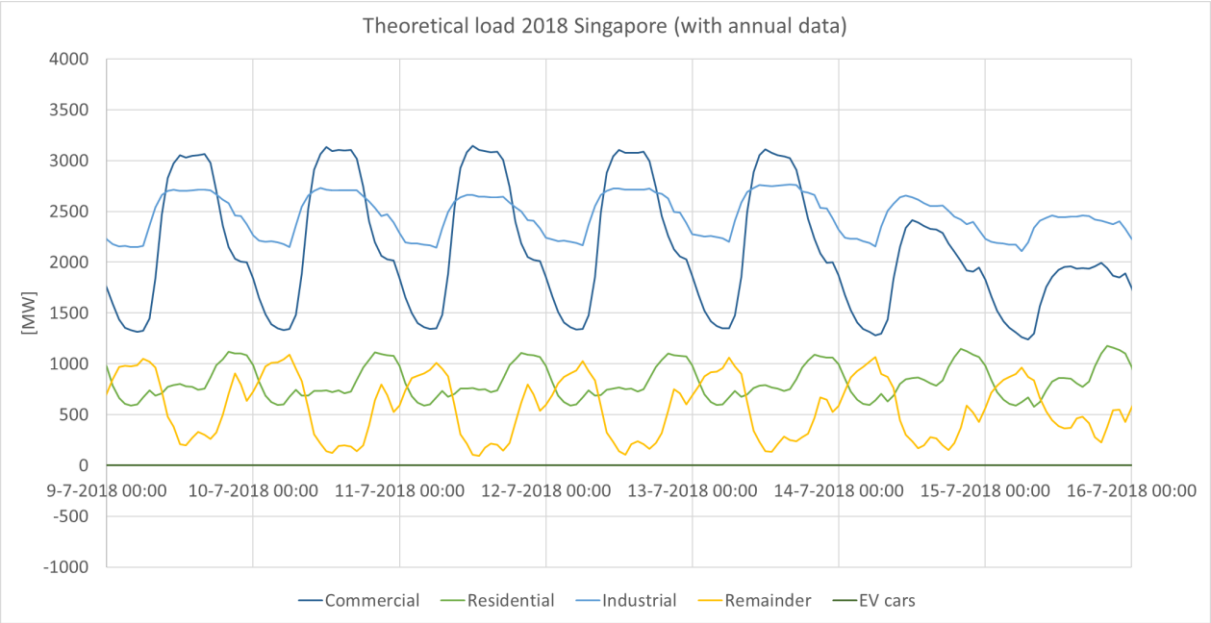

Figure 62: Decomposition of total load profile of a summer week in Singapore in 2018.

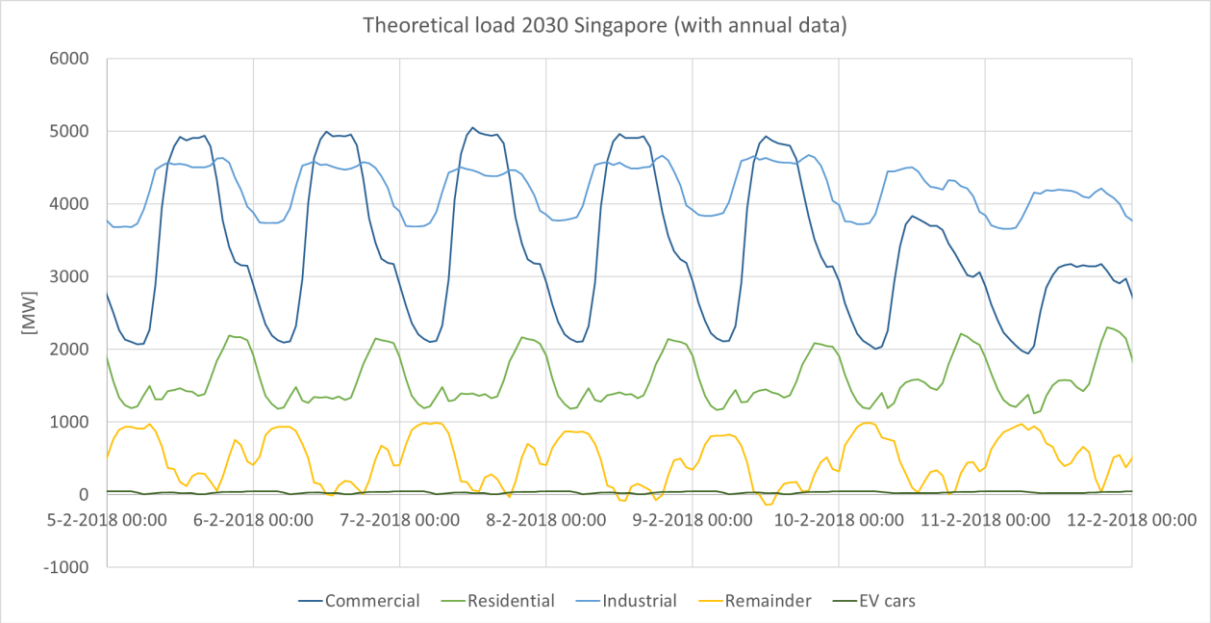

Figure 63: Decomposition of total load profile of a winter week in Singapore in 2030.

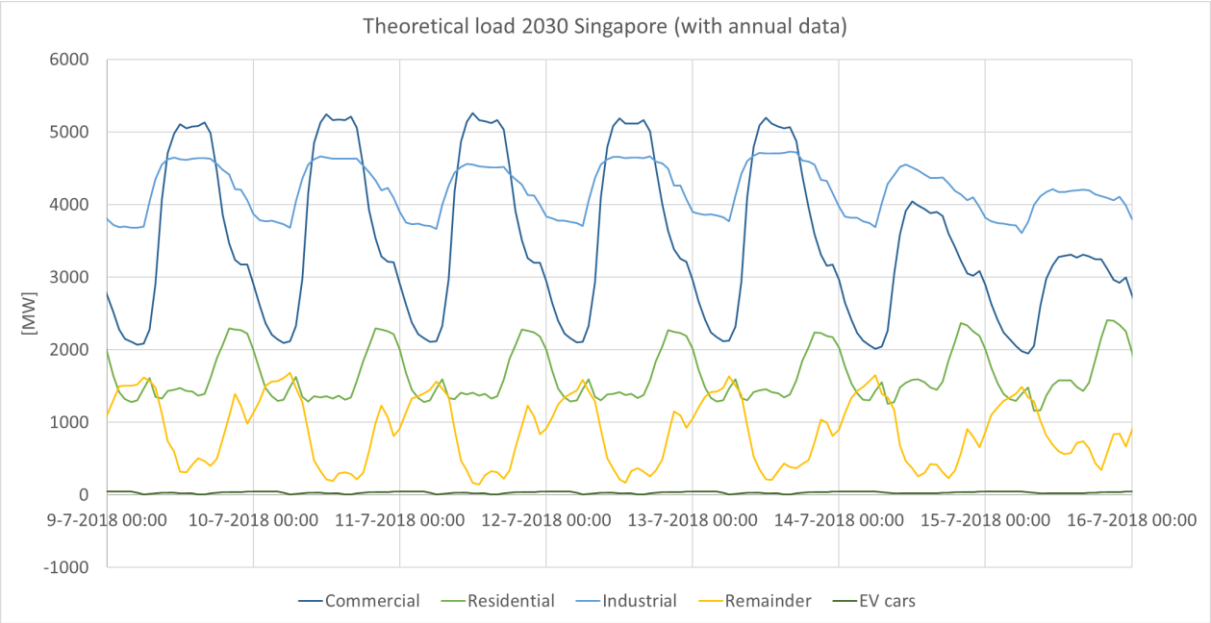

Figure 64: Decomposition of total load profile of a summer week in Singapore in 2030.

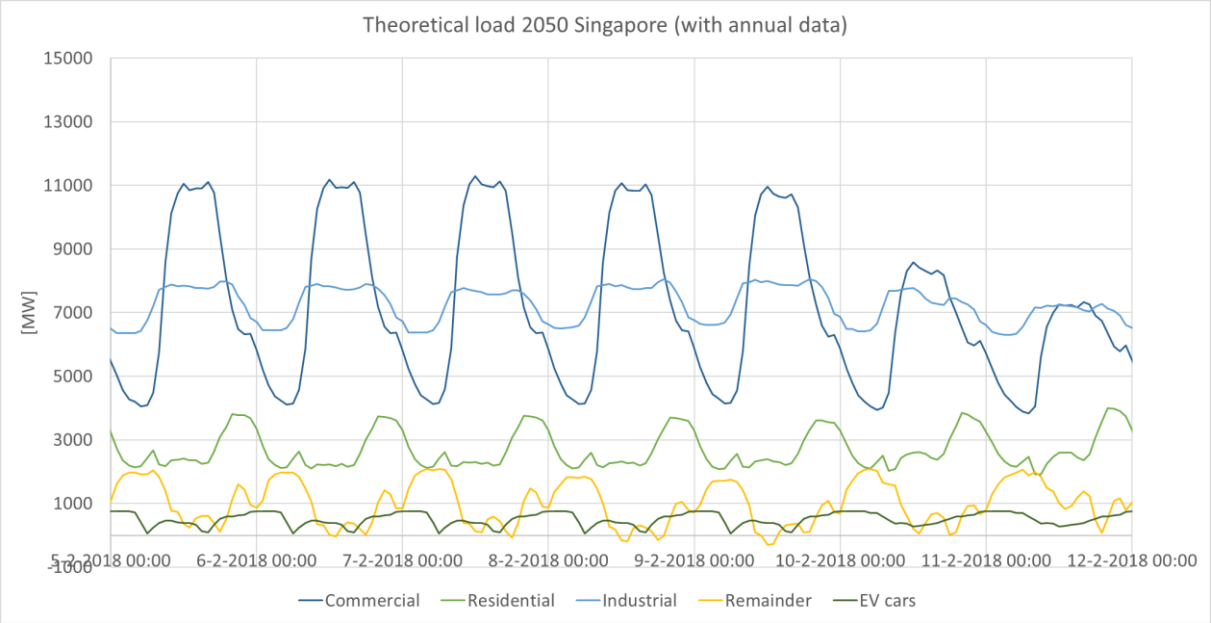

Figure 65: Decomposition of total load profile of a winter week in Singapore in 2050.

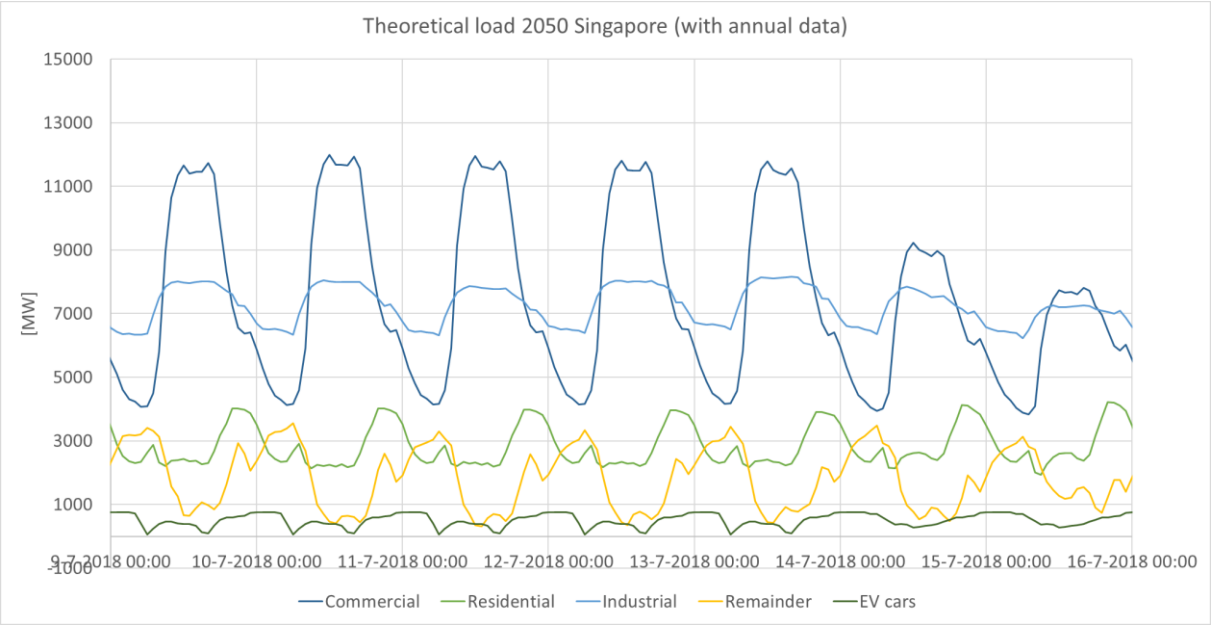

Figure 66: Decomposition of total load profile of a summer week in Singapore in 2050.

10.4 Appendix IV

10.4.1 Power frequency spectrum validation

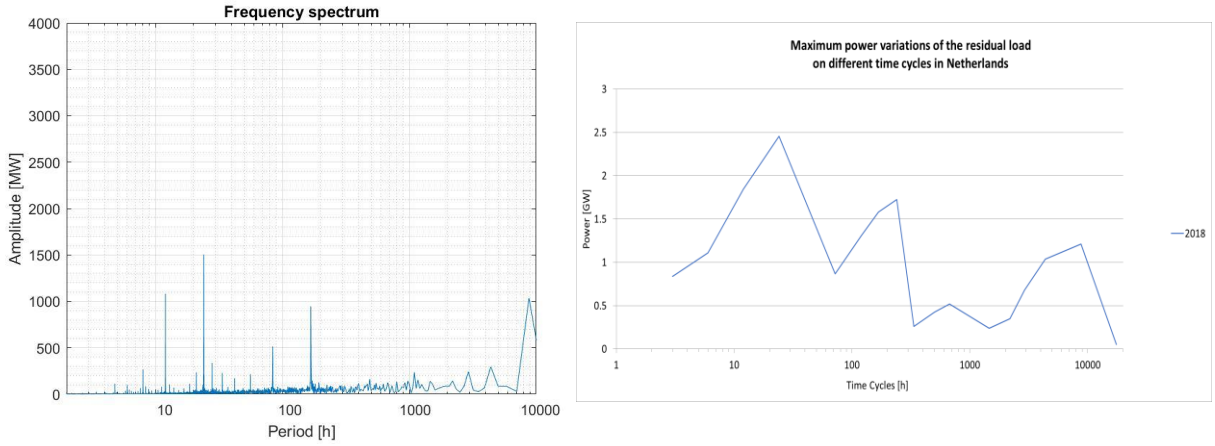

Figure 67: Power frequency spectrum calculated in MATLAB (left) and generated model (right) for Netherlands.

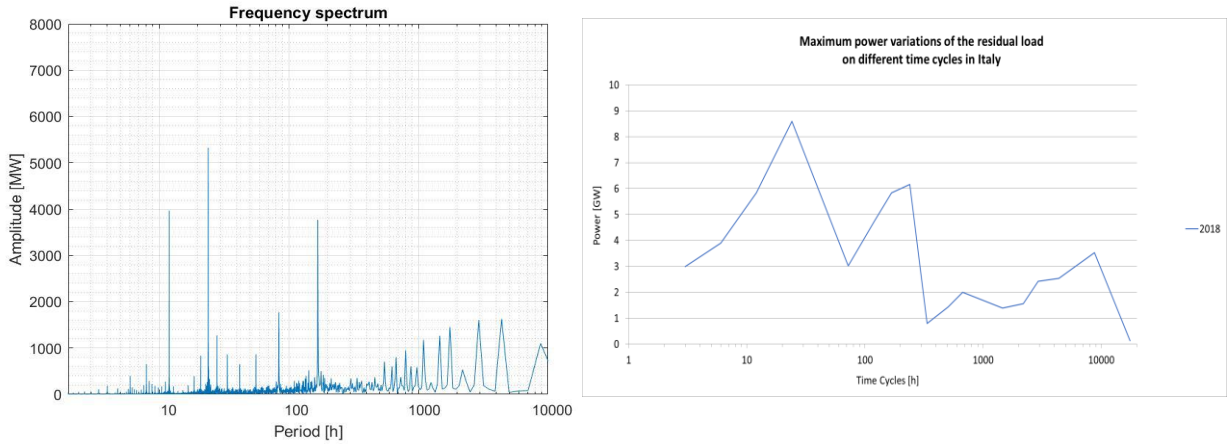

Figure 68: Power frequency spectrum calculated in MATLAB (left) and generated model (right) for Italy.

10.5Appendix V

10.5.1 Supply side (Power frequency spectrum analysis of VRES)

10.5.1.1 Netherlands (Europe North EUN)

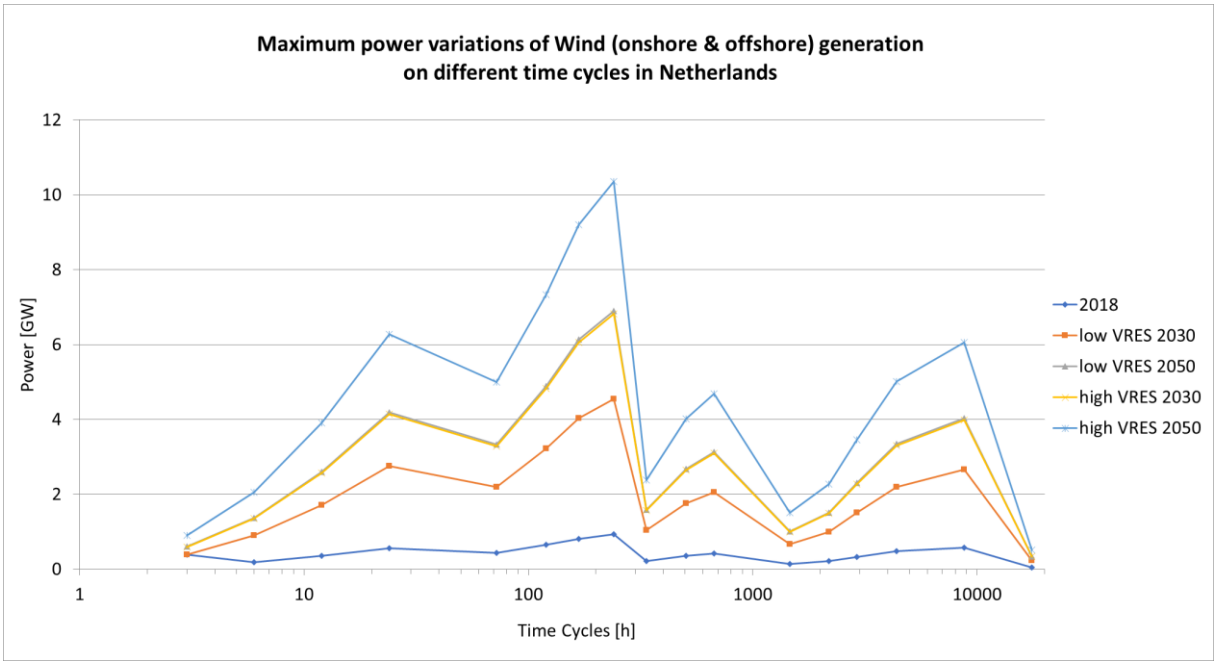

Figure 69: Power variability of Wind (onshore and offshore combined) on different time-cycles and scenarios (low and high VRES) in the Netherlands (2015 – 2018), see Table 8 for detailed description of applied time-cycles and corresponding amount of hours on the horizontal axis.

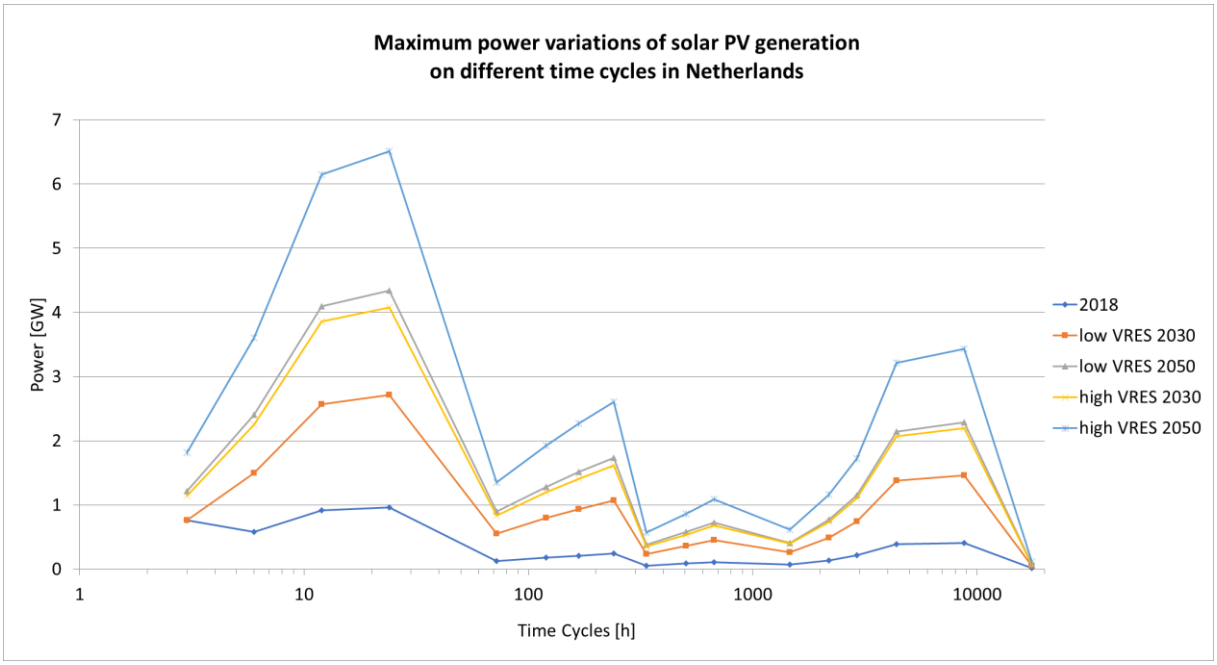

Figure 70: Power variability of solar PV on different time-cycles and scenarios (low and high VRES) in the Netherlands (2015 – 2018), see Table 8 for detailed description of applied time-cycles and corresponding amount of hours on the horizontal axis.

10.5.1.2 Italy (Europe South EUS)

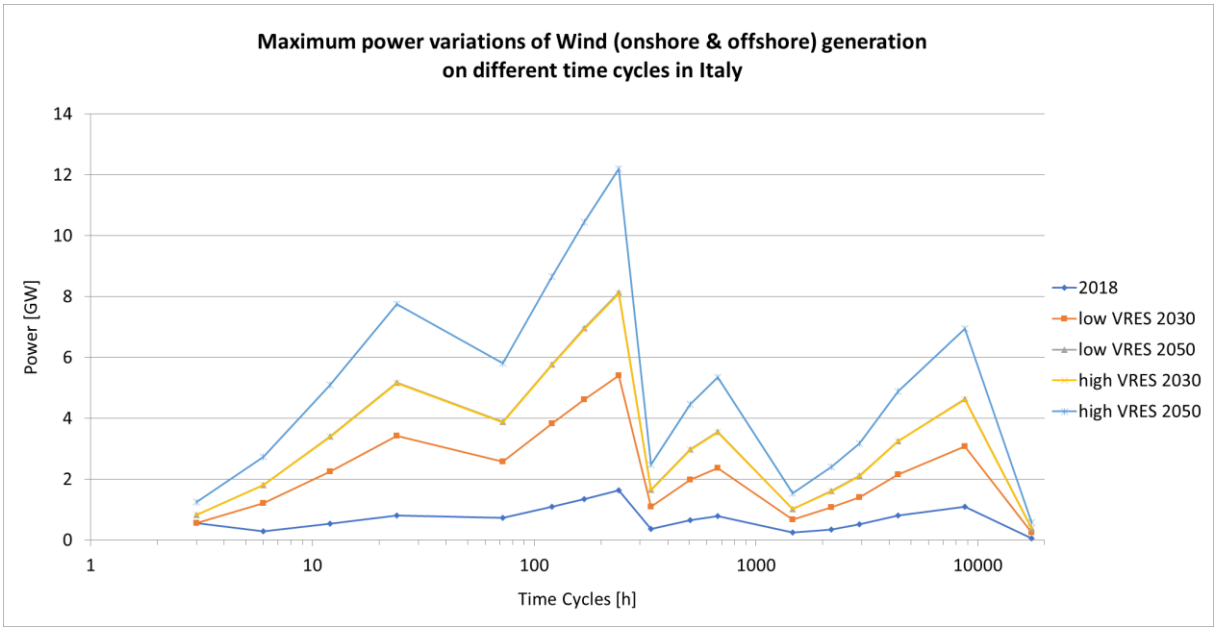

Figure 71: Power variability of Wind (onshore and offshore combined) on different time-cycles and scenarios (low and high VRES) in Italy (2015 – 2018), see Table 8 for detailed description of applied time-cycles and corresponding amount of hours on the horizontal axis.

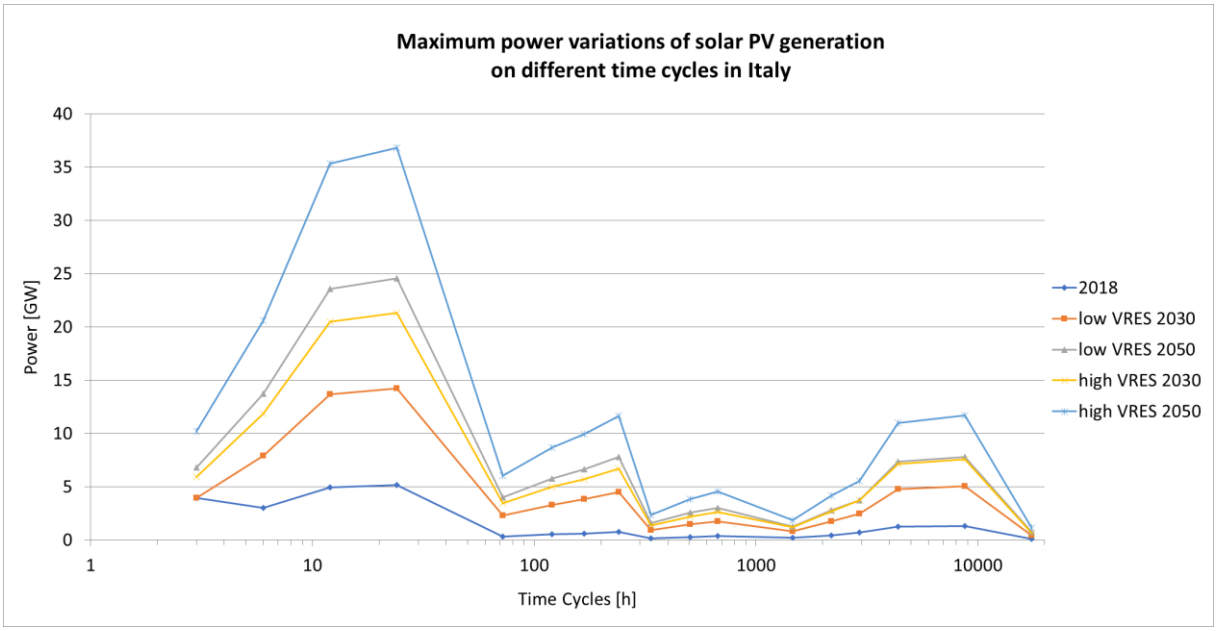

Figure 72: Power variability of solar PV on different time-cycles and scenarios (low and high VRES) in Italy (2015 – 2018), see Table 8 for detailed description of applied time-cycles and corresponding amount of hours on the horizontal axis.

10.5.1.3 Egypt (Middle East and North Africa MEA)

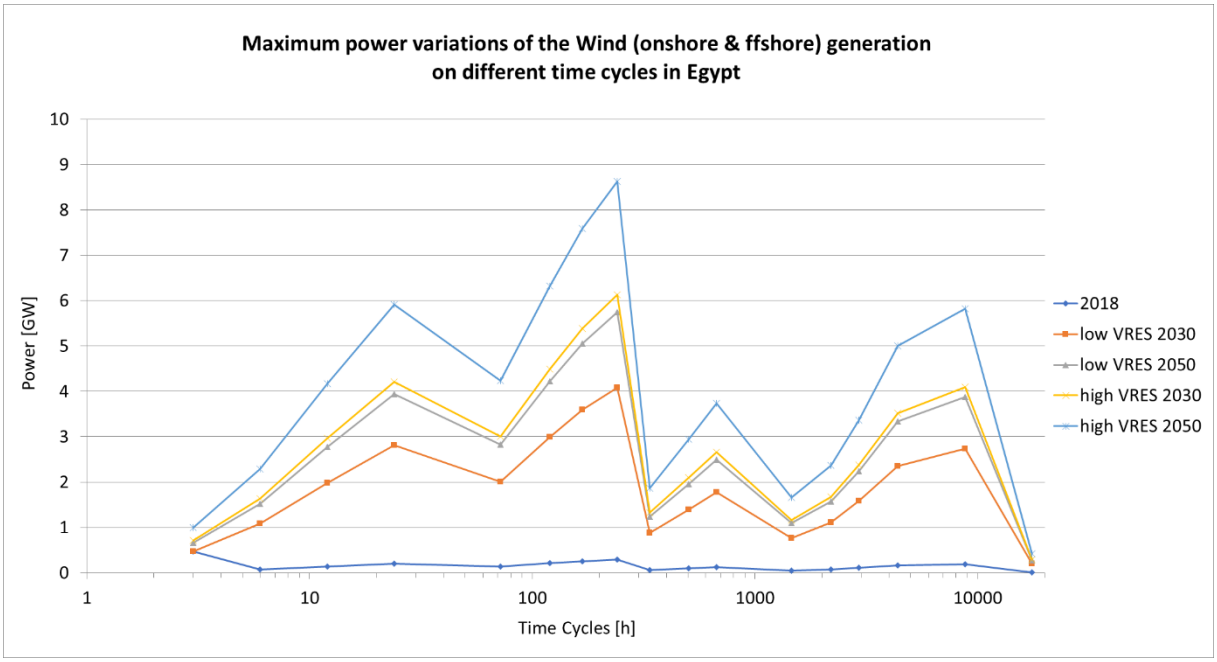

Figure 73: Power variability of Wind (onshore and offshore combined) on different time-cycles and scenarios (low and high VRES) in Egypt (2015 – 2018), see Table 8 for detailed description of applied time-cycles and corresponding amount of hours on the horizontal axis.

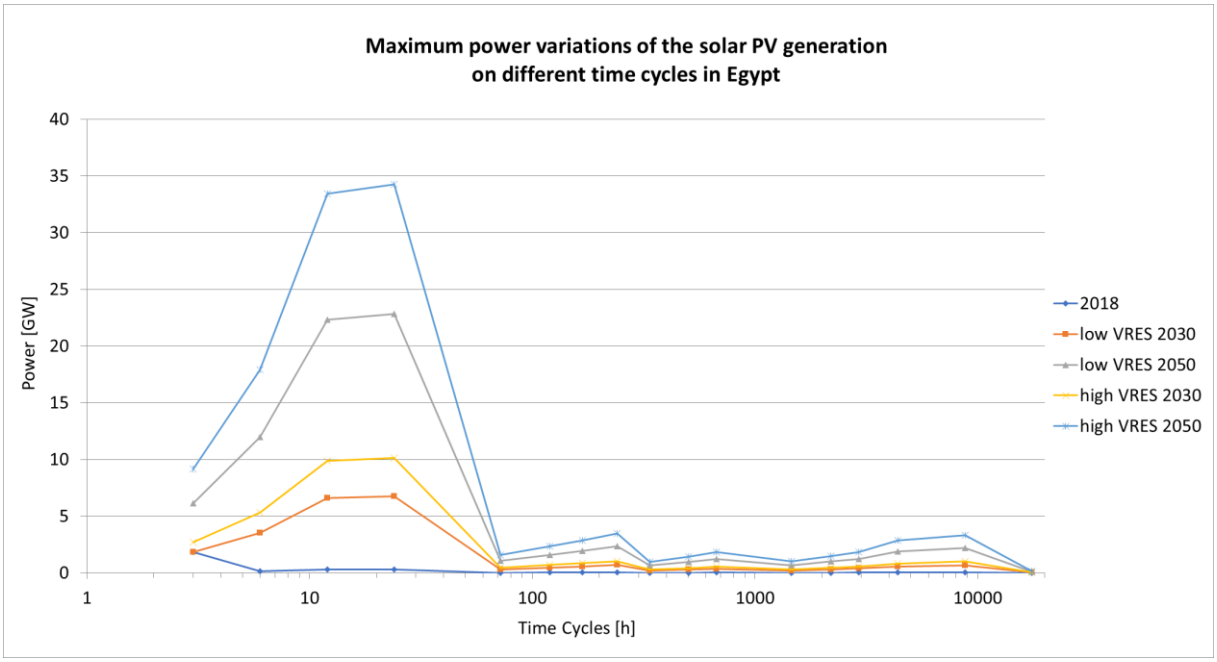

Figure 74: Power variability of solar PV on different time-cycles and scenarios (low and high VRES) in Egypt (2015 – 2018), see Table 8 for detailed description of applied time-cycles and corresponding amount of hours on the horizontal axis.

10.5.1.4 Singapore (South East Asia SEA)

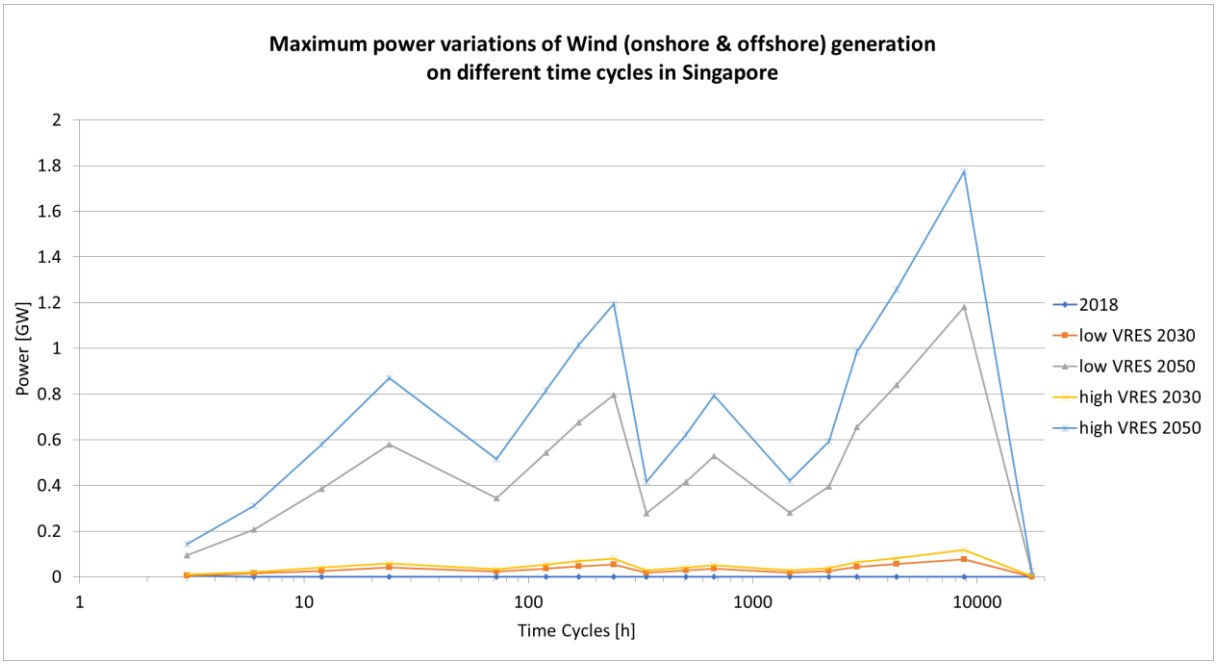

Figure 75: Power variability of Wind (onshore and offshore combined) on different time-cycles and scenarios (low and high VRES) in Singapore (2015 – 2018), see Table 8 for detailed description of applied time-cycles and corresponding amount of hours on the horizontal axis.

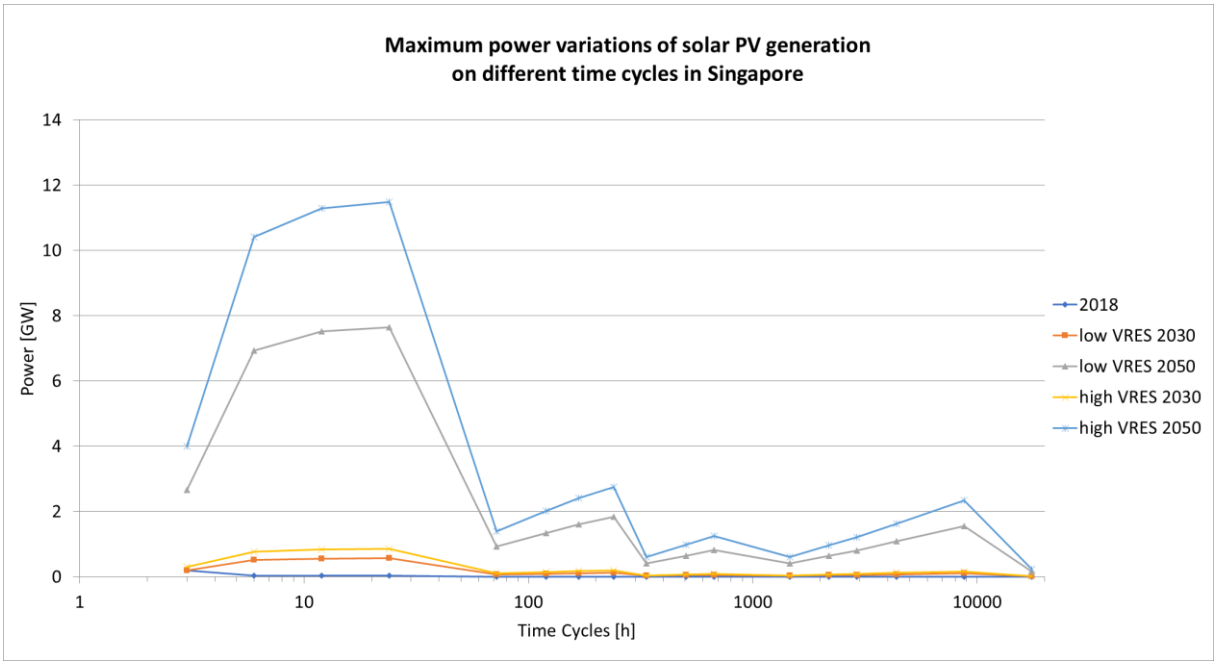

Figure 76: Power variability of solar PV on different time-cycles and scenarios (low and high VRES) in Singapore (2015 – 2018), see Table 8 for detailed description of applied time-cycles and corresponding amount of hours on the horizontal axis.

10.6 Appendix VI

10.6.1 MATLAB code, based on (van Winden, 2018).

```
%General parameters
N=length(A);
f=1 %the number of observations per unit of time.
freq=(1:(N/2))*f/N; %The frequency for graphs until the Nyquist frequency
Period=1./freq;
A_noDC=A-mean(A); %This cuts the 0 Hz DC component

%FFT execution
X=fft(A_noDC);
X_mag=abs(X);
X_amp=X_mag/N; %Normalises the magnitude into amplitude
X_ampsingle=X_amp(2:N/2+1); %Limits the plot to the Nyquist frequency
X_ampsingle(2:end-1)=2*X_ampsingle(2:end-1);

%Plots of the frequency spectrum
figure('visible','on')
subplot(1,1,1)
    semilogx(Period,X_ampsingle);
    curtick = get(gca, 'XTick'); %shows log units on x-axis
    set(gca, 'XTickLabel', cellstr(num2str(curtick(:))));
    grid on
    grid minor
    title('Frequency spectrum')
    xlabel({'Period [h]'});
    ylabel({'Amplitude [MW]'});
```